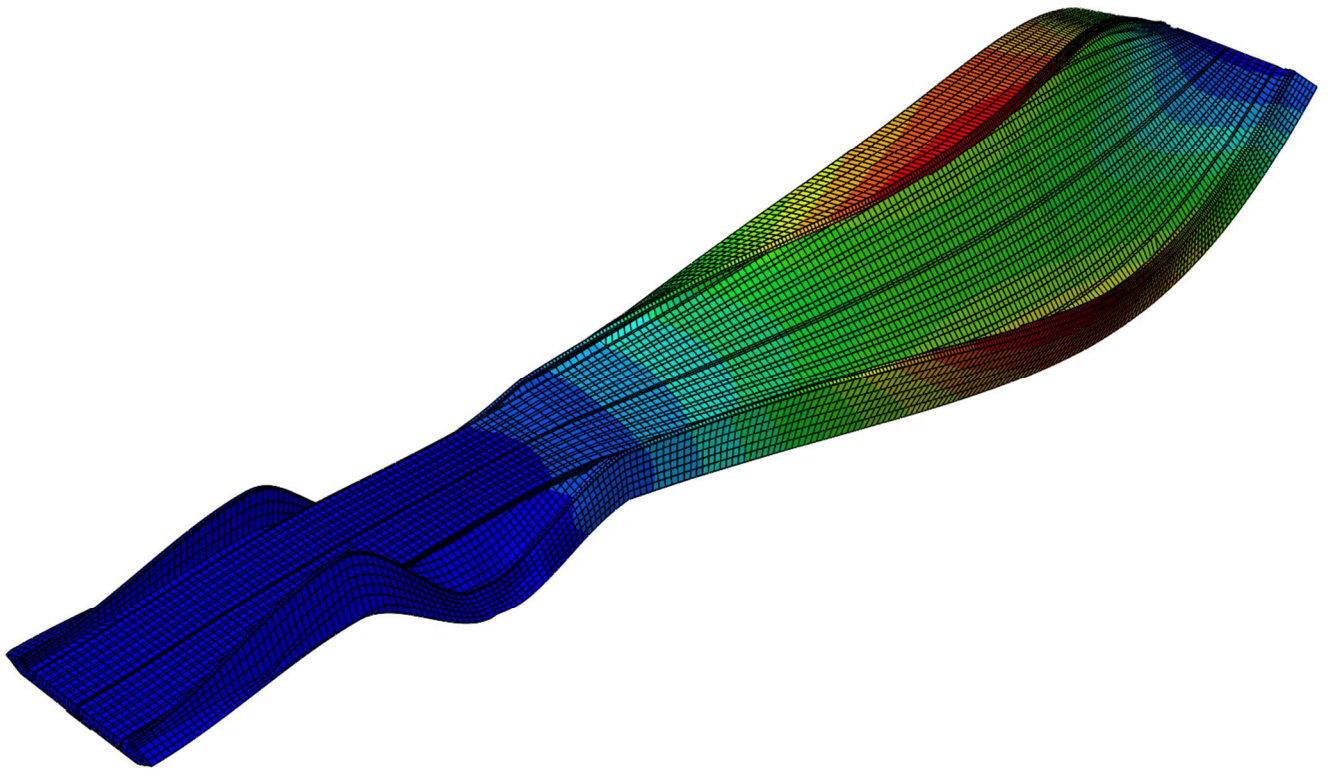# CHALMERS

Preliminary design of a fiber reinforced polymer pedestrian bridge

Master of Science Thesis in the Master's Programme Structural Engineering and Building Performance Design

CHANTHOEUN CHIV
YUBATH VOCAL

Department of Civil and Environmental Engineering
Division of Structural Engineering
Steel and Timber Structures
CHALMERS UNIVERSITY OF TECHNOLOGY
Göteborg, Sweden 2014
Master's Thesis 2015:141

Preliminary design of a fiber reinforced polymer pedestrian bridge

Master of Science Thesis in the Master's Programme Structural Engineering and Building Performance Design

CHANTHOEUN CHIV

YUBATH VOCAL

Department of Civil and Environmental Engineering
Division of Structural Engineering
Steel and Timber Structures
CHALMERS UNIVERSITY OF TECHNOLOGY
Göteborg, Sweden 2015

Preliminary design of a fiber reinforced polymer pedestrian bridge

Master of Science Thesis in the Master's Programme Structural Engineering and Building Performance Design

CHANTHOEUN CHIV
YUBATH VOCAL

Department of Civil and Environmental Engineering
Division of Structural Engineering
Steel and Timber Structures
Chalmers University of Technology
SE-412 96 Göteborg
Sweden
Telephone: + 46 (0)31-772 1000

Cover: FRP pedestrian bridge exhibiting first lateral frequency mode.

Preliminary design of a fiber reinforced polymer pedestrian bridge

Master of Science Thesis in the Master's Programme Structural Engineering and Building Performance Design
CHANTHOEUN CHIV

YUBATH VOCAL
Department of Civil and Environmental Engineering
Division of Structural Engineering
Steel and Timber *Structures*
Chalmers University of Technology

ABSTRACT

The aim of this thesis is to create a preliminary design of the bridge "Kaponjärsbron" with a fiber reinforced polymer (FRP) composite cross-section. A literature study is carried out to learn about FRP materials and how they interact with each other. Subsequently, a calculation module is developed to determine equivalent material properties that were later used to create several cross-section combinations in a finite element model (FEM) program. The FE model is then used to develop a preliminary design of the FRP composite cross-section to fulfill the design requirements for pedestrian bridges.

Key words: Fiber-reinforced-polymer; preliminary design; pedestrian bridge; dynamic analysis; Kaponjärsbron

Contents

iv

List of figures

List of tables

Preface

Nomenclature

Roman upper case letters

A_c, A_f	Area, per unit width, perpendicular to corrugation axis, of the corrugated core section and the face plate sheet, respectively, [m]
D_x, D_y	Bending stiffness for a corrugated steel sandwich panel profile, per unit width, associated with bending caused around x-, and y-axes, respectively
D_{xy}	Torsional stiffness for a corrugated steel sandwich panel profile
D_{Qy}, D_{Qx}	Transverse shear stiffness, per unit width, of a corrugated steel sandwich panel, in the y- and x-direction, respectively
E_c, E_f	Modulus of elasticity of the core and face sheet material, respectively, [Pa]
E_x, E_y	Axial stiffness in x-, and y-directions, respectively
G_c, G_f	Shear modulus of elasticity of the core material and face sheet material, respectively
S	Non-dimensional coefficient in formula for D_{Qx}

Roman lower case letters

$2p$	Corrugation pitch, [m]
f	Length of the corrugated flat segment, [m]
h	Height of sandwich profile, measured from the middle of the face sheets, [m]
h_c	Height of the core, measured from the centre lines, [m]
l_c	Length of one corrugation leg measured along the centre line, [m]
t_c, t_f	Thickness of the corrugated-core and face sheet, respectively, [m]
l_{buck}	Length of corrugation opening
f_y	Yielding strength of the material, [MPa]

Greek lower case letters

α	Corrugation angle
ν_c, ν_f	Poisson's ratio of the core and face sheet material, respectively

Abbreviations

AASHTO	American Association of State Highway and Transportation Officals
BRIGADE/STANDARD	Finite element modelling software
BRIGADE/PLUS	Finite element modelling software
CFRP	Carbon Fiber-Reinforced-Polymers
GFRP	Glass Fiber-Reinforced-Polymers
FRP	Fiber-Reinforced-Polymers
FE	Finite Element
JRC	European Commission, Joint Research Centre
LCC	Life-Cycle-Cost analysis
LCA	Life-Cycle Assessment
RIFT	Resin infusion under flexible tooling
SCRIMP	Seemann Composites Resin Infusion Manufactoring process
SLS	Serviceability Limit State
ULS	Ultimate Limite State
VARTM	Vaccum Assisted Resin Transfer Molding

1 Introduction

1.1 Background

Kaponjärsbron, which is going to be the first FRP pedestrian bridge in Sweden, is a 45 meter bridge consisting of two different span lengths. It has two spans, which are 11 meters and 34 meters as shown in Figure 1.1 and Figure 1.2 respectively. The appealing and controversial issue about this pedestrian bridge is the challenging wavy shape of the entire structure. This architectural design concept has sparked a lot of interest from the public in Sweden. Furthermore, due to the complicated geotechnical condition at the surrounding site, which is believed to have 40 meters clay and a lot of electrical wires and pipes under the ground, a lightweight structure is highly recommended as the primary solution in this project. However, to satisfy both aesthetical and geotechnical issues, what kind of material is the most appropriate one?

As the material technology has been advancing rapidly during recent decades, an advanced composite material named as Fiber Reinforced Polymer (FRP), has been introduced to the construction sector especially in the bridge industry. The primary and attractive reason for designers to choose FRP composite materials as a great promising solution for pedestrian bridges is its superior quality and advantages over several conventional construction materials. These advantages can be seen from its characteristics such as lightweight, high strength, and high durability (high corrosion and fatigue resistance). Furthermore, FRP composite materials possess the ability to be molded in any complex shape, thus it is regarded as a geometrically more efficient solution [1]. Another prominent feature of this material is the ease of prefabrication, which means fast installation, hence the construction time can be noticeably reduced compared to other conventional construction materials like reinforced concrete.

Based on a comparative case study of life-cycle cost analysis of a real bridge by Itaru Nishizaki et al [2] between FRP and prestressed concrete bridges, FRP bridges are more efficient and require much lower maintenance cost when a longer service life is required in severely hazadous environments, despite having slightly higher initial cost.

Following the distinguished characteristics of FRP composite materials, FRP pedestrian bridges have a particular fact that they are lightweight by nature. These lightweight bridges are very susceptible to human-induced-vibrations. When they are excited, they usually exhibit very low natural frequencies, which can lead to a resonance phenomenon. A practical example is the London Millennium Bridge which was initially opened in 2000 at a cost of £18.2M [1]. The bridge experienced unexpected lateral resonant vibrations due to walking and/or running and eventually was forced to close for 2 years for modifications, which cost another extra £5M. Therefore, based on such remarkable technical incident, it is strongly recommended for designers to consider not only for static loads but also the dynamic loads since already at preliminary design stage.

Due to the limited knowledge of FRP composite materials and its application in bridge industry, many design aspects are still unknown. As mentioned above, the

criterion which is interesting and probably problematic during preliminary design stage is the dynamic response of such lightweight structures. It is necessary to develop design methods specifically for the FRP structures. Therefore, Ramböll as well as the authors are part of this innovative project and are interested in deeper research of these problems.

Figure 1.1 - 3D view of the Kaponjärsbro pedestrian bridge

Figure 1.2 – Bridge's span length dimensions

1.2   Project aim and objectives

The main aim of this master thesis is to develop a preliminary design of the Kaponjärs pedestrian bridge which is entirely made of FRP composite materials. In order to archive the main aim, there are two objectives that need to be accomplished.

- Build a 3D FE model to evaluate the overall structural behavior of the entire bridge under the prescribed pedestrian loads in the Eurocode. This part includes both the methodology of how to construct the challenging irregular-shaped model step by step in FE softwares [3][4] and simple analytical designs of FRP pedestrian bridge's structural components in preliminary stage.
- Determine the dynamic response influenced by geometry, elastic modulus, fiber architecture, etc. The suggestion is to compare both acceleration and natural frequency in vertical and lateral directions in the most critical locations. However, before dynamic analysis can be assessed, the SLS requirement on deflection is chosen to be fulfilled first.

CHALMERS, *Civil and Environmental Engineering*, Master's Thesis 2015:141

1.3   Methodology

The first step in order to solve the problem in this master thesis is a study on the literature review of FRP composite materials. Each component's functionalities, characteristics, manufacturing process and modelling techniques in laminate structures are critical to understand the behavior of FRP composites. Similarly, FRP composite materials' equivalent elastic properties and design requirements (guidelines and recommendations) for FRP pedestrian bridges were studied, focusing on its dynamic behavior.

The second method is to formulate a MATLAB routine to calculate the equivalent elastic properties of the laminate structures. The MATLAB routine, which has several variables such as laminate thickness, selection of constituent materials, fiber's orientation angle, and lamina stack-up sequence, mainly bases on the instructions in *EUROCOMP Design code and Handbook* [5]. Furthermore, the purpose of programming this routine is to optimize the equivalent laminate stiffness and also to comply with the input requirements from smeared modelling technique which is briefly described later in Chapter 2.

Lastly, in order to numerically analyze the overall structural behavior by means of FE modelling, some appropriate software is required. Two FE software programs, BRIGADE STANDARD and BRIGADE/PLUS, are used to construct a beam element model and a shell element model, respectively.

1.4   Limitations

As recommended in a report from the European Commission Joint Research Center (JRC) [6] , dynamic actions and vibration behavior of the structure should be considered in an early design stage even when some important design parameters such as damping and foundation properties are unknown. Therefore, the authors decide to only focus on the dynamic analysis of the FRP pedestrian bridge at the preliminary design stage.

Due to the fact that pedestrian bridges are generally governed by Serviceability Limit State (SLS) criteria, merely SLS is regarded in this thesis.

Knowing human-induced-vibration in bridges is primarily a serviceability problem; the major requirement which is chosen to be fulfilled first in the FE model is the maximum vertical deflection of the pedestrian bridge followed by checking natural frequencies and accelerations, both in vertical and lateral directions. However, due to inadequate time for further analysis, the check on acceleration limit, also known as comfort criteria [7], is not performed.

To regulate the scope of the thesis within given timeframe, there are other limitations in this master thesis such as

- No connection design
- No consideration over hygrothermal effects
- No Ultimate Limit State (ULS) optimization on laminate configuration
- No consideration on long term effects such as creep, fatigue, etc.

1.5 Thesis outline

In this thesis, there are totally 7 chapters, a list of references, and two appendices.

Chapter 1 is an introductory section.

Chapter 2 describes the studies on literature review. It is an introduction to FRP composite materials including each component's functionalities, characteristics, manufacturing process and modelling techniques in laminate structures. Correspondingly, equivalent elastic properties and design requirements (guidelines and recommendations) for FRP pedestrian bridges focusing on its dynamic behavior.

Chapter 3 presents the development of two FE models known as beam element and shell element model.

Chapter 4 displays preliminary results obtained from the models above. The results such as maximum deflection, natural frequencies are achieved from simulation in BRIGADE STANDARD and BRIGADE PLUS.

Chapter 5 illustrates the improvement process after obtaining the preliminary results.

Chapter 6 illustrates the final result of the preliminary design.

Chapter 7 draws the main conclusions made by the authors.

Bibliography provides list of references.

Appendix A contains the MATLAB scripts.

Appendix B contains the MathCad files.

.

2   Literature Study

The application of FRP composites has been adopted since the mid 1930's. The main objective at the time was in the aviation sector due to a lightweight solution with high resistance and performance. However, its application was limited to the aerospace and defense industry.

Due to FRP's high performance and unique properties, the manufacturers have seen the possibility to grow and its potentiality in the future construction material market. This lead to a sustainable growth of research interest on different topics, and it eventually caught the attention from civil engineering industries. In recent years, the application of FRP composite materials in construction and infrastructure sectors has obviously increased. The first attempt was to use this material as reinforcement, Carbon Fiber-Reinforced-Polymers (CFRP), to strengthen and retrofit existing structures.

Before beginning to establish the model of the FRP pedestrian bridge which is the subject of this study, the understanding of each components of the material is very important. This chapter briefly describes FRP composite materials' functionalities, characteristics and relevant information that are needed for the design.

2.1   Composites properties

FRP composite materials are simply a combination between fibers, which are known as reinforcement, and matrix which functions as binders. Furthermore, they are typically arranged in the form of laminate structure. The selection in terms of type and geometry (fiber orientation's angle, stack-up sequence) of fibers and matrix mainly affect the structural properties like strength and stiffness of the laminate structure.

2.1.1 Fibers

As mentioned earlier, to serve as reinforcing component in the laminate structure, fibers must be stiff, strong, and tough comparing to matrices. Due to the fact that fibers carry most of the axial load, the strength in the laminate structure is influenced by the strength of fibers in a very direct manner. Usually, more than half of the total volume of the composite material is occupied by fibers.

Fibers, which are usually utilized in civil engineering applications, are glass, aramid, and carbon fibers. The properties of these fibers are shown in Table 2.1 below.

Table 2.1 – Properties of glass, aramid and carbon fiber [7]

Typical properties	Fibers					
	Glass		Aramid		Carbon	
	E-Glass	S-Glass	Kevlar 29	Kevlar 49	High strength	High modulus
Density ρ [g/cm³]	2.60	2.50	1.44	1.44	1.80	0.19
E-modulus E [GPa]	72	87	100	124	230	370
Tensile strength [MPa]	1.72	2.53	2.27	2.27	2.48	1.79
Extension [%]	2.40	2.90	2.80	1.80	11.00	0.50

2.1.1.1 Glass fibers

Glass fibers are considered as the most commonly used fibers in the civil infrastructure applications due to the fact that it has low cost, high tensile strength, as well as comprising of certain glass' natural properties such as corrosion resistance and chemical inertness. There are a variety of glass-fiber common forms which are used as the reinforcement of the matrix material, and they are illustrated in the Figure 2.1. Furthermore, a number of different glass-fiber types are available in the FRP industry; however, the two main types are E-glass and S-glass. Among all the commercial reinforcing fibers, E-glass provides the lowest cost together with its superior durability performance. This is the reason that E-glass is the most widely used in relevant practical FRP application especially in infrastructure sector. However, some disadvantages of glass-fibers can be addressed such as relatively low young's modulus of elasticity and fatigue resistance, low abrasive resistance (which usually diminishing fiber's tensile strength), low long-term strength due to stress rupture, high density (comparing to other fiber-types) and high hardness.
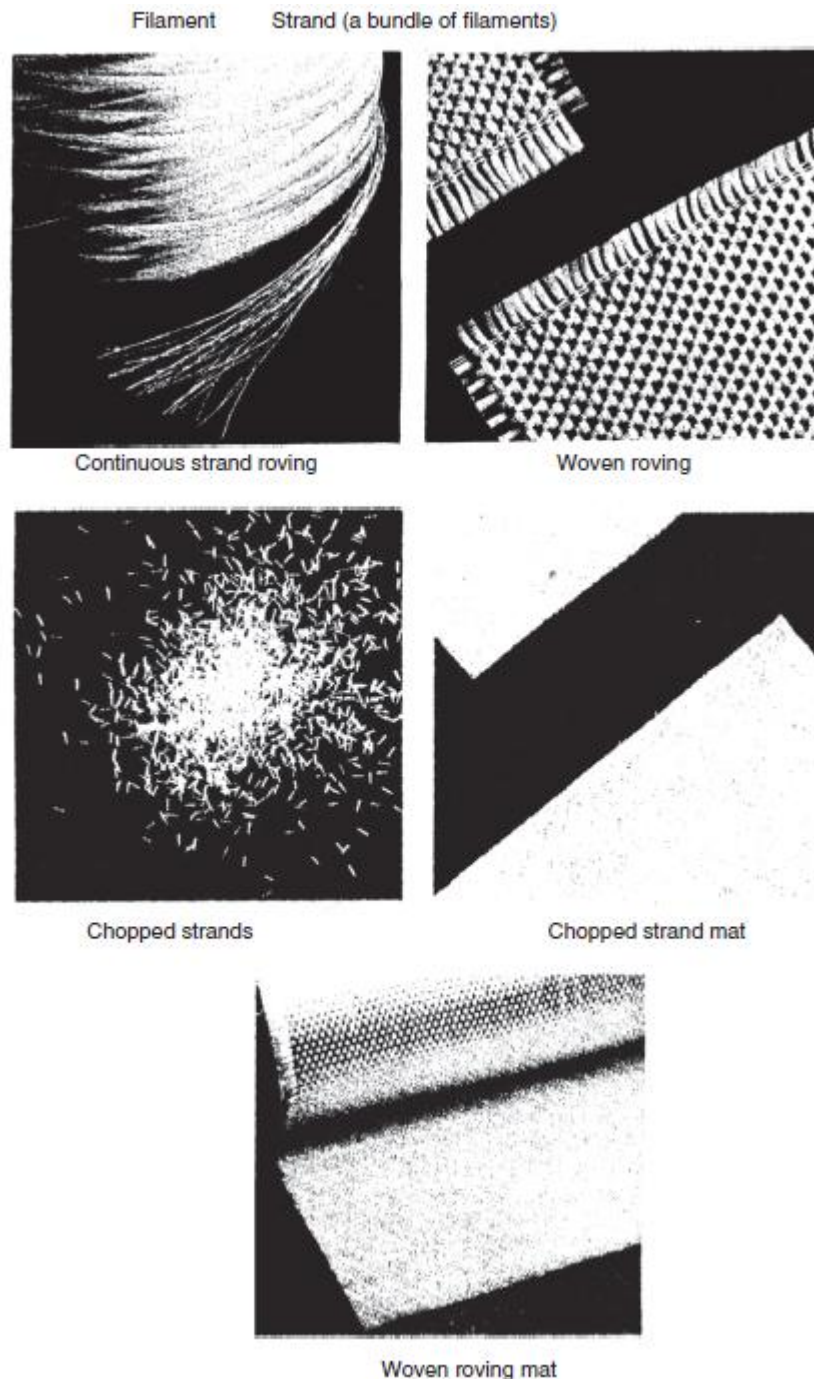
Figure 2.1 – Common forms of glass fiber (Courtesy of Owens Fiberglass Corporation)

2.1.1.2 Aramid fibers

Having the lowest density along with high strength-weight ratio and exceptional heat resistance among other reinforcing bars, aramid fibers, *see* Figure 2.2, also known as highly crystalline aromatic polyamide fibers, are very appealing to some areas which require high performance characteristics such as marine and aerospace applications. Moreover, aramid fibers are also used in civil infrastructure applications. The most common type of aramid fibers is known as Kevlar, the most commercially recognized brand. Kevlar is also well known by its interesting applications such as bullet-resistant vests, soft lightweight body armors and helmets used by the police officers and military personnel for more than 25 years. The principal disadvantages of

the aramid fibers are considered to be having low compressive strength and difficulty in cutting and machining. Moreover, other drawbacks are the reduced long-term strength (stress rupture), susceptibility to creep, sensitivity to UV radiation, moisture absorption, temperature-dependent mechanical properties, and relatively high cost [8], [9].
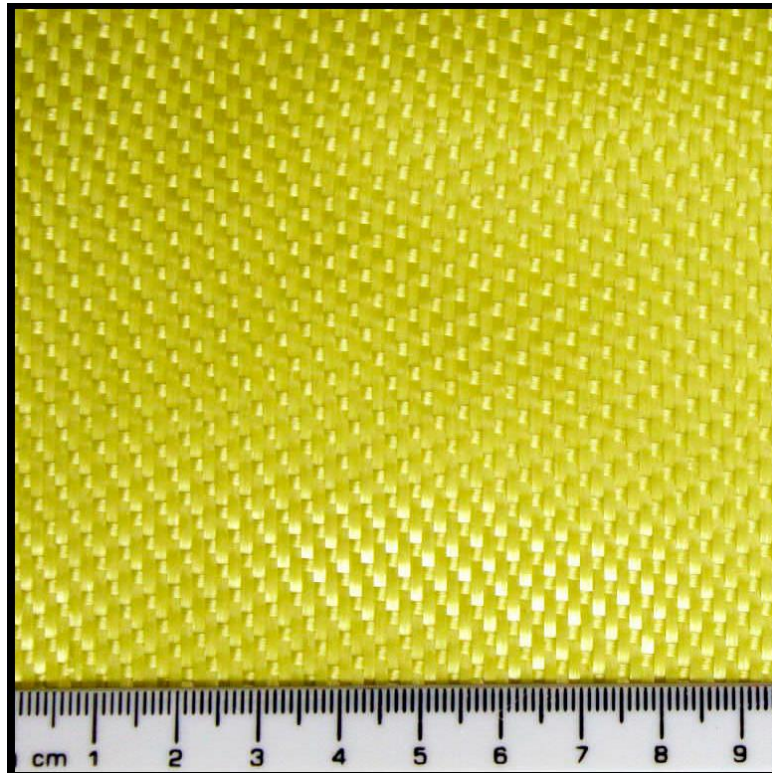
Figure 2.2 – Aramid fiber fabric [10]

2.1.1.3 Carbon fibers

Carbon fibers, *see* Figure 2.3, are usually chosen only within limited civil infrastructure applications due to its high cost among others. Despite high cost, CFRP composites are found in some critical infrastructure applications which are specifically involved in strengthening, retrofitting, and seismic rehabilitation of the existing structures. This is due to the fact that carbon fibers are a type of high performance fiber possessing exceptionally high tensile strength-weight ratios as well as tensile modulus-weight ratios, high specific stiffness and also high fatigue strength. Moreover, carbon fibers are found to be having higher service life than aramid and glass fibers. Commercially, carbon fibers are categorized in three basic forms, known as, long and continuous tow, chopped (6-50 mm long), and milled (30-3000 µm long) [8]. Additionally, their disadvantages are relatively high cost, high electrical conductivity, and low impact resistance.
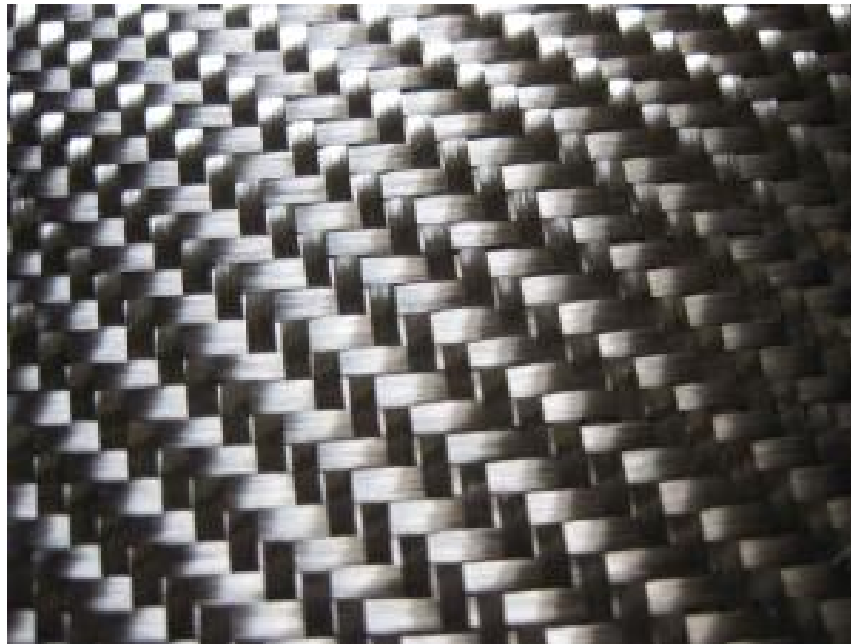
Figure 2.3 – Carbon fiber fabric [11]

2.1.2 Matrix

Matrix, one of the main constituents in composite materials, is serving as a binder to keep the reinforcement together and also to transfer the loads to the reinforcement. Moreover, it behaves as protection barriers for the reinforcement against possible damages such as damage due to handling or from adverse environment, etc. Matrix material has significant influence over many mechanical properties of the composite materials such as transvers modulus and strength, shear and compressive strength. Conventionally, there are three types of matrix available for different applications; they are polymers, metals and ceramics. However, polymers are the most commonly used one for fiber composites because of their low cost, low density, ease of processability, and good chemical resistance.

Polymers basically can be categorized into thermosets and thermoplastics. The most important thermosets in use are epoxy, polyester/vinylester, phenolics, bismaleimide (BMI), and polymides. And, commonly used thermoplastics are polyethylene, polystyrene, polypropylene, polyetheretherketone (PEEK), polyetherimide (PEI), polyethersulfone (PES), polyphenylene sulfide, and polyamide-imide (PAI).

Thermosets

- Undergoes permanent reactions when subjected to high temperature
- Is not recyclable
- Exhibits brittle behavior
- Is widely applied in civil infrastructure application

Thermoplastics

- Undergoes temporary physical change only when subjected to high temperature

- Is recyclable
- Exhibits more ductile behavior
- Is not preferred in civil infrastructure application

Below is a list of polymers that are commonly used in civil and infrastructure applications today [12]:

- Orthophthalic polyester
- Isophthalic polyester
- Vinylesters
- Epoxies

Table 2.2 – The mechanical properties of different polymers with and without glass fiber reinforcement

Polymers type		Compressive strength [MPa]	Tensile strength [MPa]	Tensile modulus [MPa]	Heat deflection temperature [°C*]
Orthophtalic polyester	Without reinforcement	NA	49.6-58.6	3.1-4.55	79.4
	With reinforcement	NA	151.7	11.7	
Isophtalic polyester	Without reinforcement	117.2	50-75	3.1-4.6	90.6
	With reinforcement	206.8	158.6	11.7	
Vinylester	Without reinforcement	NA	75.8-87.5	3.17-3.93	100
	With reinforcement	206.8	158.6	11	
Epoxy	Without reinforcement	NA	60-85	2.6-3.8	49-104
	With reinforcement	241.3	206.8	12.4	

*Heat deflection temperature is the temperature when polymers start to soften and lose the strength

2.2 Manufacturing process

There are many manufacturing processes which could be categorized into 3 groups:

- Manual processes: hand lay-up and bag molding process.

- Semi-automated processes: resin infusion under flexible tooling and compression molding.
- Automated processes: pultrusion, resin transfer molding.

2.2.1 Hand lay up

The hand layup technique is one of the first techniques used to produce fiber reinforced composites, still commonly used these days. Labor intensive and slow production time are some of the reasons why manufacturers have chosen more efficient methods. There may be small variations in the manufacturing process but the main idea is to lay sheets of fiber reinforcement over the mold, these could be chopped fibers, woven fibers, or stitched fibers. Subsequently, liquid resin is poured by hand, this process could be repeated until the desired fiber and resin volumes are reached. Finally, to make sure the resin fully saturates all the layers and to remove the air voids, squeegees and/or metal hand rollers are applied over the final composite.

This process can easily be transformed into a semi-automated process by applying the resin and chopped fibers with a spray gun. It reduces the process time but the quality is not as good due to the lack of control.
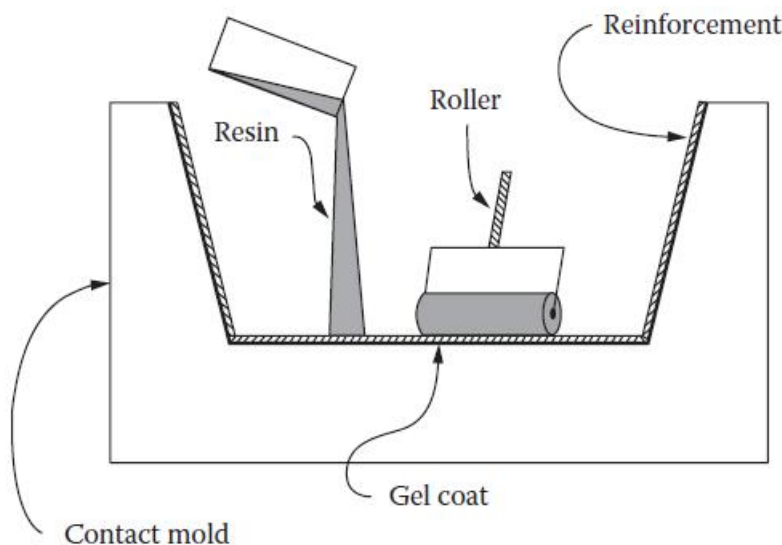
Figure 2.4 – Schematic of the hand lay-up manufacturing process [13]

2.2.2 Vacuum bag molding process

If big volume production is not a concern then the bag molding process is an interesting approach, the aerospace industry has chosen this type of process for this reason. This procedure begins with a so called "prepreg", a mixture of partially cured epoxy resin and fibers, with a percentage between 50%-60% of fiber material. After the prepreg plies are ready they can be arranged in the desired way into the mold, a certain sequence and orientation. When all the layers are arranged over the mold a porous release cloth is placed on top and a few layers of bleeder to absorb the resin excess. To complete the whole layout the following materials are needed such as a

Teflon-coated glass fabric separator, a caul plate, and a thin heat-resistant vacuum bag. All these have to be sealed all around and then it is placed inside an autoclave. The autoclave is a pressure chamber that applies heat and pressure at the same time to consolidate and densify separate plies into a solid laminate. The vacuum will remove air and volatiles.
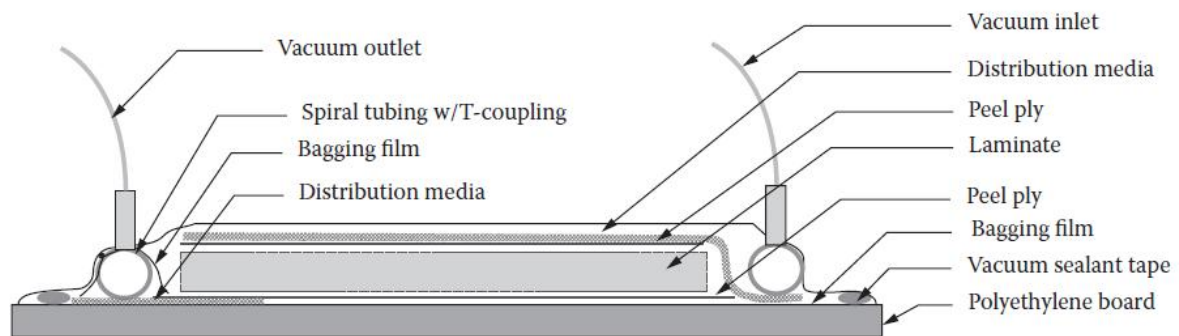
Figure 2.5 – Cross-section of the bag molding process [13]
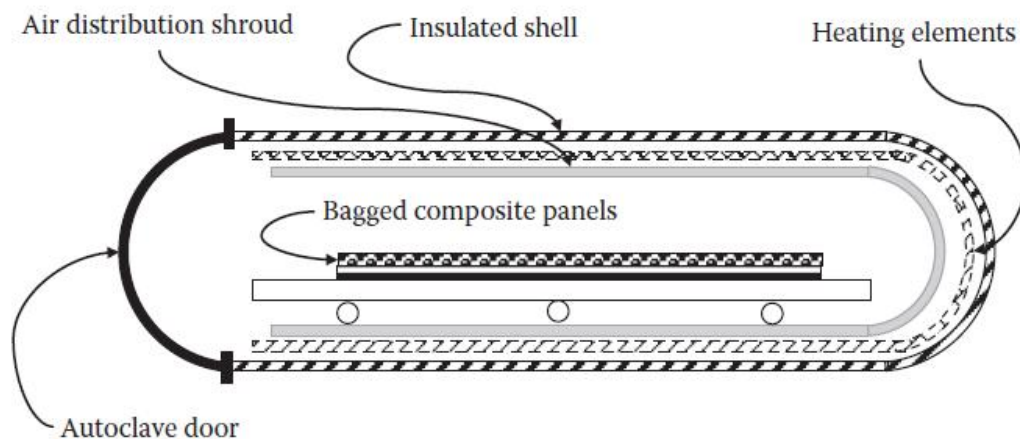
Figure 2.6 – Configuration and elements of autoclave [13]

2.2.3 Resin infusion under flexible tooling (RIFT)

Resin infusion under flexible tooling (RIFT) is a process very similar to the compression mold technique, described later, with a small variation in which one of the mold faces is replaced by a polymer film or a thin composite mold tool. The purpose of having a different mold face is to reduce tooling costs and styrene emissions, providing a healthier work environment. The process starts by placing dry fiber reinforcement inside the mold followed by infusing resin under vacuum conditions to supply enough resin saturation with the fibers. The choice of the flexible tool is done according to the required shape and the conditions for each particular case. Retrofitting is a common use of the RIFT technique; the fiber reinforcement is placed in the preform and transported to the site to be later attached to the structure. After the fiber reinforcement is in place, resin is injected and a vacuum bag is used to consolidate the composite and the bond. There are many patented variations of the

RIFT process, and two remarkable processes among them are Seemann Composites Resin Infusion Manufactoring Process (SCRIMP) and Vacuum Assisted Resin Transfer Molding (VARTM) [13].

In such a way that the wavy shape of Kaponjärbron is very challenging, a proper manufacturing process is highly required in the production stage. The authors believe that RIFT is the most appropriate manufacturing process that can satisfy the geometrical requirements of the bridge since any complex moulds can be formed using this process.
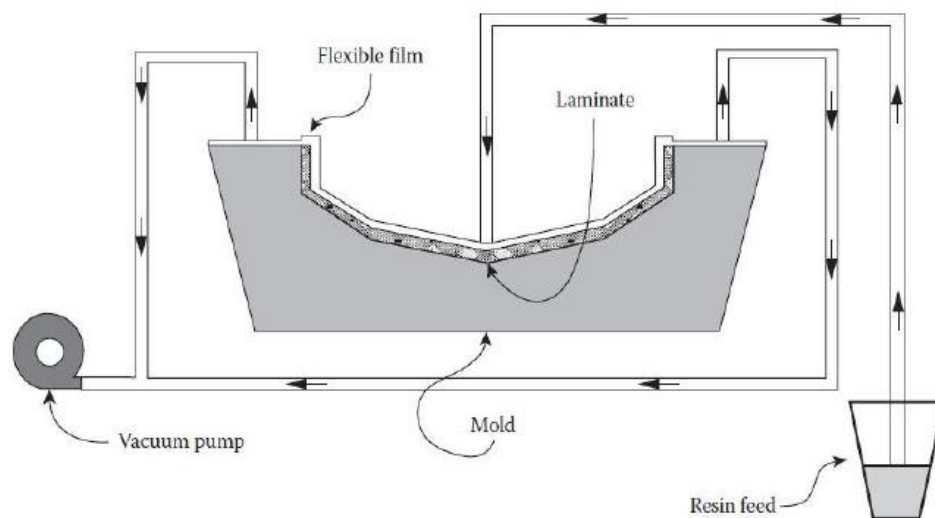
Figure 2.7 – Schematic of SCRIMP manufacturing process [13]

2.2.4 Compression molding

Within the fully automated processes, compression molding could be considered as one of them, even though most manufacturers choose to do part of the process manually to avoid costly automation tools. The first step in this process is the preparation of the preform compound which can be bulk molding compound (BMC) or sheet-molding compound (SMC). The purpose of these preforms is to have previously put together a proper combination of resin and fibers to be molded uniformly without voids. Immediately after, the preform is placed in between the molds and a top force closes the molds and keeps them in place. Heat and pressure is applied to ensure the curing takes place until it is fully cured and the final shape is obtained. The biggest advantage of this process is the possibility to create complex and high strength shapes in a moderate high volume rate.
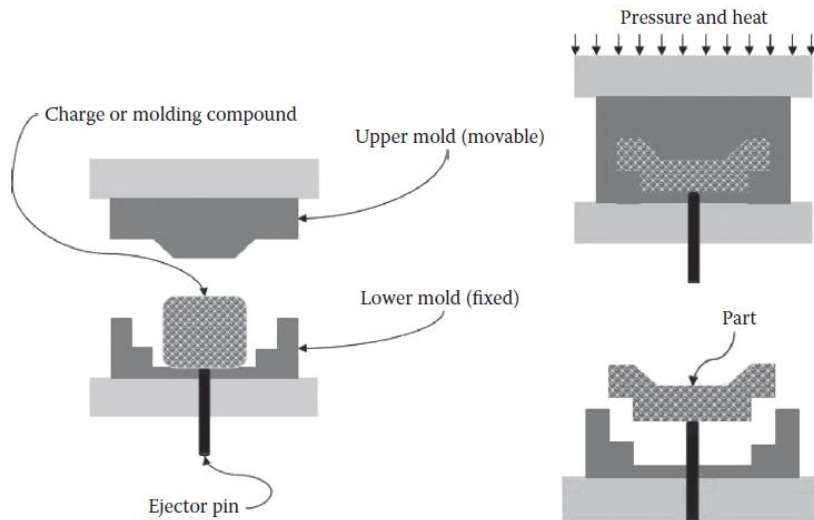
Figure 2.8 – Compression molding manufacturing process [13]

2.2.5 Pultrusion

Pultrusion is one of the manufacturing processes in FRP composite materials production categorized in the fully-automated method. It is basically a continuous process for manufacturing various structural shapes of FRP profiles having constant cross-sections. Moreover, up to the current technology in relevant industry, pultrusion process is ensured to provide high reliability in the professional level in term of consistent quality. The pultrusion process can be described with the initiation of a continual pulling of fibers/rovings (reinforcement materials) passing through a resin impregnation tank (resin bath) leading the fibers completely impregnated by matrix material. Then, the combined mixture with the addition of surfacing material is pulled out toward preform die. The material is shaped according to the desired geometry and cured in a heated die. Finally, the cut-off saw is used to cut the final constant cross-sections into the predetermined lengths. The various stages of pultrusion process are illustrated in Figure 2.9.
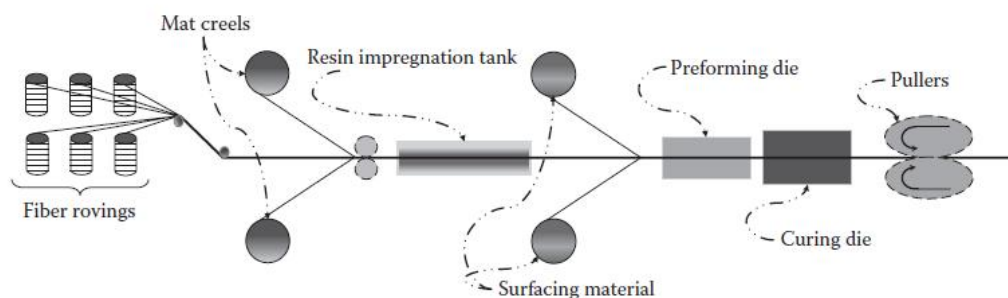
Figure 2.9 – Component and stages of the pultrution manufacturing process [13]

2.2.6   Resin transfer molding

The resin transfer molding (RTM) process is one of the fully automated processes which produces parts with high mechanical properties and smooth surface finish. Dry fiber material is placed between the upper and lower solid molds and thermosetting resin is pumped into the mold, usually through an opening located in the lowest part of the whole cavity (mold). The resin fills the mold soaking the fiber and a vacuum is applied to remove air voids. The fiber reinforcement can be performed which is an advantage when dealing with complex shapes and the trimming operation is avoided. After the resin has filled up the mold evenly it can be cured at room temperature or in an oven depending on the materials used.

The preform of the fiber reinforcement can be arranged in many ways, levels and orientations with many techniques depending on the requirements. The mold needs to be well designed to let the resin fill it uniformly, to have a constant distribution along the whole section.
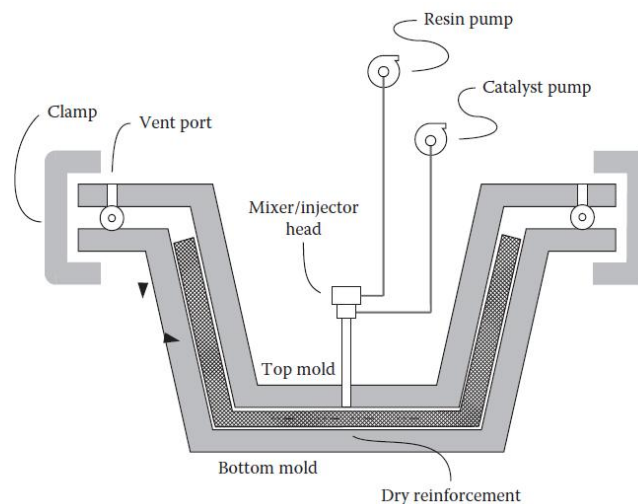
Figure 2.10 – Component and representatives configuration in the RTM process [13]

2.3   Prediction of equivalent elastic properties

Since composites are formed by different materials (matrix and fiber reinforcement), their structural behavior and properties are by nature more complicated than that of homogenous materials. They do not have plastic deformation and behave elastically till the end of failure point. Composites are considered as orthotropic materials implying that their properties differ in different directions. So how are elastic properties of composite materials computed?

 In composite materials, a single lamina, also known as ply, is a combination between matrix and fiber constituent materials. Several laminae bonded together in the thickness direction with specified stack-up sequence and various fiber's orientation angle form a complete body of laminate structure, *see* Figure 2.11. Moreover, the loading directions have strong influence on the overall behavior of the laminate structure due to the fact that each layer of the laminate will behave differently and have its own stiffness. Therefore, in order to integrate all the

respective directional properties from each lamina, a concept of formulating "equivalent" elastic properties of the composite materials has been introduced. This concept considers the entire laminate structure as an "equivalent" single layer which have elastic properties that are "equivalent" to the multi-layered structure.

Before making such calculation, some basic fundamental principles such as lamination theory should be reviewed. Since our purpose is to determine the laminate stiffness and equivalent elastic properties, reviews on some parts of lamination theory like lamina and laminate constitutive relations will be briefly described. Furthermore, in laminate structures, two coordinate systems are used, and they are known as lamina (local) coordinate and laminate (global) coordinate. Lamina axes are represented by numbers 1, 2, and 3, and laminate axes are represented by x, y, and z, *see* Figure 2.12. These coordinates are very important when the local stresses and strains from each lamina are needed to transform into global stresses.
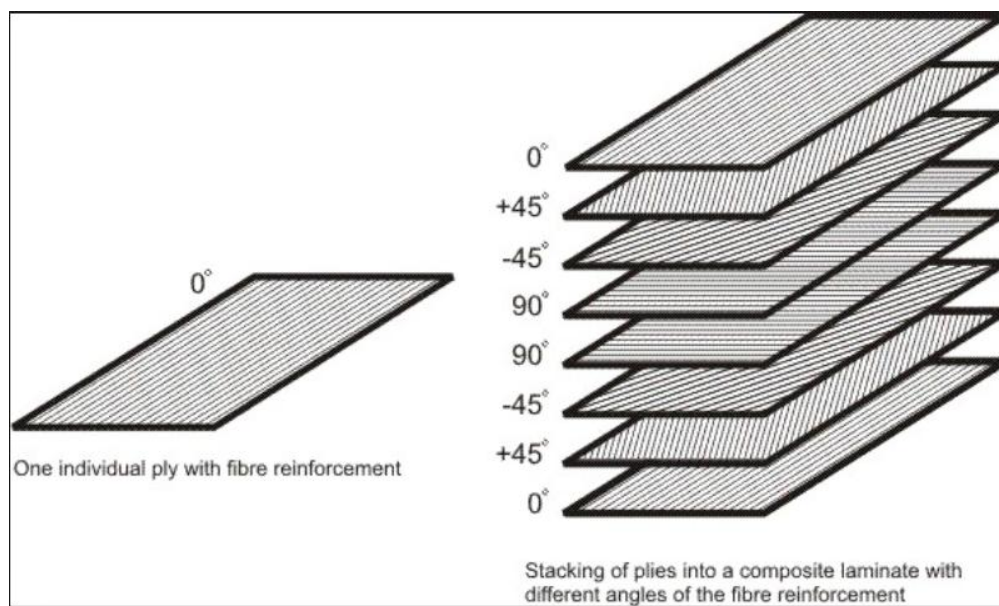
Figure 2.11 – Stacking up sequence of a composite laminate [14]
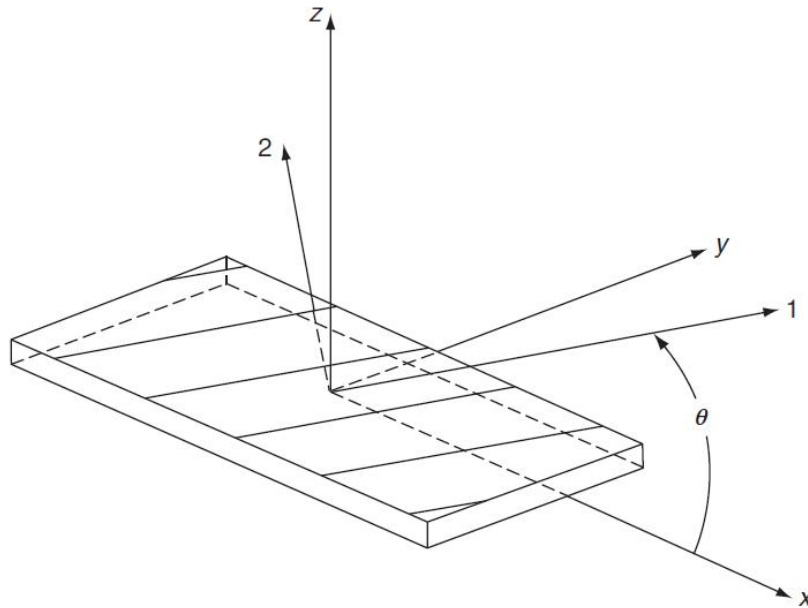
Figure 2.12 – Definition of principal material axes and loading axes for a lamina [8]

2.3.1 Notations

One should be aware of the typical notations of modulus of elasticity, Poisson's ratio, and shear modulus in lamina properties. Conventionally, they are denoted by two subscripts. The first subscript indicates the direction of loading, and the second subscript indicates the direction in which specific property is determined. For instance, Poisson's ratio v_{ij} is the ratio between strain in j-direction and the applied strain in i-direction $\left(v_{ij} = -\frac{\varepsilon_j}{\varepsilon_i}\right)$.

This also applies to the notations of stresses and strains. Likewise, they are denoted by two subscripts. The first subscript indicates the direction of the outward normal to the plane in which the stress component acts. The second subscript indicates the stress component's direction. For instance, for shear stress component τ_{zy}, the subscript z indicates the direction of the outward normal to the yx plane and the subscript y indications its direction. The stress components σ_{xx}, σ_{yy}, and τ_{xy} are called in-plane (intralaminar) stresses, whereas σ_{zz}, τ_{xz}, and τ_{yz} are called interlaminar stresses.
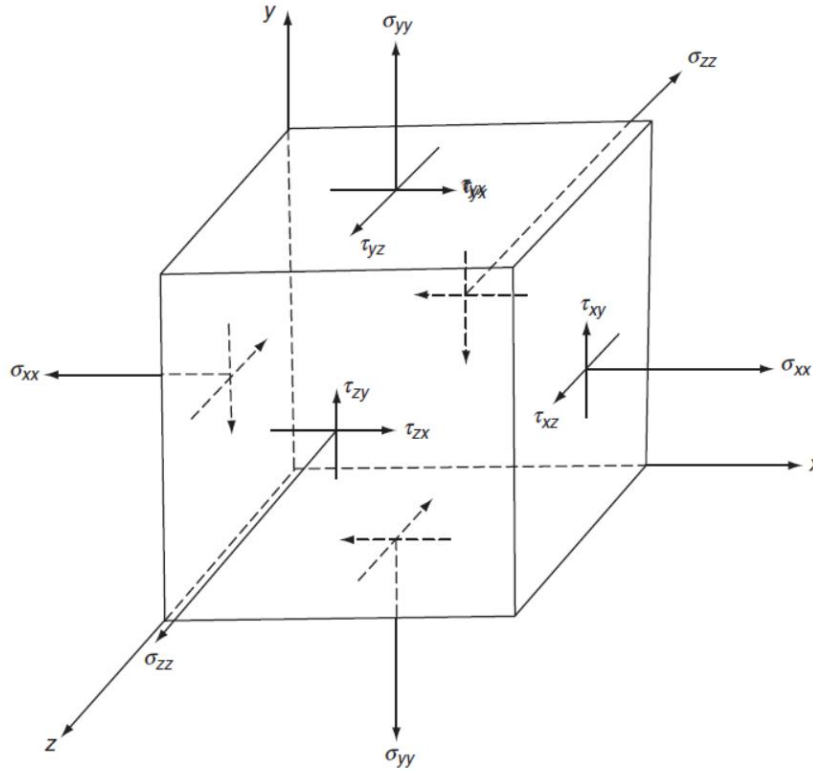
Figure 2.13 – Normal stress and shear stress component [8]

2.3.2 Lamina constitutive relations

Generally, the constitutive relations for an orthotropic material in 3 dimensions can be expressed as $\{\sigma\} = [Q]\{\varepsilon\}$. The constitutive matrix $[Q]$ is a 6-by-6 matrix, as shown in *Eq. (2-1)*.

The constitutive relation for an orthotropic material in 3 dimensions is written as:

$$
\begin{bmatrix} \sigma_{11} \\ \sigma_{22} \\ \sigma_{33} \\ \tau_{23} \\ \tau_{13} \\ \tau_{12} \end{bmatrix} = \begin{bmatrix} Q_{11} & Q_{12} & Q_{13} & Q_{14} & Q_{15} & Q_{16} \\ Q_{12} & Q_{22} & Q_{23} & Q_{24} & Q_{25} & Q_{26} \\ Q_{13} & Q_{23} & Q_{33} & Q_{34} & Q_{35} & Q_{36} \\ Q_{14} & Q_{24} & Q_{34} & Q_{44} & Q_{45} & Q_{46} \\ Q_{15} & Q_{25} & Q_{35} & Q_{45} & Q_{55} & Q_{56} \\ Q_{16} & Q_{26} & Q_{36} & Q_{46} & Q_{56} & Q_{66} \end{bmatrix} \begin{bmatrix} \varepsilon_{11} \\ \varepsilon_{22} \\ \varepsilon_{33} \\ \gamma_{23} \\ \gamma_{13} \\ \gamma_{12} \end{bmatrix}
\qquad (2\text{-}1)
$$

2.3.2.1 For specially orthotropic lamina ($\theta = 0°\ or\ 90°$)

Since each lamina is rather thin, thin plate theory is applicable. The assumption of plane stress state is valid; it means there are no stresses in the thickness direction. Then, the constitutive matrix $[Q]$ can be reduced to a 3-by-3 matrix as shown in *Eq. (2-2)*.

For plane stress state, the constitutive relations can be rewritten as follow:

$$\begin{Bmatrix} \sigma_{11} \\ \sigma_{22} \\ \tau_{12} \end{Bmatrix} = \begin{bmatrix} Q_{11} & Q_{12} & \mathbf{0} \\ Q_{12} & Q_{22} & \mathbf{0} \\ \mathbf{0} & \mathbf{0} & Q_{66} \end{bmatrix} \begin{Bmatrix} \varepsilon_{11} \\ \varepsilon_{22} \\ \gamma_{12} \end{Bmatrix}$$

(2-2)

Where:

$\llbracket Q \rrbracket$ is the constitutive matrix for specially orthotropic lamina

$$Q_{11} = \frac{E_{11}}{1 - \nu_{12}\nu_{21}}$$

$$Q_{12} = \frac{\nu_{21}E_{11}}{1 - \nu_{12}\nu_{21}}$$

$$Q_{22} = \frac{E_{22}}{1 - \nu_{12}\nu_{21}}$$

$$Q_{66} = G_{12}$$

E_{11} is the longitudinal modulus of elasticity

E_{22} is the transverse modulus of elasticity

ν_{12} is the major Poisson's ratio or Poisson's ratio of the plane 12

ν_{21} is the minor Poisson's ratio or Poisson's ratio of the plane 21

G_{12} is the in-plane shear modulus

$$\nu_{21} = \nu_{12}\frac{E_{22}}{E_{11}}$$

$$G_{23} = \frac{E_{22}}{2(1+\nu_{23})}$$

$$\nu_{23} = \frac{\nu_{12}(1-\nu_{21})}{(1-\nu_{12})}$$

Note: see Figure 2.16 for the picking the values of $E_{11}, E_{22}, \nu_{12}, G_{12}$ above.

2.3.2.2 For general orthotropic lamina ($\theta \neq 0° \ or \ 90°$)

The constitutive relation for general orthotropic lamina is written as:

$$\begin{Bmatrix} \sigma_{xx} \\ \sigma_{yy} \\ \tau_{xy} \end{Bmatrix} = \begin{bmatrix} \bar{Q}_{11} & \bar{Q}_{12} & \bar{Q}_{16} \\ \bar{Q}_{12} & \bar{Q}_{22} & \bar{Q}_{26} \\ \bar{Q}_{16} & \bar{Q}_{26} & \bar{Q}_{66} \end{bmatrix} \begin{Bmatrix} \varepsilon_{xx} \\ \varepsilon_{yy} \\ \gamma_{xy} \end{Bmatrix}$$

(2-2)

Where:

$\llbracket \bar{Q} \rrbracket$ is the constitutive matrix for general orthotropic lamina

$$\bar{Q}_{11} = Q_{11}\cos^4\theta + 2(Q_{12} + 2Q_{66})\sin^2\theta\cos^2\theta + Q_{22}\sin^4\theta$$

$$\bar{Q}_{12} = Q_{12}(\sin^4\theta + \cos^4\theta) + (Q_{11} + Q_{22} - 4Q_{66})\sin^2\theta\cos^2\theta$$

$$\bar{Q}_{22} = Q_{11}\sin^4\theta + 2(Q_{12}+2Q_{66})\sin^2\theta\cos^2\theta + Q_{22}\cos^4\theta$$

$$\bar{Q}_{16} = (Q_{11} - Q_{12} - 2Q_{66})\sin\theta\cos^3\theta + (Q_{12-}Q_{22} + 2Q_{66})\sin^3\theta\cos\theta$$

$$\bar{Q}_{26} = (Q_{11} - Q_{12} - 2Q_{66})\sin^3\theta\cos\theta + (Q_{12-}Q_{22} + 2Q_{66})\sin\theta\cos^3\theta$$

$$\bar{Q}_{66} = (Q_{11} + Q_{22} - 2Q_{12} - 2Q_{66})\sin^2\theta\cos^2\theta + Q_{66}(\sin^4\theta + \cos^4\theta)$$

Or by using trigonometric identities, the matrix $[\bar{Q}]$ can be simplified as

$$\bar{Q}_{11} = U_1 + U_2\cos 2\theta + U_3\cos 4\theta$$

$$\bar{Q}_{12} = \bar{Q}_{21} = U_4 - U_3\cos 4\theta$$

$$\bar{Q}_{22} = U_1 - U_2\cos 2\theta + U_3\cos 4\theta$$

$$\bar{Q}_{16} = \frac{1}{2}U_2\sin 2\theta + U_3\sin 4\theta$$

$$\bar{Q}_{26} = \frac{1}{2}U_2\sin 2\theta - U_3\sin 4\theta$$

$$\bar{Q}_{16} = U_5 - U_3\cos 4\theta$$

$$U_1 = \frac{1}{8}(3Q_{11} + 3Q_{22} + 2Q_{12} + 4Q_{66})$$

$$U_2 = \frac{1}{2}(Q_{11} - Q_{22})$$

$$U_3 = \frac{1}{8}(Q_{11} + Q_{22} - 2Q_{12} - 4Q_{66})$$

$$U_4 = \frac{1}{8}(Q_{11} + Q_{22} + 6Q_{12} - 4Q_{66})$$

$$U_5 = \frac{1}{2}(U_1 - U_4)$$

2.3.3   Laminate (general) constitutive relations

The constitutive relations of the laminate structures are derived by combining equilibrium, kinematics (strain-displacement relations) and stress-strain relations from *Eq. (2-2)* [13], and finally the constitutive equations known as force-strain curvature relationships are able to be expressed as below:

$$\begin{bmatrix}N\\M\end{bmatrix} = \begin{bmatrix}A & B\\B & D\end{bmatrix}\begin{bmatrix}\varepsilon^\circ\\\kappa\end{bmatrix} \qquad (2\text{-}3)$$

Or it can be rewritten in the form below:

$$\begin{bmatrix} N_{xx} \\ N_{yy} \\ N_{xy} \\ \hline M_{xx} \\ M_{yy} \\ M_{xy} \end{bmatrix} = \begin{bmatrix} A_{11} & A_{12} & A_{16} \\ A_{21} & A_{22} & A_{26} \\ A_{61} & A_{62} & A_{66} \\ B_{11} & B_{12} & B_{16} \\ B_{21} & B_{22} & B_{26} \\ B_{61} & B_{62} & B_{66} \end{bmatrix} \begin{bmatrix} \varepsilon_{xx}^{\circ} \\ \varepsilon_{yy}^{\circ} \\ \gamma_{xy}^{\circ} \end{bmatrix} + \begin{bmatrix} B_{11} & B_{12} & B_{16} \\ B_{21} & B_{22} & B_{26} \\ B_{61} & B_{62} & B_{66} \\ D_{11} & D_{12} & D_{16} \\ D_{21} & D_{22} & D_{26} \\ D_{61} & D_{62} & D_{66} \end{bmatrix} \begin{bmatrix} \kappa_{xx} \\ \kappa_{yy} \\ \kappa_{xy} \end{bmatrix}$$

Where

N_{xx} is the normal force resultant in the x direction (per unit width)

N_{yy} is the normal force resultant in the y direction (per unit width)

N_{xy} is the shear force resultant (per unit width)

N_{xx} is the normal force resultant in the x direction (per unit width)

M_{xx} is the bending moment resultant in the yz plane (per unit width)

M_{yy} is the bending moment resultant in the xz plane (per unit width)

M_{xy} is the twisting moment (torsion) resultant (per unit width)

ε_{xx}° and ε_{yy}° are the midplane normal strains in the laminate

γ_{xy}° is the midplane shear strains in the laminate

$\kappa_{x}x$ and κ_{yy} are the bending curvatures in the laminate

κ_{xy} is the twisting curvature in the laminate

$[A], [B],$ **and** $[D]$ are called the elements in stiffness matrices

$[A]$ is called extentional stiffness matrix for the laminate [N/m]

$[B]$ is called coupling stiffness matrix for the laminate   [N]

$[D]$ is called beding stiffness matrix for the laminate   [Nm]

$$[A] = A_{ij} = \sum_{k=1}^{n} (Q_{ij})_k (h_k - h_{k-1})$$

$$[B] = B_{ij} = \frac{1}{2} \sum_{k=1}^{n} (Q_{ij})_k (h_k^2 - h_{k-1}^2)$$

$$[D] = D_{ij} = \frac{1}{3} \sum_{k=1}^{n} (Q_{ij})_k (h_k^3 - h_{k-1}^3)$$
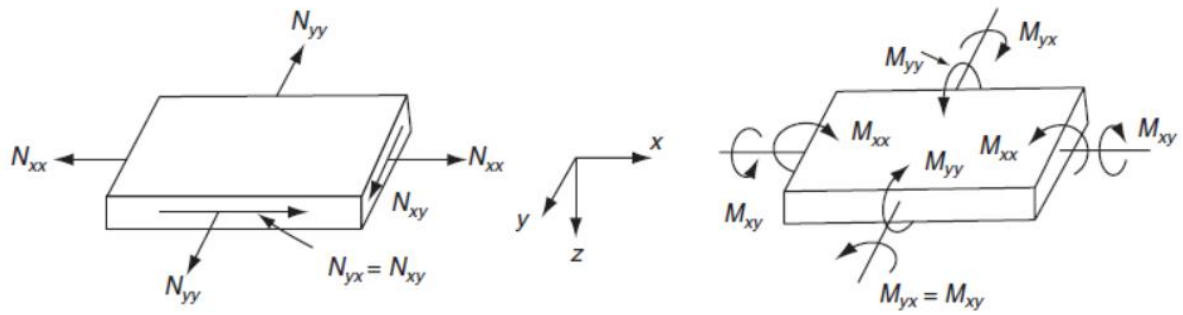
Figure 2.16 – In-plane, bending, and twisting loads applied on a laminate. [8]

2.3.3.1 Calculation of equivalent elastic properties

There is a step-by-step instruction of how to calculate the laminate stiffness and its equivalent elastic properties from *EUROCOMP Design Code and Handbook* [5], *see* Figure 2.17. The key factors to predict the equivalent elastic properties are the selection of constituent materials, fiber's orientation angle, lamina stack-up sequence, and laminate thickness.

Obtain lamina properties like
$E_{11}, E_{22}, G_{12}, v_{12}, h \ (ply \ thickness), \theta \ (fiber \ orientation \ angle)$

Step 1: Determine lamina reduced values Q_{ij}

Step 2: Determine lamina transformed reduced stiffness $\bar{Q}_{ij}$

Step 3: Determine coordinates h_k for lamina from bottom surface

Step 4: For a given angle of orientation per lamina, caculate $A_{ij} \ B_{ij} \ D_{ij}$ matrices

Step 5: Invert the laminate stiffness matrix and calculate $a_{ij} \ b_{ij} \ d_{ij}$

Step 6: Calculate equivalent laminate elastic properties $E_x, E_y, G_{xy}, v_{xy}, v_{yx}$

Figure 2.17 – Flowchart for calculation of laminate stiffness and equivalent elastic properties

[5]

CHALMERS, *Civil and Environmental Engineering*, *Master's Thesis 2015:141*

❖ **Step 1: Determine lamina reduced stiffness values $[Q_{ij}]$**

The lamina elastic properties like $E_{11}, E_{22}, G_{12}, \nu_{12}, \nu_{21}$ can be either pre-calculated or obtained from Figure 2.16 below. Then the lamina reduced stiffness values $[Q_{ij}]$ can be calculated.

$$Q_{11} = \frac{E_{11}}{1 - \nu_{12}\nu_{21}}$$

$$Q_{12} = \frac{\nu_{21}E_{11}}{1 - \nu_{12}\nu_{21}}$$

$$Q_{22} = \frac{E_{22}}{1 - \nu_{12}\nu_{21}}$$

$$Q_{66} = G_{12}$$

$$[Q] = \begin{bmatrix} Q_{11} & Q_{12} & 0 \\ Q_{12} & Q_{22} & 0 \\ 0 & 0 & Q_{66} \end{bmatrix}$$

A.5 TYPICAL MECHANICAL PROPERTIES OF UNIDIRECTIONAL CONTINUOUS FIBER COMPOSITES

Property	Boron—Epoxy	AS Carbon—Epoxy	T-300—Epoxy	HMS Carbon—Epoxy	GY-70—Epoxy	Kevlar 49—Epoxy	E-Glass—Epoxy	S-Glass—Epoxy
Density, g/cm³	1.99	1.54	1.55	1.63	1.69	1.38	1.80	1.82
Tensile properties								
Strength, MPa (ksi), 0°	1585 (230)	1447.5 (210)	1447.5 (210)	827 (120)	586 (85)	1379 (200)	1103 (160)	1214 (176)
90°	62.7 (9.1)	62.0 (9)	44.8 (6.5)	86.2 (12.5)	41.3 (6.0)	28.3 (4.1)	96.5 (14)	—
Modulus GPa (Msi) 0°	207 (30)	127.5 (18.5)	138 (20)	207 (30)	276 (40)	76 (11)	39 (5.7)	43 (6.3)
90°	19 (2.7)	9 (1.3)	10 (1.5)	13.8 (2.0)	8.3 (1.2)	5.5 (0.8)	4.8 (0.7)	—
Major Poisson's ratio	0.21	0.25	0.21	0.20	0.25	0.34	0.30	—
Compressive properties								
Strength, MPa (ksi), 0°	2481.5 (360)	1172 (170)	1447.5 (210)	620 (90)	517 (75)	276 (40)	620 (90)	758 (110)
Modulus, GPa (Msi), 0°	221 (32)	110 (16)	138 (20)	171 (25)	262 (38)	76 (11)	32 (4.6)	41 (6)
Flexural properties								
Strength, MPa (ksi), 0°	—	1551 (225)	1792 (260)	1034 (150)	930 (135)	621 (90)	1137 (165)	1172 (170)
Modulus, GPa (Msi), 0°	—	117 (17)	138 (20)	193 (28)	262 (38)	76 (11)	36.5 (5.3)	41.4 (6)
In-plane shear properties								
Strength, MPa (ksi)	131 (19)	60 (8.7)	62 (9)	72 (10.4)	96.5 (14)	60 (8.7)	83 (12)	83 (12)
Modulus, GPa (Msi)	6.4 (0.93)	5.7 (0.83)	6.5 (0.95)	5.9 (0.85)	4.1 (0.60)	2.1 (0.30)	4.8 (0.70)	—
Interlaminar shear strength, MPa (ksi) 0°	110 (16)	96.5 (14)	96.5 (14)	72 (10.5)	52 (7.5)	48 (7)	69 (10)	72 (10.5)

Source: From Chamis, C.C., *Hybrid and Metal Matrix Composites*, American Institute of Aeronautics and Astronautics, New York, 1977. With permission.

Figure 2.16 – Mechanical properties of composite materials [8]

❖ **Step 2: Determine lamina transformed reduced stiffness $\left[\bar{Q}_{ij}\right]$**

In this step, any arbitrary fiber's orientation angle θ can be inserted here.

$$\bar{Q}_{11} = U_1 + U_2 \cos 2\theta + U_3 \cos 4\theta$$

$$\bar{Q}_{12} = \bar{Q}_{21} = U_4 - U_3 \cos 4\theta$$

$$\bar{Q}_{22} = U_1 - U_2 \cos 2\theta + U_3 \cos 4\theta$$

$$\bar{Q}_{16} = \frac{1}{2}U_2 \sin 2\theta + U_3 \sin 4\theta$$

$$\bar{Q}_{26} = \frac{1}{2}U_2 \sin 2\theta - U_3 \sin 4\theta$$

$$\bar{Q}_{16} = U_5 - U_3 \cos 4\theta$$

$$U_1 = \frac{1}{8}(3Q_{11} + 3Q_{22} + 2Q_{12} + 4Q_{66})$$

$$U_2 = \frac{1}{2}(Q_{11} - Q_{22})$$

$$U_3 = \frac{1}{8}(Q_{11} + Q_{22} - 2Q_{12} - 4Q_{66})$$

$$U_4 = \frac{1}{8}(Q_{11} + Q_{22} + 6Q_{12} - 4Q_{66})$$

$$U_5 = \frac{1}{2}(U_1 - U_4)$$

$$[\bar{Q}] = \begin{bmatrix} \bar{Q}_{11} & \bar{Q}_{12} & \bar{Q}_{16} \\ \bar{Q}_{12} & \bar{Q}_{22} & \bar{Q}_{26} \\ \bar{Q}_{16} & \bar{Q}_{26} & \bar{Q}_{66} \end{bmatrix}$$

❖ **Step 3: Determine coordinates for h_k each lamina from the bottom surface**

In this step, the laminate thickness can be designed here.

By definition, h_{k-1} is the distance from the midplane of the laminate to the top surface of the kth layer, and h_k is the distance from the midplane to the lower layer sureface of the kth layer, *see* Figure 2.19.
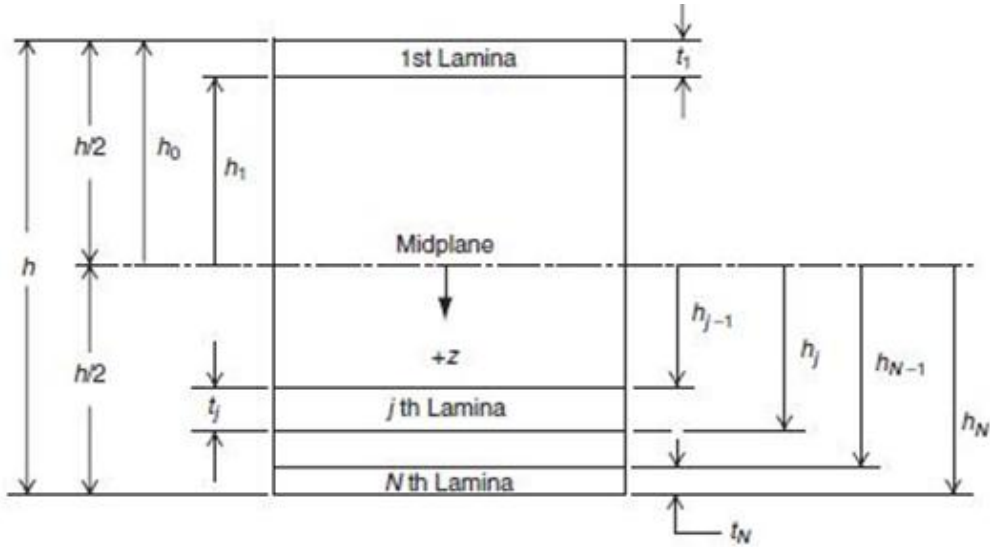
Figure 2.19 – Geometry of a laminate [8]

❖ **Step 4: Determine the laminate stiffness matrices $[A],[B],[D]$**

It is recommended to design laminate as balanced (symmetric) laminates to decrease residual stress, buckling loads, twisting, and warpage [15]. When balanced laminates are used, the coupling stiffness matrix $[B]$ will be always equal to zero.

$$[A] = A_{ij} = \sum_{k=1}^{n} (Q_{ij})_k (h_k - h_{k-1})$$

$$[B] = B_{ij} = \frac{1}{2} \sum_{k=1}^{n} (Q_{ij})_k (h_k^2 - h_{k-1}^2)$$

$$[D] = D_{ij} = \frac{1}{3} \sum_{k=1}^{n} (Q_{ij})_k (h_k^3 - h_{k-1}^3)$$

❖ **Step 5: Determine laminate compliances $[a],[b],[d]$**

By inverting the stiffness matrices $[A],[B],[D]$, the laminate compliances can be easily obtained.

$$[a] = [A]^{-1}$$
$$[b] = [B]^{-1}$$
$$[d] = [D]^{-1}$$

❖ **Step 6: Determine the equivalent laminate elastic properties**

There are two types of equivalent laminate elastic properties depending on laminate's loading condition.

The equivalent membrane elastic constants are

$$E_{xx}^N = \frac{1}{h * a_{11}}$$

$$E_{yy}^N = \frac{1}{h * a_{22}}$$

$$G_{xy}^N = \frac{1}{h * a_{66}}$$

$$\nu_{xy}^N = -\frac{a_{12}}{a_{11}}$$

$$\nu_{yx}^N = -\frac{a_{12}}{a_{22}}$$

The equivalent bending elastic constants are

$$E_{xx}^M = \frac{12}{h^3 * d_{11}}$$

$$E_{yy}^M = \frac{12}{h^3 * d_{22}}$$

$$G_{xy}^M = \frac{1}{h^3 * d_{66}}$$

$$\nu_{xy}^M = -\frac{d_{12}}{d_{11}}$$

$$\nu_{yx}^M = -\frac{d_{12}}{d_{22}}$$

Where

h is the total laminate thickness [m]

2.4 Dynamic analysis for the FRP pedestrian bridge

2.4.1 Design requirement

2.4.1.1 Deflection

As previously mentioned, there is a strong recommendation to consider the dynamic behavior of the pedestrian bridges at the preliminary design stage. However, since the human-induced-vibration of the pedestrian bridge is a serviceability problem, prior to performing dynamic analysis of the structure, the deflection requirement was chosen to be fulfilled first. According to *"Guide Specifications for Design of FRP PEDSTRIAN BRIDGES"* [16] published by American Association of State Highway and Transportation Officials (AASHTO), the recommended value for the allowable vertical deflection due to service pedestrian load and the allowable horizontal deflection due to lateral wind load should not be greater than $\frac{1}{400}$ of the length of the longest span.

$$\delta_{v,max} \leq \frac{L}{\mathbf{400}}$$

$$\delta_{h,max} \leq \frac{L}{\mathbf{400}}$$

$(2\text{-}4)$
$(2\text{-}5)$

Where:

$\delta_{v,max}$ is the allowable vertical deflection [cm]

$\delta_{h,max}$ is the allowable lateral deflection [cm]

L   is the span length [m]

In "LRFD Guide Specifications for Design of Pedestrian Bridges" [17] from AASHTO, for conventional construction materials like steel, concrete, wood, and aluminium, it suggests that the allowable vertical deflection due to service pedestrian load and the allowable horizontal deflection due to lateral wind load should not be greater than $\frac{1}{500}$ of the length of the longest span. This implies that, the maximum deflection limits of the FRP pedestrian bridges are more liberal than the conventional-material-bridges. Since FRP composite materials have high strength but low stiffness (low elastic modulus), so when the same pedestrian loads are applied on the FRP pedestrian bridges, they tend to be subjected to lower stresses. Therefore, it is reasonable to give more freedom in terms of deflection limits to the FRP pedestrian bridges.

2.4.1.2 Vibrations

Due to lightweight characteristics of composite materials, the FRP pedestrian bridges are more prone to suffer excessive vibrations which are caused by dynamic actions from pedestrians. Therefore, after fulfilling the deflection limits, the next step is to evaluate the natural frequencies of the bridges.

In the same guide specifications from AASHTO [16] mentioned above, it states that in order to avoid the resonance phenomenon induced by the 2nd harmonic of pedestrian loads, the vertical and longitudinal natural frequencies should be higher than 5 Hz. Furthermore, the fundamental natural frequency in lateral movement

induced by 1st harmonic of pedestrian loads should be higher than 3 Hz (2.5 Hz according to the Eurocode EN 1990 [7]). It is necessary to note that pedestrians react much more sensibly to lateral vibrations than the vertical ones [6].

To insure that the vibrations from the FRP pedestrian bridges can be acceptable, the vertical and lateral natural frequencies induced by people walking or running must comply with the conditions below:

$$f_v \geq \mathbf{5} \, Hz \qquad \text{(2-6)}$$
$$f_h \geq \mathbf{3} \, Hz \qquad \text{(2-7)}$$

Where:

f_v is the designed vertical natural frequency [Hz]

f_h is the designed lateral natural frequency [Hz]

In another design guidelines from European Commission JRC [6] and the Eurocode EN 1990 [7], two critical ranges of natural frequencies, *see* Table 2.3, with pedestrian excitation are provided. The guideline states that if the natural frequencies of the pedestrian bridges are outside these critical ranges, the dynamic vibrations are acceptable.

Table 2.3 – The critical ranges of natural frequencies for pedestrian bridges

Critical range of natural frequencies	For vertical and longitudinal vibrations	For lateral vibrations
European Commission JRC [6]	$\mathbf{1.25} \, Hz \leq f_i \leq \mathbf{4.6} \, Hz$	$\mathbf{0.5} \, Hz \leq f_i \leq \mathbf{1.2} \, Hz$
Eurocode EN 1990 [7]	$f_i \leq \mathbf{5} \, Hz$	$f_i \leq \mathbf{2.5} \, Hz$

2.4.2 Design guideline of lightweight pedestrian bridges for human-induced-vibrations

From the elaboration above, it indicates that it is of vital importance to not only consider static loads but also the dynamic performance of the bridges. However, there are still no standardized codes or regulations for such design available yet. The key factors to study the dynamic response of the bridges are their mass, stiffness, and damping. Should designers directly make modification of these factors when they find out that the natural frequencies of the pedestrian bridges fall within the critical ranges? How will designers know if the pedestrian bridge meets comfort requirements set by the client?

In a conclusion of a study on dynamic characteristics of FRP footbridge [18], it states that between frequency and acceleration indicator, through test measurement, the

acceleration is found to be more significant than frequency for the evaluation of the vibration comfort.

According to European Commission JRC [6], In the situation that the natural frequencies of the pedestrian bridges fall within the critical ranges, a dynamic assessment must be performed. Basically, the dynamic assessment is categorized into two main classes which contain traffic classes, and comfort classes. Based on this assessment, designers can decide if modification of mass and frequency, or additional damping devices are required or not. A design guideline which illustrates about how to evaluate the dynamic behavior of pedestrian bridges is provided, see Figure 2.20.
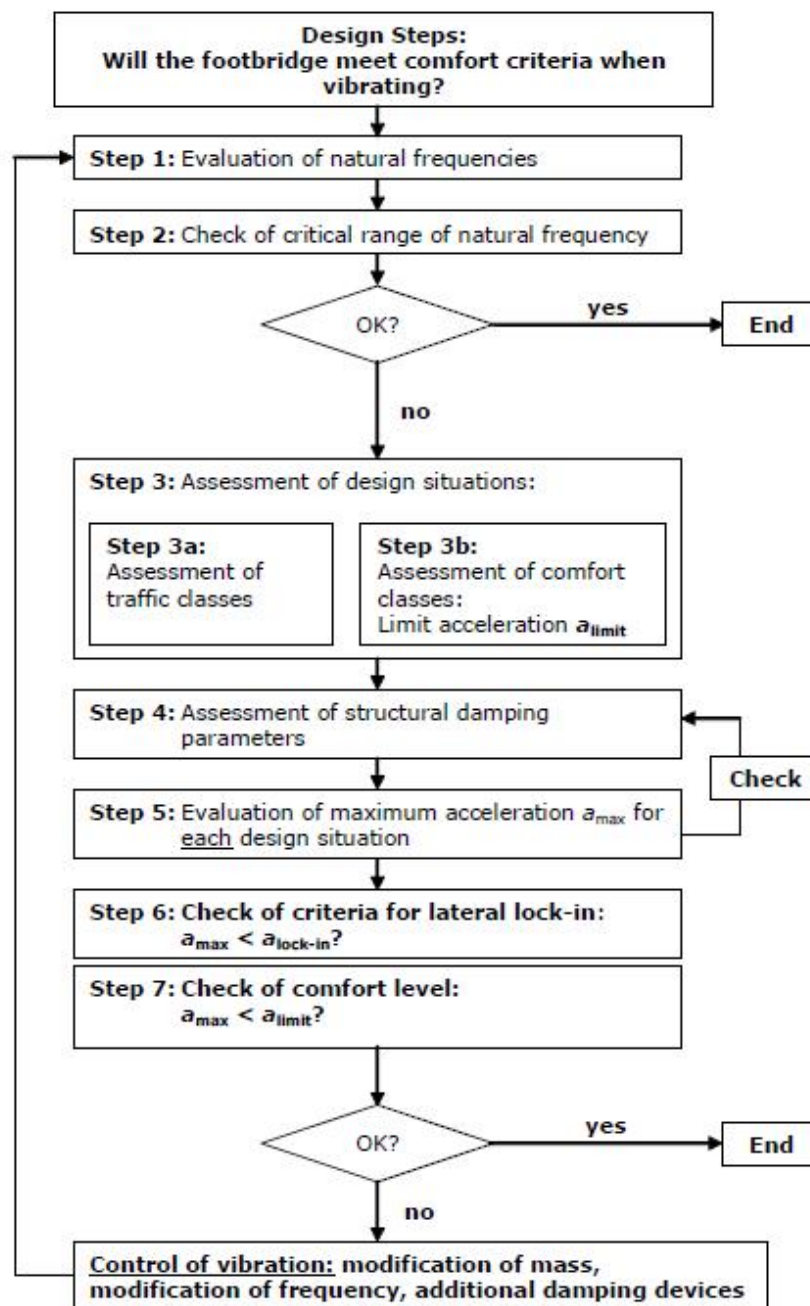

Figure 2.20 – Flowchart for the use of the design guideline [6]

CHALMERS, *Civil and Environmental Engineering*, Master's Thesis 2015:141

2.5   Modelling techniques of composite materials

In BRIGADE/PLUS, there are 3 main different modelling techniques for composite materials that can be applied based on the objective of the analysis. They are:

2.5.1   Microscopic modelling

Literally, this technique looks at the model at microscopic level. The two components of composite materials like matrix and fiber are separately modelled as deformable continua. They are regarded as single homogenous material which is either matrix or fiber phase. This technique is suitable to be applied in material engineering application.

2.5.2   Layered modelling (Lay-up model)

In this technique, different materials, which refer to specific ply (combination between matrix and fiber), are layered up in each element, and each element has its own degree of freedom (DOF). It implies that this layered modelling can become very expensive if a lot of plies are used.

2.5.3   Smeared modelling

In this modelling, the entire composite material is modelled as an equivalent homogenous material with stacked or single element configuration. Each laminate configuration has its own equivalent elastic properties such as stiffness and poison's ratio that can represent the multi-layered structure.

The MATLAB routine which is formulated to calculate the equivalent elastic properties of the laminate structure mentioned in the APPENDIX A – MATLAB scriptsis intended to apply in this smear modelling. The routine gives equivalent values of the elastic properties of the composite materials, and those values can directly be inserted into the material module in BRIGADE/PLUS.
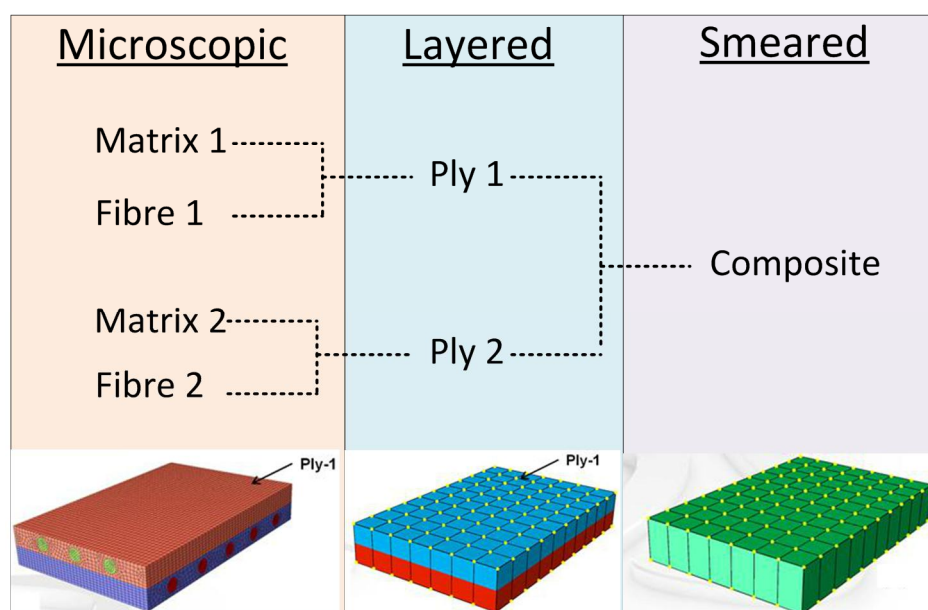

Figure 2.21 – Three different modelling techniques in composite materials

3 Modelling

This chapter illustrates the establishment of two 3D FE models which are used for evaluating the dynamic behavior of the FRP pedestrian bridge. These models are called as beam element model and shell element model.

Due to the complexity of the geometry and many uncertainties in material properties of the bridge, a simple beam element model should be made first at an early stage of the design before moving to a more complex model. The purpose of this beam element model is initially to have a general feeling on the structural behavior of the bridge when it is subjected to service pedestrian load. Authors want to quickly investigate the deformation and dynamic response of the bridge. After the beam model is studied, the shell element model, which entails a time-consuming process and much more complicated analysis, is successively constructed. BRIGADE/STANDARD and BRIGADE/PLUS are used for the modelling of beam element and shell element model, respectively.

3.1 Beam element model

In order to have a quick investigation on the bridge, an easy and approximate model using beam element is established at the first attempt. This could help understanding the estimated response of the entire bridge such as rough deflection and frequency etc. To construct this simple model, BRIGADE/STANDARD is used.

Necessary 3D drawings of the bridge with approximate geometry and necessary information such as boundary condition and technical support to implement the FE program are sufficiently provided by Ramböll AB. To simplify the work, only six cross-sections are chosen to build up the structure; therefore, particular section cuts over the specified locations which are considered as critical cross sections are executed, see Figure 3.2Figure 1.2 – Bridge's span length dimensions. Then, the dimensions of those cross-sections are modified to fulfill the design requirements, see Figure 3.1. In BRIGADE/STANDARD, linear interpolation between cross-sections is by default carried out when the combination of all cross-sections to obtain single bridge structure is needed; see Figure 3.3, Figure 3.4, and Figure 3.5.

The boundary conditions of each end are chosen to be simply supported and the mid support is fixed (free rotations). The bridge is subjected to its own self weight and service pedestrian surface load (5 kN/m^2). Normally, the density of glassfibers range between 1700-1900 kg/m^3, for the sake of simplification and to be more conservative, the density of the beam and the deck are chosen to be 2100 kg/m^3 and 1 kg/m^3, respectively. Furthermore, the deck has 300 mm thickness and damping ratio is chosen to be 2% as recommended by AASTHHO [16] .

Section A-A   Section B-B   Section C-C

Section D-D   Section E-E   Section F-F
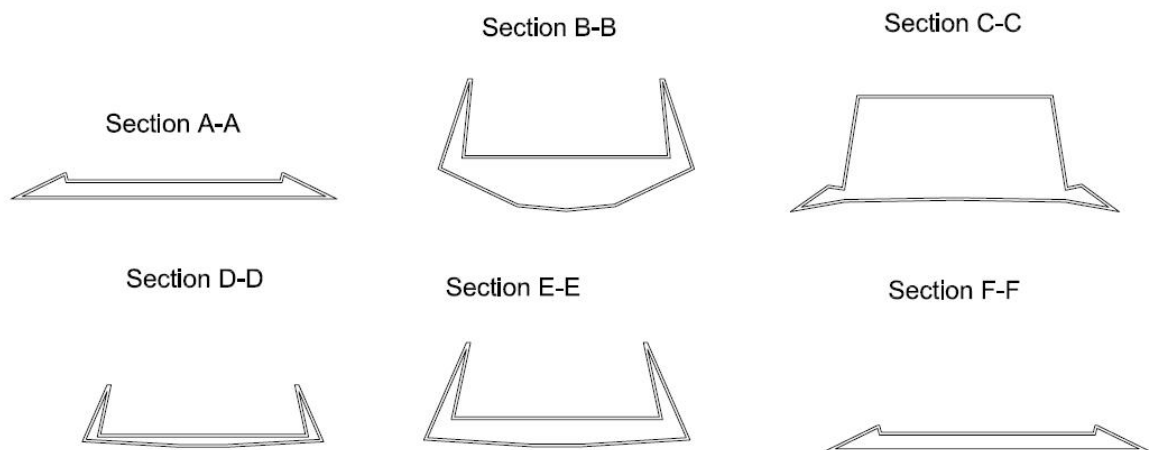
Figure 3.1 – Beam element cross-sections for Brigade Standard
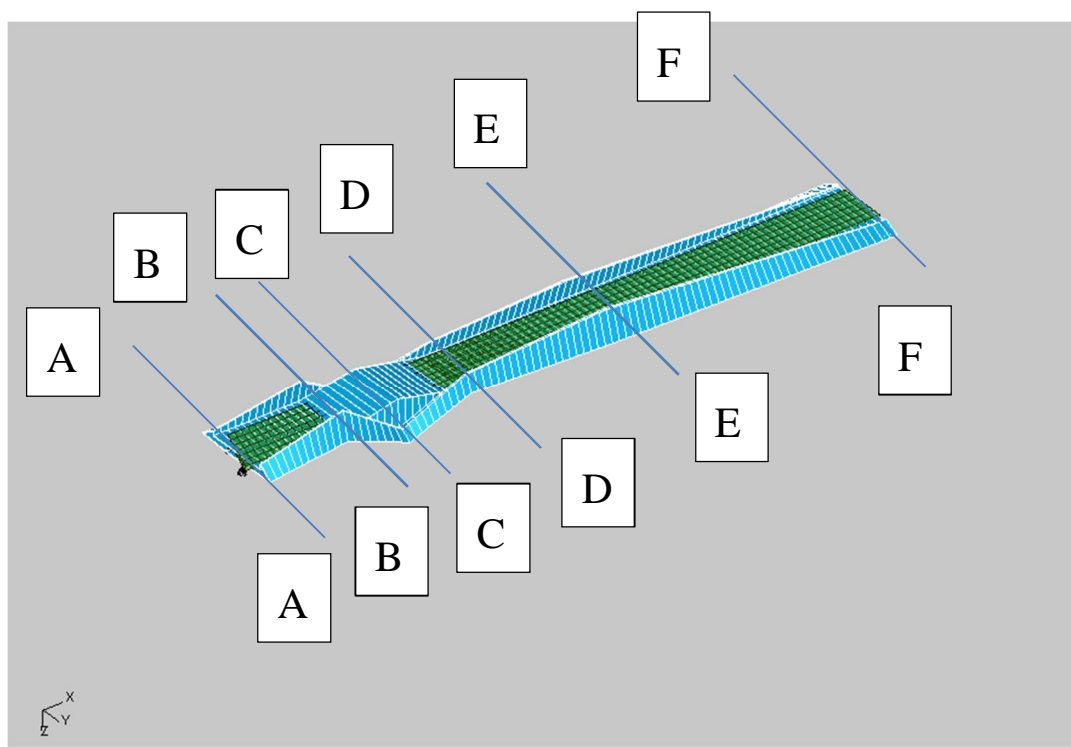
Figure 3.2 – Perspective view of the pedestrian bridge in beam element model
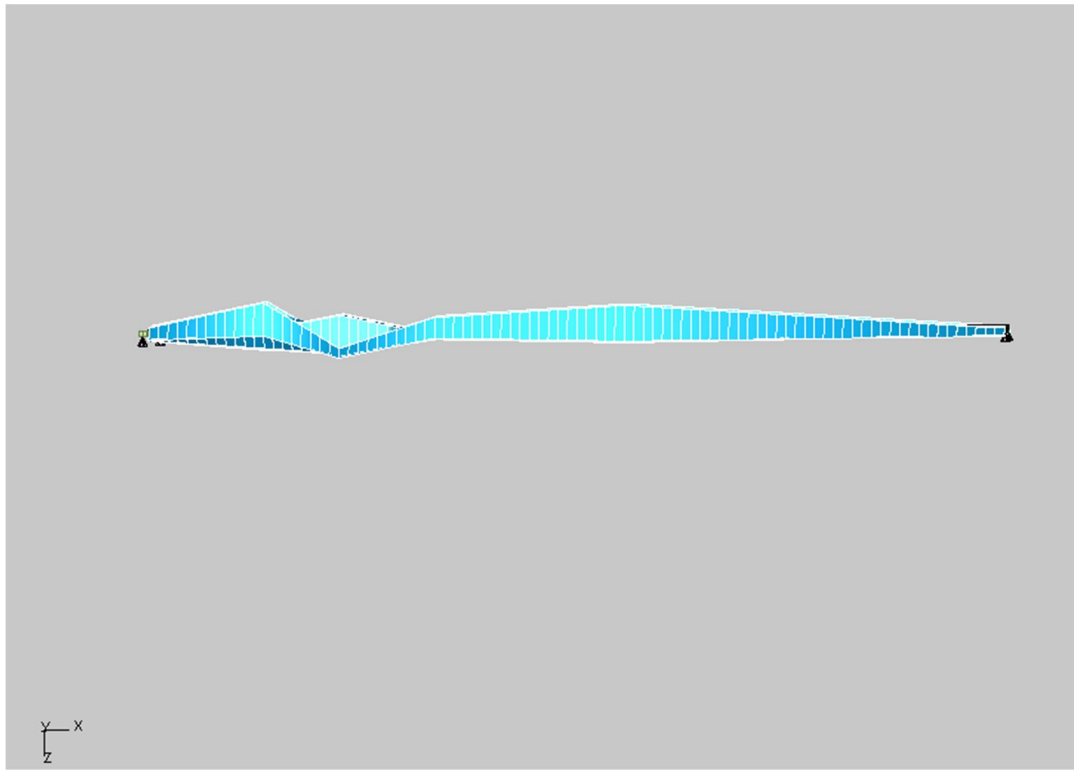
Figure 3.3 – Side view of the pedestrian bridge in the beam element model
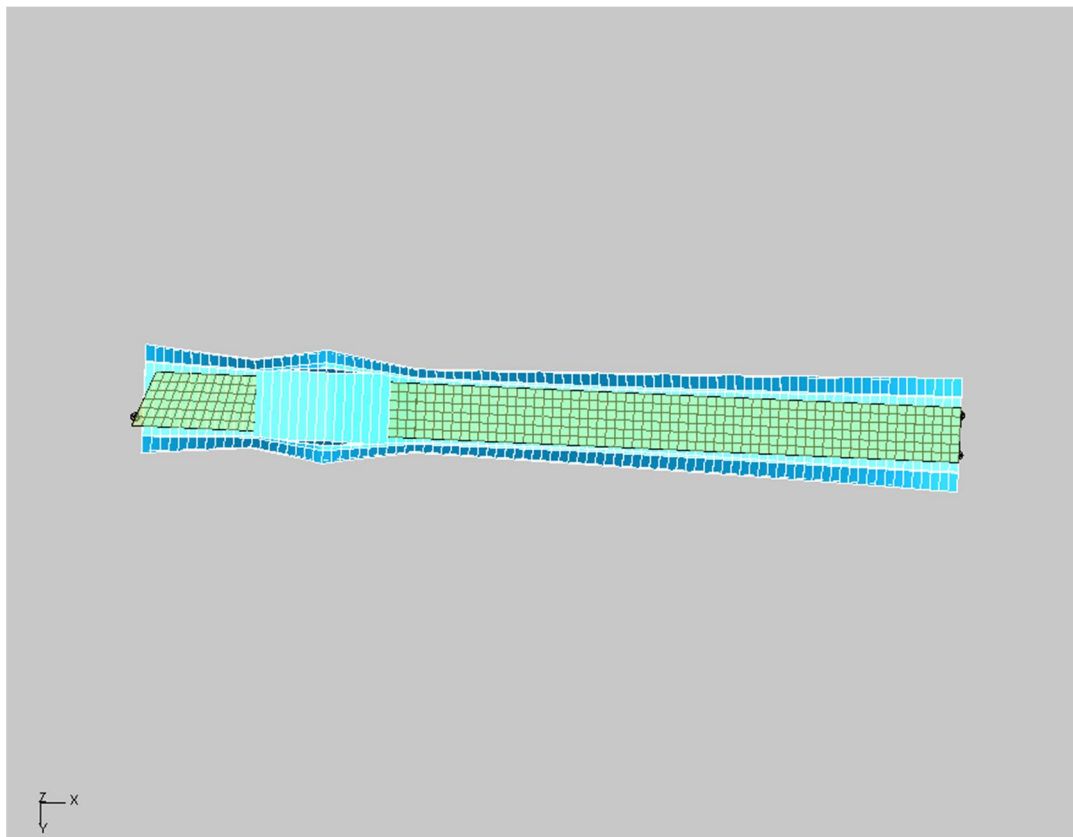
Figure 3.4 – Top view of the pedestrian bridge in the beam element model

CHALMERS, *Civil and Environmental Engineering*, Master's Thesis 2015:141
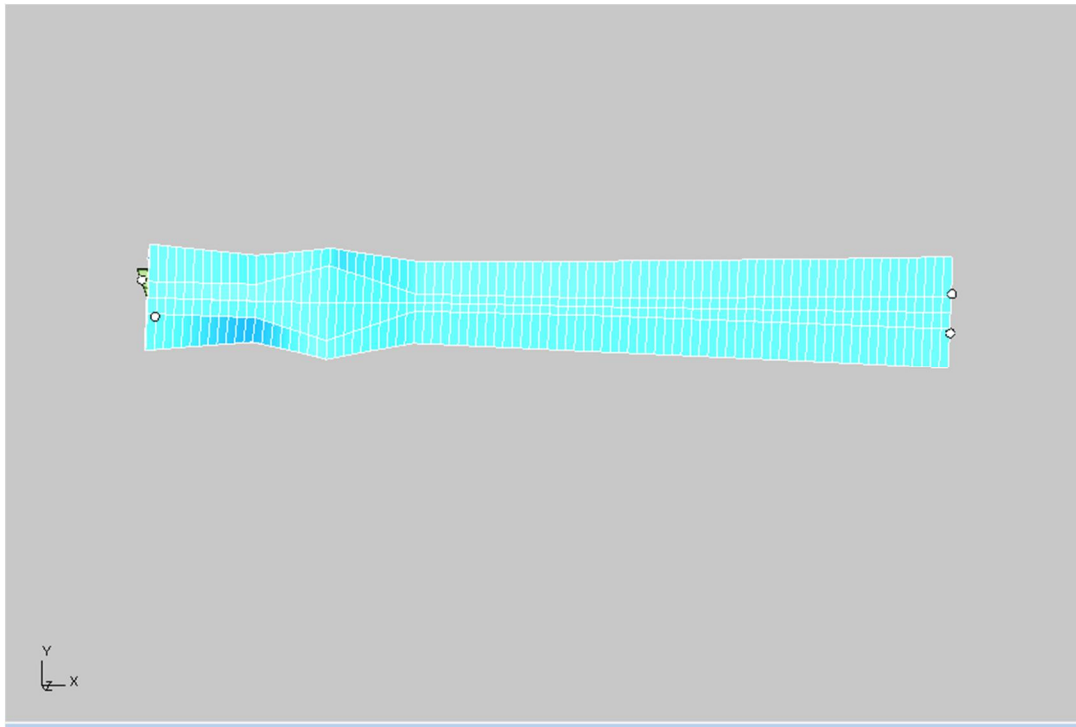
Figure 3.5 – Bottom view of the pedestrian bridge in the beam element model

These pictures shown above can illustrate the rough approximation made with a beam element model, however the results of the analysis will be further discussed in Chapter 4 to compare them with the shell element model.

3.2 Shell element model

As it was stated previously, the beam element model is a very simplified model but after obtaining the necessary information from it a more accurate model is needed. This method can represent more complex shapes, different material configurations and provides much more information in terms of stresses, forces, displacements and reactions.

This section of the thesis will explain the different steps in the process of creation of the shell element model.

Ramböll provided the latest drawings used for the project in order to have the most recent data available.

1. Modelling space: 3D, deformable type, plane stress
2. Base feature: Shell element, extrusion.

3.2.1 Parts

As it was mentioned earlier, six simplified cross-sections are required to build up the structure; therefore, particular cuts over the specified locations which are considered as critical cross sections are performed, *see* Figure 3.6.

Figure 3.6 – Location of the cross-sections at critical points

The cross-sections are slightly different than the ones used in the beam element model due to an update of the drawings in the project, *see* Figure 3.7. In the same manner the required cross-sections were obtained and subsequently simplified to be able to model them in BRIGADE/PLUS, *see* Figure 3.8.
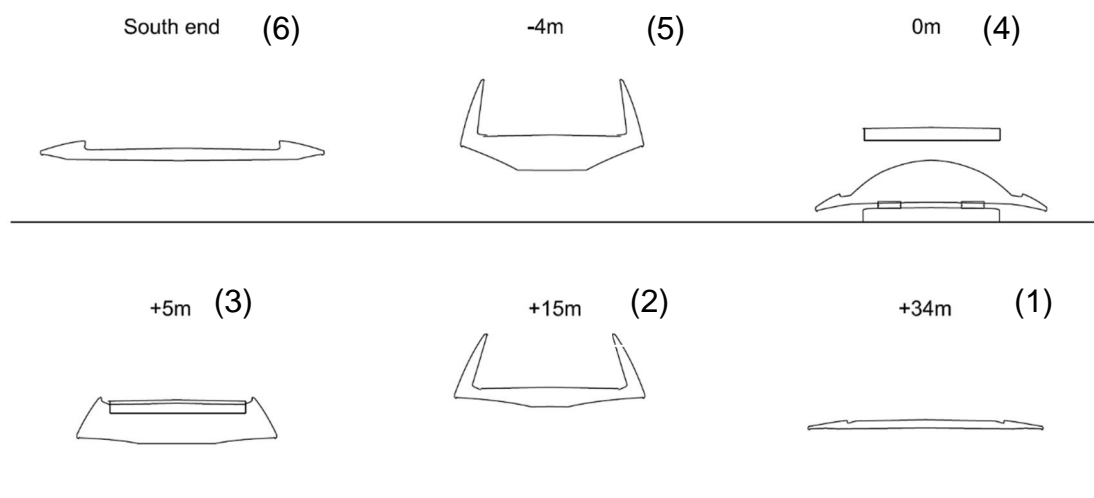
Figure 3.7 – Cross-section obtained to use in the modelling
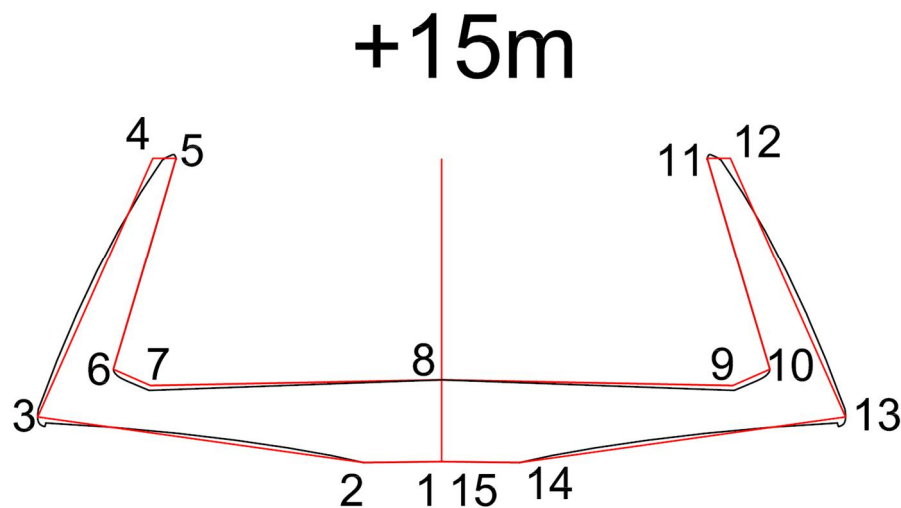
Figure 3.8 – Simplified cross-section and node numbering
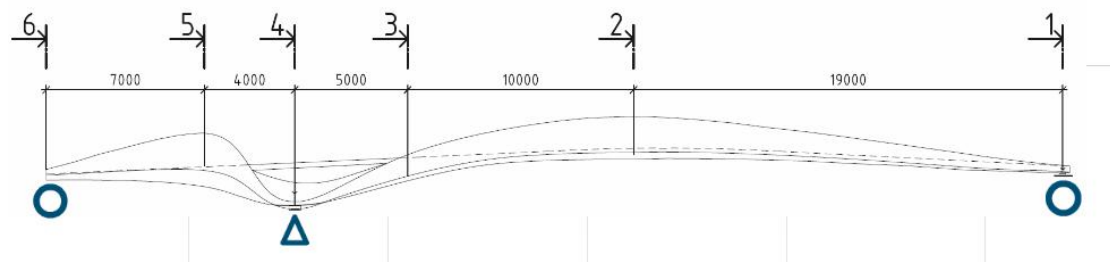
These six cross-sections, *see* Figure 3.7, will divide the bridge into five different pieces, the main objective of this procedure is to model all these five pieces individually in Brigade/Plus and then assemble them together to have the one complete structure modelled.

The creation of these pieces will be done using two cross-sections for each piece and interpolating the faces into one shell piece, *see* Figure 3.9. There could be different ways to build these pieces using the program Brigade/Plus, the one that the authors found most suitable for this case was the *LOFT* function. The main idea is to provide this function with two cross-sections, preferably with the same amount of nodes (corners). That is why all the simplified cross-sections have the same amount of nodes, fifteen in this case, *see* Figure 3.8. This function will interpolate the path between all the nodes and create a surface with these paths, leaving a hollow section in the middle and a shell around it.

The first step is to draw these cross-sections in Autocad and then import them into Brigade/plus as a Sketch, if drawn correctly the program will recognize the corners automatically, *see* Figure 3.9. After many attempts of trial and error it has been understood that the LOFT function will work correctly only if the number of edges is the same and that there are no extra lines or segments. To be sure the drawing is correct it is possible to create points in all the edges using Brigade's own drawing tools, then all the lines can be erased and drawn again to avoid hidden mistakes. It should be noted that each cross-section is positioned in the correct Y-coordinates (elevation).
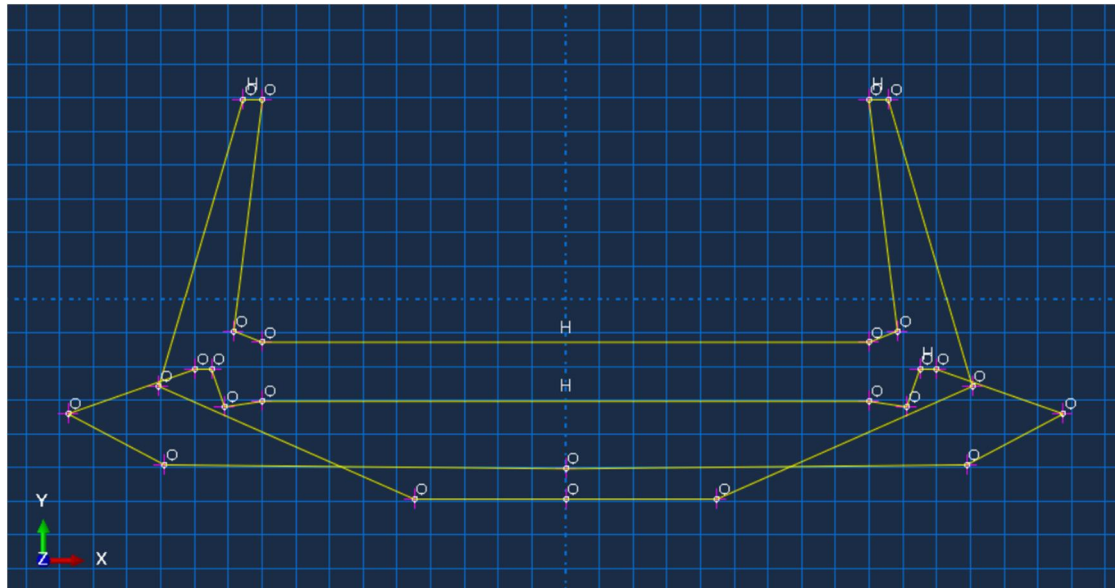
Figure 3.9 – Cross-section drawn in the Sketch module of Brigade Plus

After the SKETCH is done correctly, avoiding extra lines, segments and edges, the next step is to create a PART with this SKETCH. Subsequently, the next step is to extrude this drawing in the z-direction, the objective of the extrusion is to have both cross-sections in the same plane but at different coordinates in the z-axis. The piece used for this example is 4 meters long, so the extrusion has to be 4 meters in the z-axis, *see* Figure 3.10.
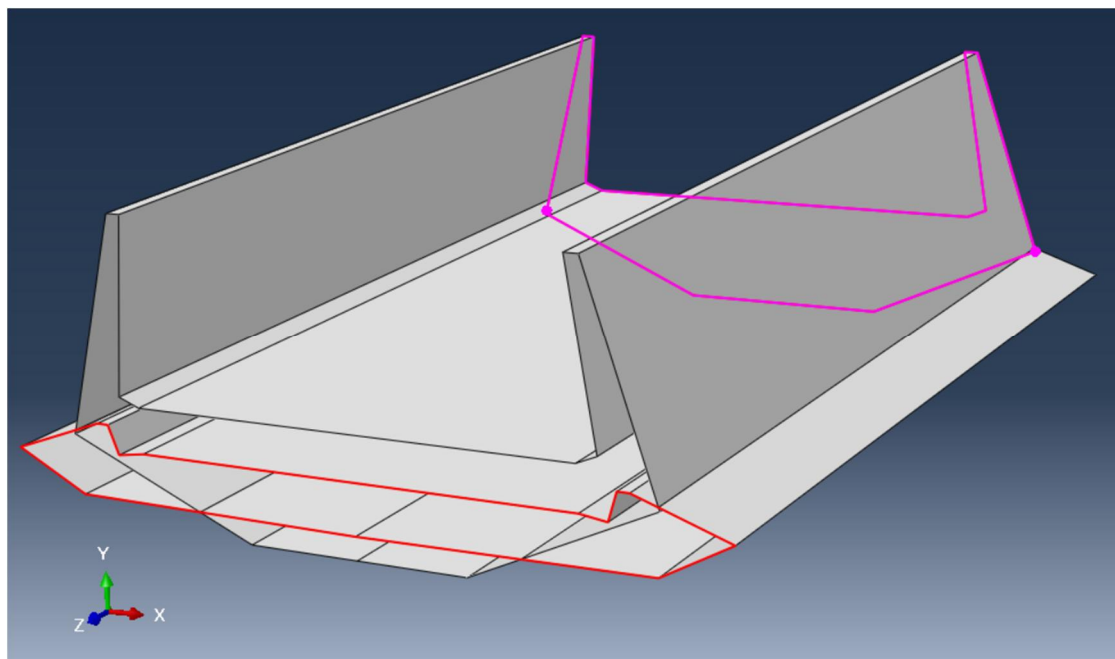
Figure 3.10 – Extrusion of a cross-section

Figure 3.10 shows how the Extrusion function has created a surface connecting the edges of the cross-section, having now two cross-section overlapping each other. The Extrusion function and the Loft function will be combined to obtain the desired piece. The LOFT function needs a starting face and an ending face, Figure 3.10

CHALMERS, *Civil and Environmental Engineering*, Master's Thesis 2015:141

shows the red cross-section as the beginning face and the pink cross-section as the ending face. If the option PREVIEW is selected it is possible to see a preview of the paths connecting the edges, it is very helpful to use this option to examine if the paths are connecting the correct edges and find other possible mistakes, *see* Figure 3.11.
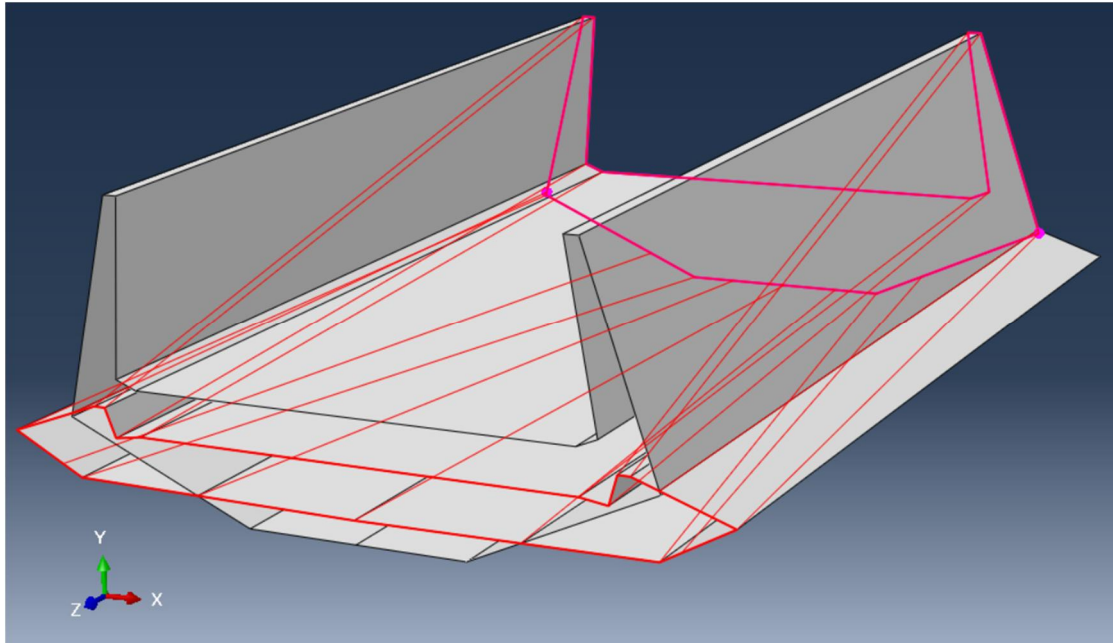
Figure 3.11 – Preview of the paths connecting the edges of the cross-section

Subsequently, the LOFT function can be executed and a piece will obtained but one small detail is still missing. Looking at the entire bridge it can be seen that the shape of the bridge is very "wavey" which is not resembled by the straight paths seen in Figure 3.11. Fortunately, there is an option in the LOFT function in which it is possible to modify the paths to have a more similar shape like the original bridge. This option will allow the user to decide the angle at which the path will start and end at each cross-section, *see* Figure 3.12. After several attempts it was possible to obtain a very similar shape to the real one, *see* Figure 3.13.
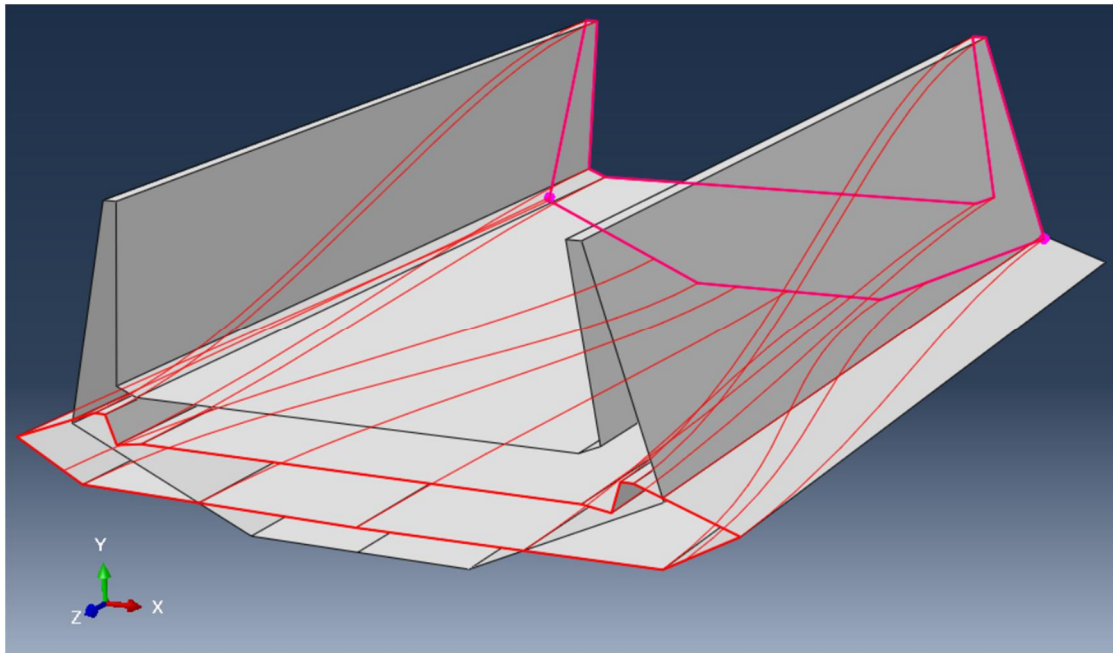
Figure 3.12 – Angled paths modified in the Loft function

Finally, the LOFT function creates the paths connecting the edges and creates a surface around them. The only thing left would be to remove the residual surfaces and the final piece is obtained, *see* Figure 3.13.
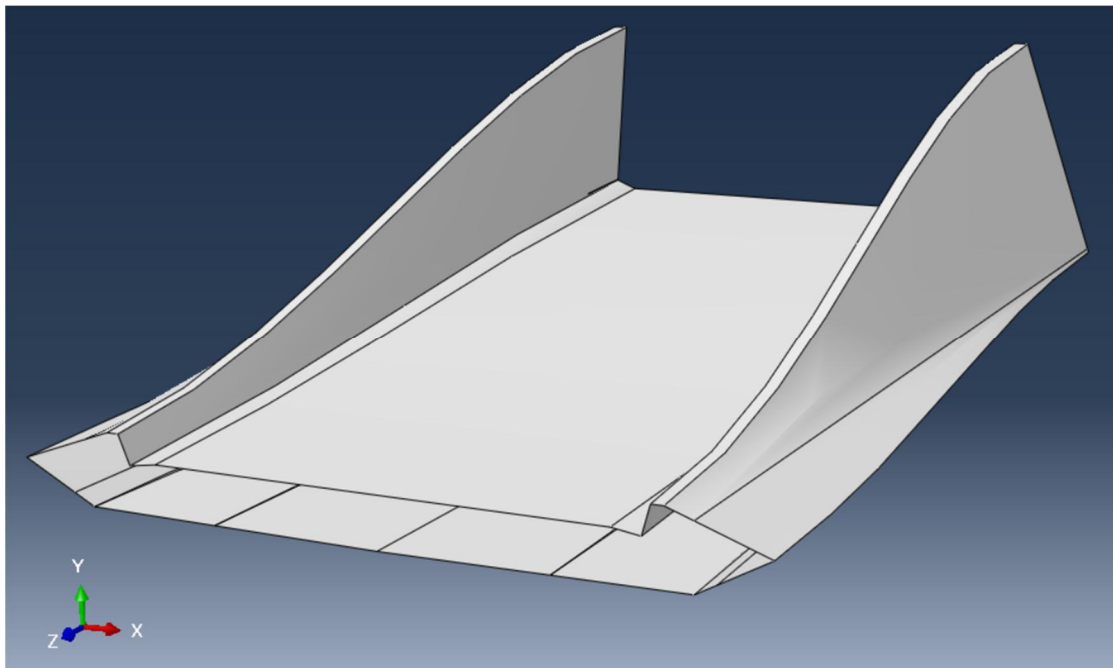
Figure 3.13 – Final surface created with the Loft function

This procedure has to be repeated for the remaining four pieces of the bridge, paying attention to the same details mentioned earlier it should be easy to avoid any mistakes. Since the next piece to be created will begin with the same cross-section with which the first one ended it is obvious that all the pieces will fit perfectly with each other.

3.2.2 Material properties

FE modelling of the composite materials such as FRP is normally more complicated regarding material properties and local coordinates for the fiber orientation of each laminate. Since FRP is described as an orthotropic material, it requires more inputs such as different young's modulus and poisson's ratio in different directions.

Although the modelling process of the material properties in Brigade/plus can get complicated as one increases the accuracy, a simple way to model the properties of FRP is to define the material as isotropic. The first attempt of the shell model was done with an isotropic material, this means that the material had the same properties in all directions and only the Young's modulus is needed. An average value for fiberglass composite as an isotropic material is 21 MPa.

3.2.3 Stiffness improvement

The first attempt of the shell model showed that the entire structure lacked stiffness, it could be seen in the extreme deformations and displacements. Correspondingly, the immediate reaction was to look for ways to increase the stiffness of the bridge. Many alternatives were analyzed taking into account program capabilities, available knowledge and practicality.

Having considered all these aspects, the chosen option was to stiffen the bridge with "stiffeners". Looking at the model it was evident that the hollow middle section had to be reinforced with "ribs" as seen in Figure 3.14.

Figure 3.14 – Stiffeners along the inner section of the bridge

These ribs were placed into the model in both x and z direction with a spacing of approx. 1 meter and 3 meters respectively. The material properties of the ribs were still the same as the entire model, isotropic equivalent Glass fiber. In order to acquire a higher mom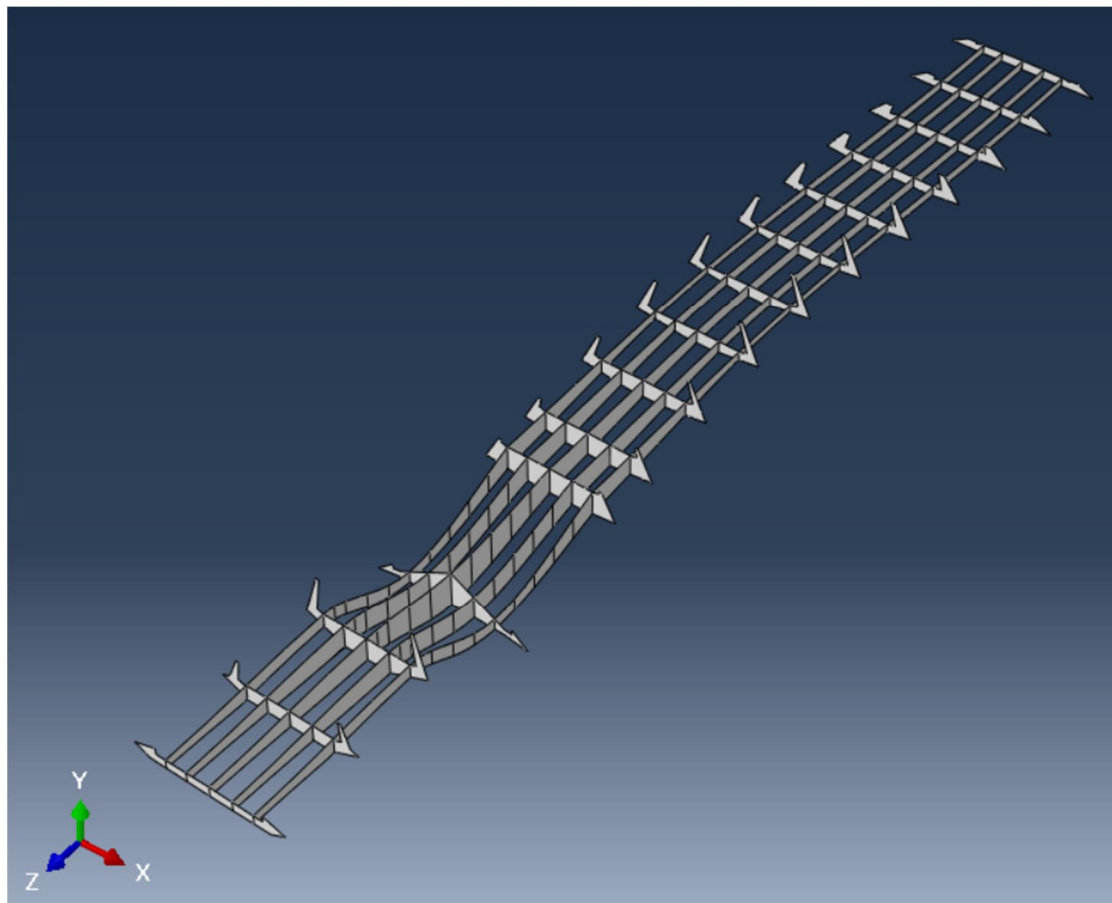ent of inertia the ribs are thin but long in the y-direction. This configuration of the ribs is meant to increase the stiffness of the structure and to connect all the faces to work together as one whole piece.

3.2.4 Step

If one is familiar with the FE program Abaqus or in this case Brigade/Plus then one is familiar with the two main types of analysis available in these programs. Both analysis are important depending on what type of behavior is intended to examine. In order to analyze this structure and retrieve all the necessary information it is fundamental to make two types of analysis, static general analysis and frequency analysis.

3.2.4.1 Static general analysis

This analysis is the most common and important one. All the loads are considered such as self-weight, pedestrian load and the point load representing the snowplow. This analysis will provide the necessary stresses, deflections and reactions.

3.2.4.2 Frequency analysis

The frequency analysis does not consider extra loads besides the self-weight. The main factors influencing the frequency of the structure are the stiffness and the mass of the structure. For this matter it is important to disable all the loads on the bridge to obtain accurate results.

3.2.5 Application of Load and Boundary conditions

3.2.5.1 Loads

As it was mentioned earlier, the main problem with glass fiber composites is the low modulus of elasticity. Accordingly, the deflection will be the designing criteria besides the frequency of the structure. To analyze the deflection of the structure, the corresponding load is the Pedestrian load with a value of 5 kN/m2 according to the Eurocode [21]and the Handbook.

pedestrian load (SS-EN 1991-2 chapter 5.3.2.1) and the point load representing the snowplow (SS-EN 1991-2 chapter 5.3.2.3).

The earlier mentioned pedestrian load was modelled in the program as a Surface Pressure in the y-direction over the entire surface of the deck along the bridge. This load in particular was used to design the bridge with regard to the global deflection limit.

Focusing on the local aspect of the bridge, the deck was designed using the load of ta 12-ton snow plow (maintenance vehicle) according to the Eurocode [21]. This load has 2 axes with a load of 40kN and 80kN respectively with a separation of 3 meters.

As these load are used in the Serviceability Limit State all partial factors are equal to 1 for a characteristic load combination as stated in the Eurocode [7] section 6.5.

3.2.5.2 Boundary conditions

At the moment of realizing this thesis the Kaponjärsbron project was still at an early stage but being the foundation a critical aspect to choose a FRP composite solution, the boundary conditions were defined from the beginning.

The main foundation of the bridge is located in the middle of the river over a concrete pile called coffer-dam, preventing only displacement in all directions. Both ends of the bridge have a "gaffel type" support, which means that displacement is restricted in the vertical and horizontal direction. The only displacement is allowed in the longitudinal direction; for both end supports, *see* Figure 3.15.
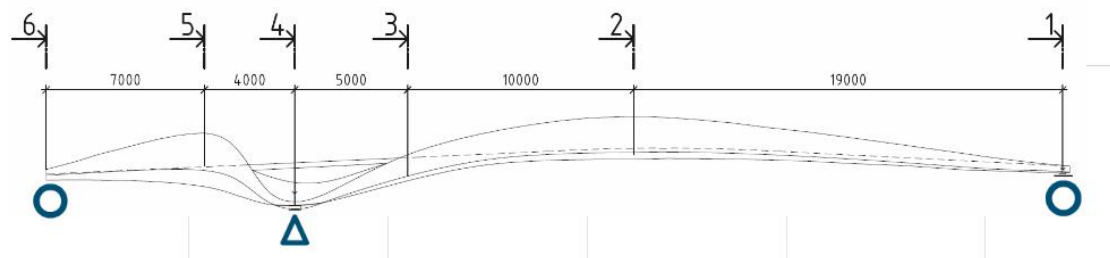
Figure 3.15 – Simplified drawing showing boundary conditions

- Load: Self weight and pedestrian load 5 kN/m2
- BC: End support, roller
- Mid support: fixed in translation and rotation allowed

3.2.6 Meshing

The accuracy of a FE analysis depends on the type of mesh with which it's analyzed; this section will explain partially how the mesh was realized for this project. A lot of options exist for this matter, depending on the type of structure, form, complexity and accuracy.

3.2.6.1 Element shape

This module select the element shape for the mesh of the model, it can be Free, Structured or Sweep. The FREE option will create the elements randomly adopting the shape that best fits the form of the piece or section. For this reason, it is not recommend using the FREE option given that the elements are created randomly giving much uncertainty, errors and convergence problems.

The other option is the Structured/Sweep option, where the elements are shaped according to a selected amount of edges in these elements. Accordingly, the elements can be shaped with 3 edges (Tri) or with 4 edges (Quad), more edges will provide more points of integration and consequently deliver a higher accuracy in the results.

3.2.6.2 Element Size

The size of the elements are chosen relative to the size of the bridge, they should be small enough to provide enough integration points along the different cross-sections, *see* Figure 3.16. The size of the elements used for this model is 20 cm square elements (4 nodes), considering that some of the elements differ in shape in some of the complicated areas. An element of this size is considered small enough to provide accurate results, the convergence study showed that smaller elements don't increase the accuracy of the results significantly.

- Element shape: Quad/Quad-dominated
- Element type: Standard
- Geometric order: Linear
- Family: Shell
- Mesh size: 0.20 m
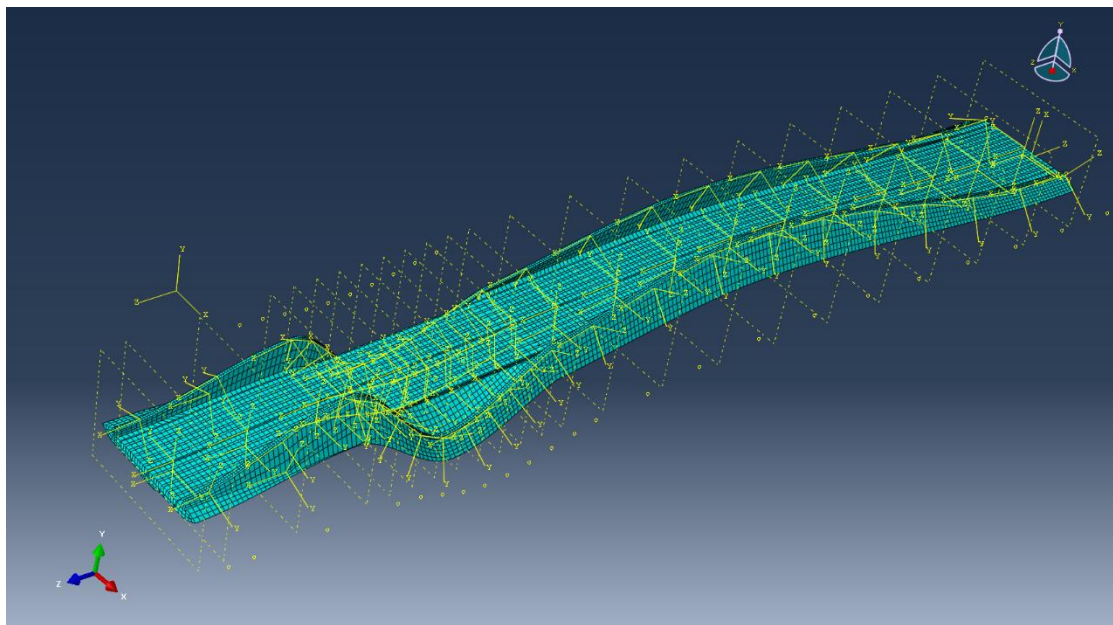
Figure 3.16 – Mesh of the structure with an element size small enough

4 Preliminary Results

Different types of models were chosen at the beginning of the thesis, with different purposes and with different results. These results are analyzed in order to retrieve preliminary information and develop the model with help of these.

4.1 Beam element model

This particular model had the purpose to provide a first impression of the behavior of the bridge under a distributed pedestrian load. However, the beam model in the program Brigade Standard is only a beam provided with cross-sections to approximate the stiffness of each section. Furthermore, the information available after the analysis is reactions force, moment, shear forces and deflection.

After running the analysis it was possible to see that the deflection of the bridge was as expected. The longer span deflected downwards reaching a maximum displacement near the mid span and the short span had a deflection upwards reacting as a continuous beam, *see* Figure 4.1. Curve 1 depicts the deformation of the bridge due to self-weight and curve 2 depicts the deformation with pedestrian load.
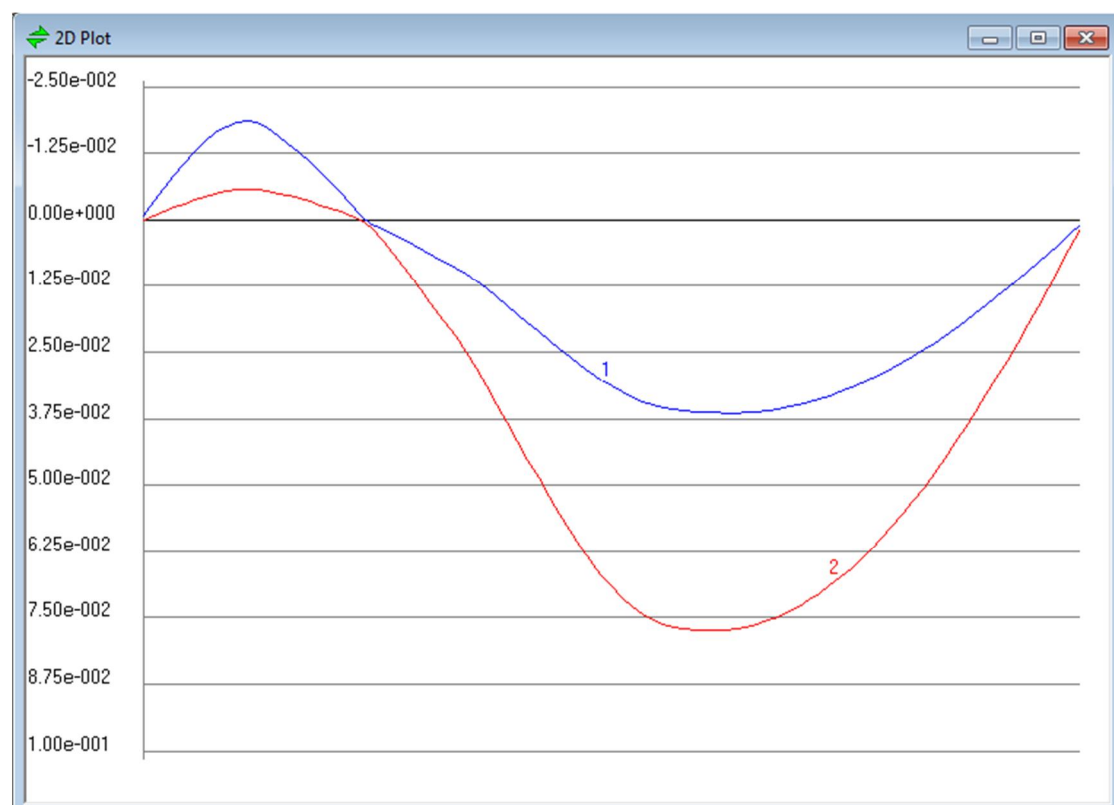
Figure 4.1 – Deflection of the bridge, Brigade Standard (units in meters)

It is however, important to note that even though the approximations of the cross-sections are accurate, the results from the analysis are not as reliable. Nevertheless, the deflection at the longest mid span is approximately 8cm, which is a reasonable

value in comparison with the allowable vertical deflection ($\frac{L}{400} = \frac{3400}{400} = \mathbf{8.5}cm$) as stated in section 2.4.2.1.

4.2 Shell element model

A more accurate alternative is the shell model where the stresses across the whole cross-section can be obtained and the entire modelling process is more precise.

The model was loaded with the basic loads as stated in chapter 3.2.5.1 in the Serviceability Limit State and the material properties of an isotropic glass fiber:

- Self-weight: 2500 kg/m3
- Pedestrian load: 5 kN/m2
- Glass fiber E-modulus: 21 MPa

The first model created in Brigade Plus was analyzed only with its self-weight to confirm that the deflections where reasonable and that the model was working correctly. It is predominant to fulfil the deflection criteria first before the frequency is analyzed; the deflection of the structure is the first thing to look at in the results. Figure 4.2 shows the deflection in the long span as 25cm only with self-weight and it is also perceivable that the deflections in the deck near the mid span bend beyond the structure itself.
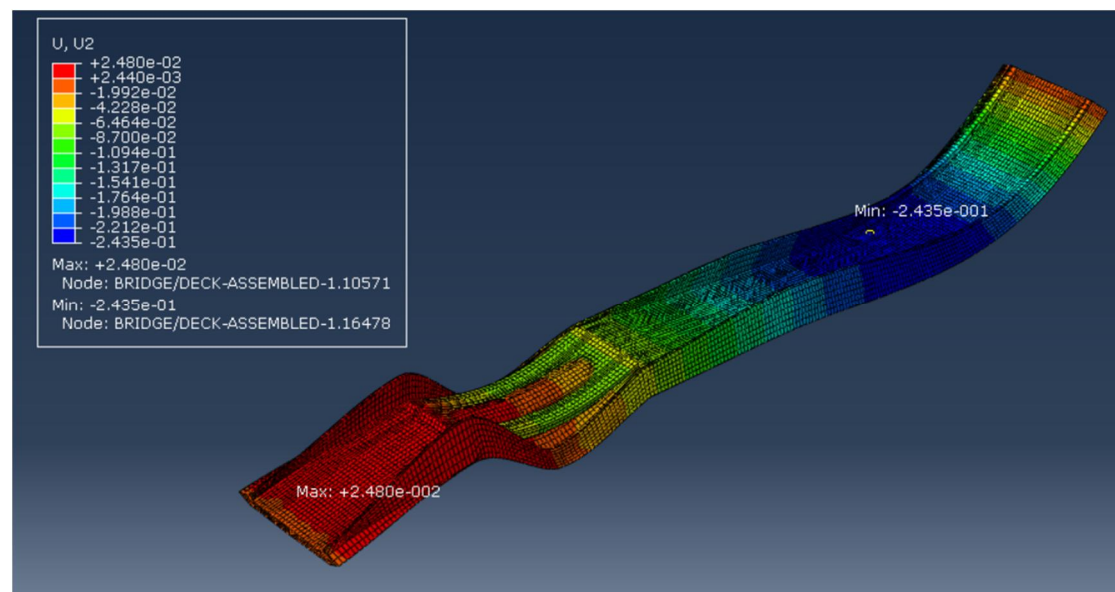
Figure 4.2 – Deflection angle view, Shell Model Brigade Plus (units in meters)
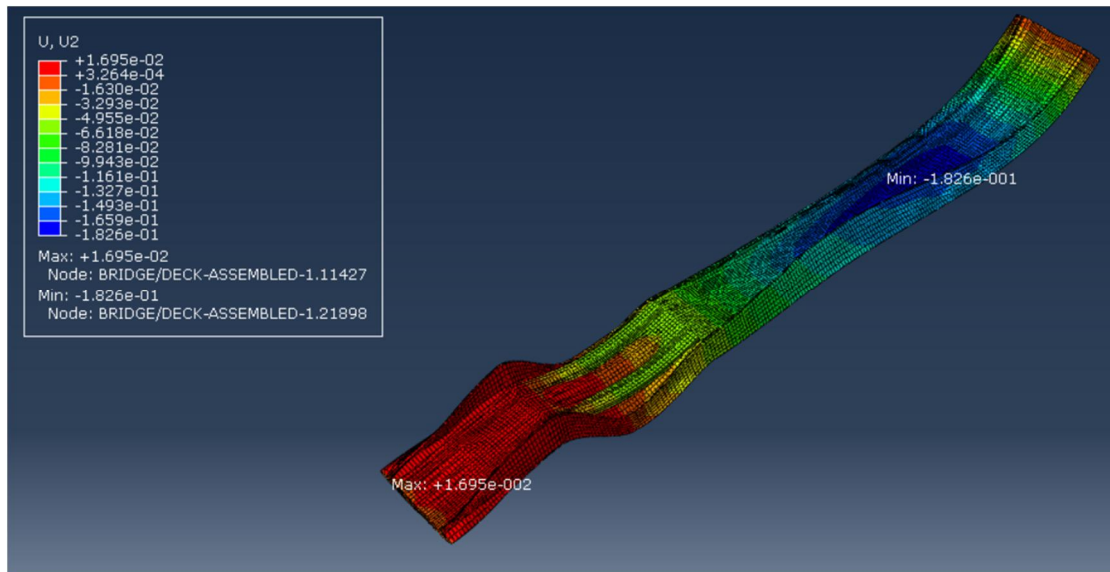
Figure 4.3 – Deflection top view, Shell model Brigade Plus (units in meters)
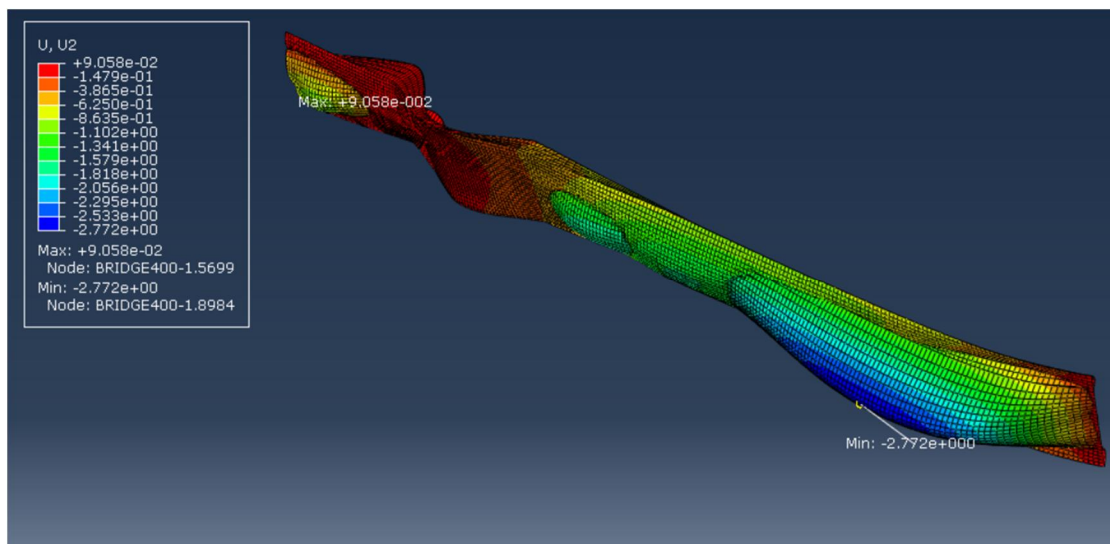
Figure 4.4 – Deflection bottom view, Shell model Brigade Plus (units in meters)

Looking at the other views in Figure 4.3 and Figure 4.4 it is more noticeable to see how the deflections increase to more than 2 meters and the faces of the shell deflect with no restrains. Consequently, it is possible to conclude that the structure lacks stiffness, the only stiffness provided is the thickness of the material in the faces of the shell (15 cm) which is clearly not enough. In this way, another observation to the behavior of the structure is how the top and bottom faces cross each other meaning that a connection should exist between them to make them work together. For this reason, the improvement to be made to the structure is to increase the stiffness of the structure and to somehow connect the faces of the shell to make them work together.

5 Improvement of the bridge model

After experimenting with early models of the bridge it became easier to identify the problems in the structure and the material. Having identified these problems a series of improvements were necessary to design a structure that met the requirements, these improvements will be explained in this chapter.

5.1 Sandwich panel

The results of the stiffeners in the bridge resulted in a very heavy structure with excessive deflection in the long span, therefore new alternatives have to be considered to solve this issue. Therefore, the new alternative is to implement a sandwich panel instead an isotropic glass fiber material.

In this case a sandwich is composed by glass fiber plies in different directions and foam in the middle, *see* Figure 5.1. The orientation of the plies will be stacked according to the need of strength in the required directions and the foam is a very light material which has the function to displace the fiber plies away from the neutral axis to increase the moment of inertia, hence increasing the stiffness.

Figure 5.1 – Sandwich panel configuration (10 mm thick example)
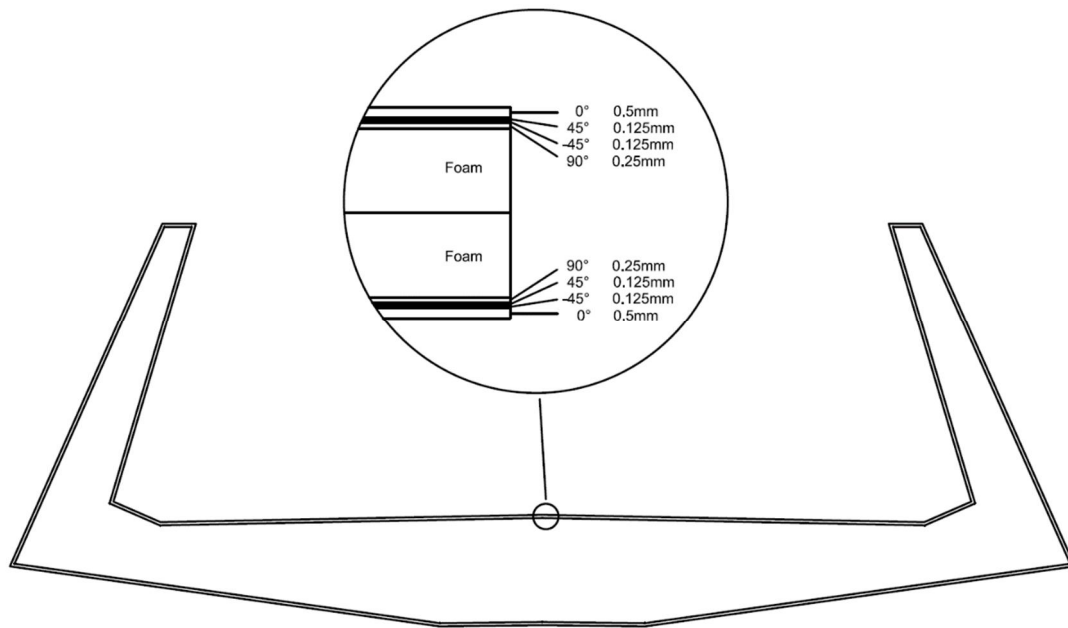
Figure 5.2 – Sandwich panel position into the entire cross section

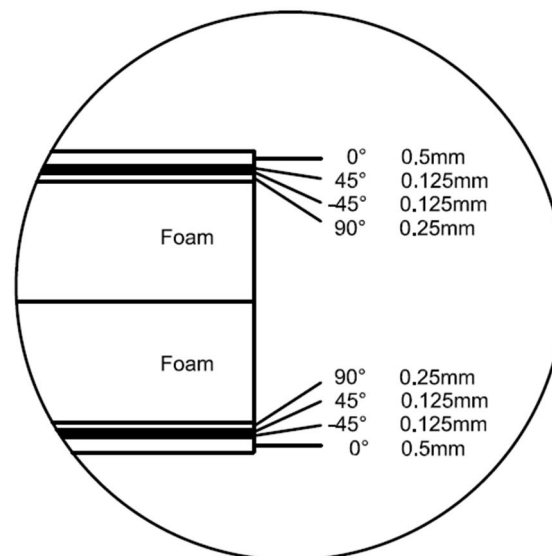At this point the material properties change, the isotropic glass fiber can no longer be used and an orthotropic material has to be implement in order to take advantage of the sandwich panel's qualities. A routine has been developed in MatLab to predict the equivalent properties of the sandwich panel because the material will be modelled in Brigade Plus as a homogenous material with orthotropic properties.

Orthotropic materials have different properties in different directions, due to this fact these two properties have to be modelled in the program. Correspondingly, for these two properties a coordinate has to be defined for each one of them. As the bridge changes direction in the X, Y and Z axis, the bridge is divided into small parts to approximate the material's behavior as much as possible.

5.2   Corrugated deck

At the same time as the sandwich panel alternative was determined to be used in the model of the bridge, another aspect of the bridge had been observed. The stiffeners on the bridge were too heavy, despite the low density of the sandwich panel, a better solution had to be implemented.

 The reasoning behind the other alternative is to shift the sectional area as far away from the neutral axis as possible. This would increase the second moment of area by having a sectional area with a bigger lever arm to the neutral axis. Due to this observation it was possible to understand that the stiffeners were acting as very long slender beams with a big sectional area but a low second moment of area.

A corrugated deck, this is the new alternative and solution to have a structure capable of resisting the acting loads on the deck and to increase the stiffness of the entire bridge. Chalmers provided this new design based on the 12 ton snowplow required for maintenance. Accordingly, Figure 5.3 shows the configuration of the new cross section and it is possible to observe that most of the sectional area is located far away from the neutral axis. However, the ribs that compose the corrugated deck

are made of a homogenous orthotropic glass fiber composite, not a sandwich panel. Only the deck has this type of material to be able to resist the pedestrian and service vehicle point loads, the rest of the cross section is made with the sandwich panel.
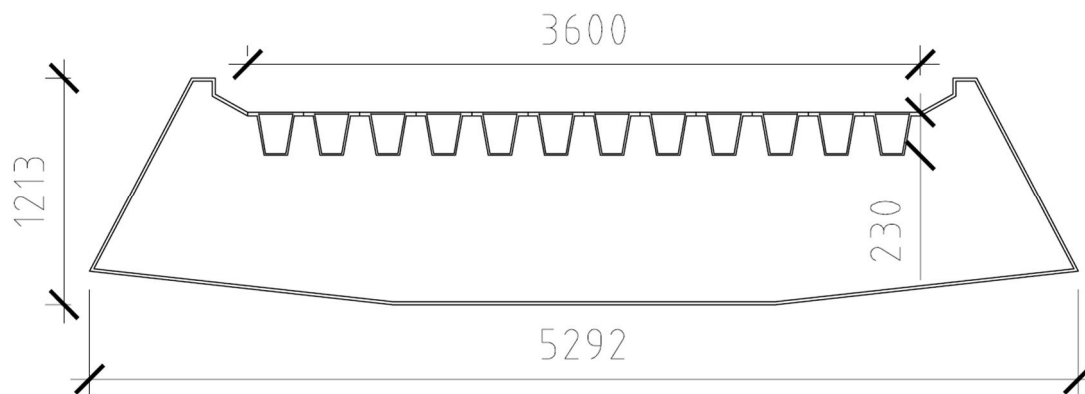
Figure 5.3 – Cross section with the position of the corrugated deck (dimensions in mm)

The corrugated deck as seen in Figure 5.3 was designed as a simple supported beam with a span of 3 meters, distance between transversal stiffeners in the new design of the bridge but with a sandwich panel cross section. Again, deflection was the designing parameter for this corrugated part, having two cases for which the deflection shouldn't be larger than L/400. The two different cases were the distributed pedestrian load of 5 kN/m2 and the 12 ton maintenance vehicle (snowplow). It is important to note however that the corrugated deck is a continuous structure across the entire bridge, supported by transversal stiffeners every 3 meters. The design was made as simple supported, on the safe side (simple supported implies a larger deflection at mid span), due to the time constraints and uncertainties that the entire concept of fiber composites carries.

After having a final design of the deck it was possible to move on to design the entire cross section taking into account the great contribution of the corrugated deck in its corresponding position. Moreover, having a bridge with a very complex and varying geometry, the contribution to the stiffness of the bridge varies constantly. The design of the remaining parts of the bridge was done by modelling the new cross section in Brigade Plus. This would enable the possibility to experiment with different sandwich panel configurations and study its behavior.

5.3   New cross section with corrugated deck

The modelling of the corrugated deck brought more difficulties than expected, despite having acquired lots of skills and knowledge with the previous model attempts. As it was mentioned before, the first step is to create a sketch in Brigade Plus with the new cross section and then extrude it, *see* Figure 5.4.
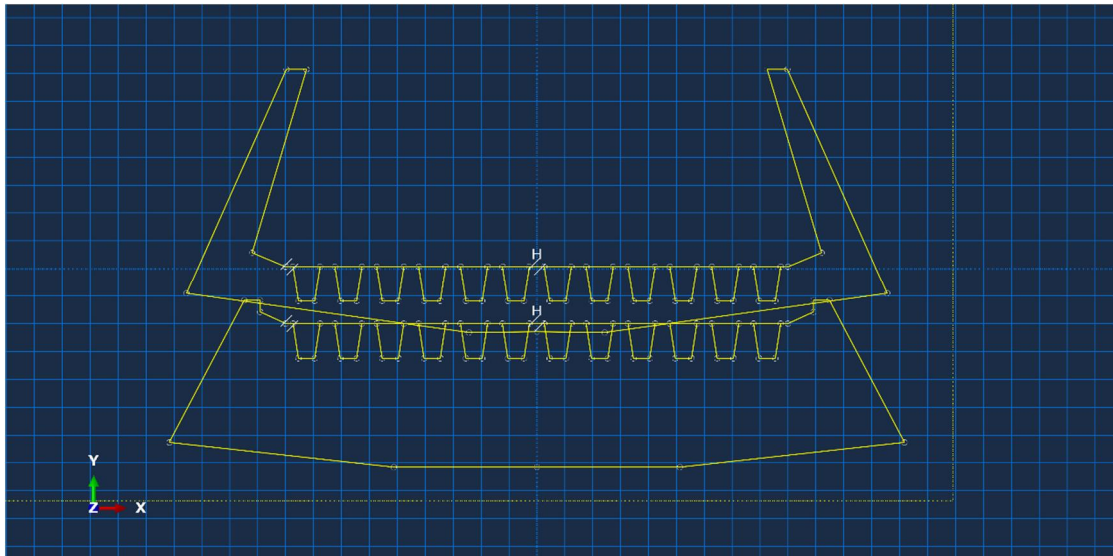
Figure 5.4 – Drawing of the new cross section with the corrugated deck

A first attempt was to draw the corrugated deck into the 6 different cross section that were used earlier to build the entire bridge, then these were imported into the sketch module of Brigade Plus to proceed with the same steps as in the earlier model. Shortly after, the two cross sections were extruded and the Loft function was put into use, *see* Figure 5.5.
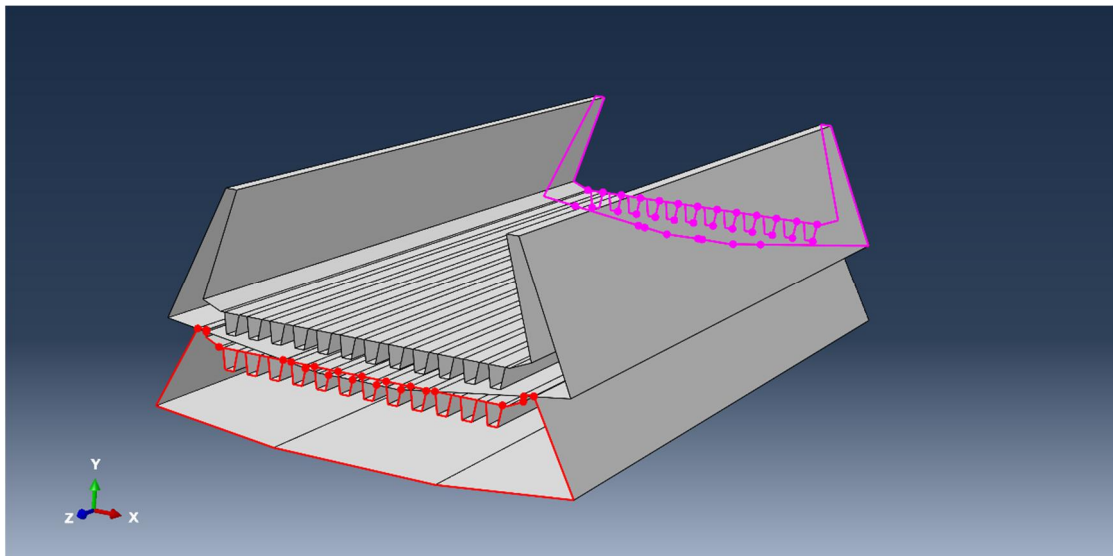
Figure 5.5 – First attempt of the Loft function in the new cross sections

Figure 5.5 shows how the two faces had been selected to create the paths to connect the edges, but this was not possible due to the fact that the Loft function only was able to proceed if the faces were one continuous loop of segments. This was not the case because the ribs were one loop of its own in another loop which was the entire cross section. In addition, the LOFT function does not work correctly when the amount of edges is too high so another alternative had to be found.

Despite the great amount of failed attempts, a new solution could be found to model this particular type of cross section. Some minor modification had to be made to the original cross sections in order to use another function in the program. To build one entire piece two steps were necessary in this case, and two different functions were used. For this reason, all the cross sections had to be modified to have a straight and continuous width of the deck along the entire bridge. The deck varied slightly in width and had a small bank, after the adjustment the deck was straight and the width was constant, it is believed that these minor adjustments shouldn't affect the behavior of the structure considerably.

The first step is to model one piece of the bridge with its corresponding new cross sections using the Loft function as it was done earlier. However, this time the corrugated deck will not be included and only the cross section with the top part of the deck will be modeled, *see* Figure 5.6.
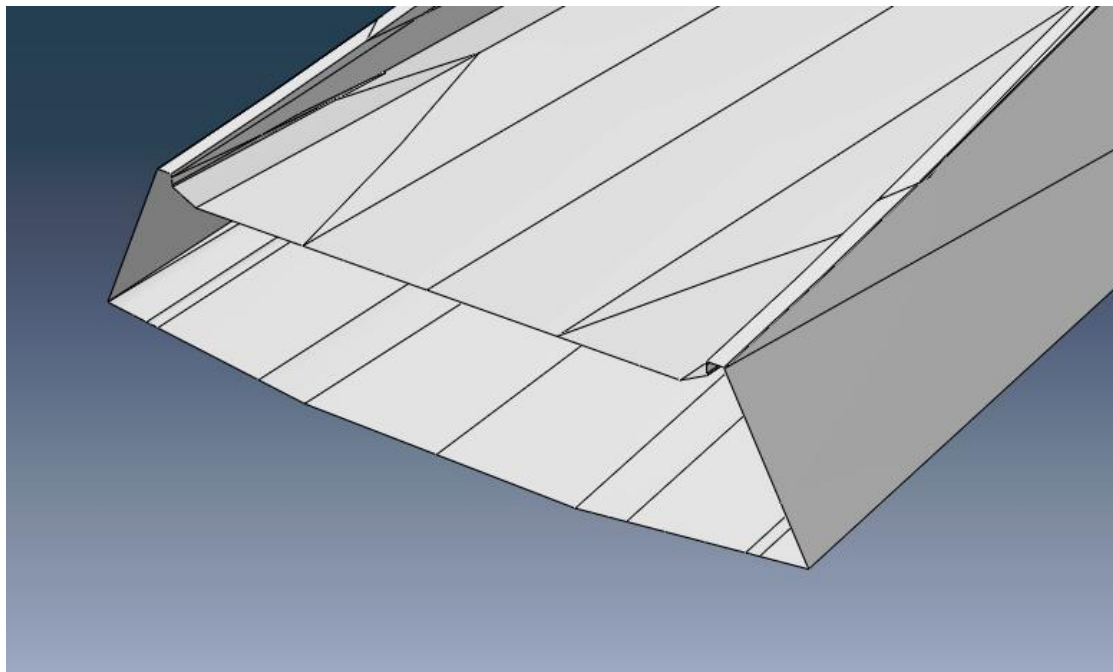
Figure 5.6 – Part of the bridge with a straight deck and no ribs

The second step is to model only the corrugated deck using the Sweep function, with this function it is possible extrude a cross section along a path that can be defined by the user.

The main idea is to model a piece with the cross sections without the ribs, then the corrugated deck will be modeled using the Sweep function following the same path as the deck in the previous model. Consequently, the modeled corrugated deck would fit perfectly with the remaining cross section and it would just be a matter of putting them together, *see* Figure 5.7.
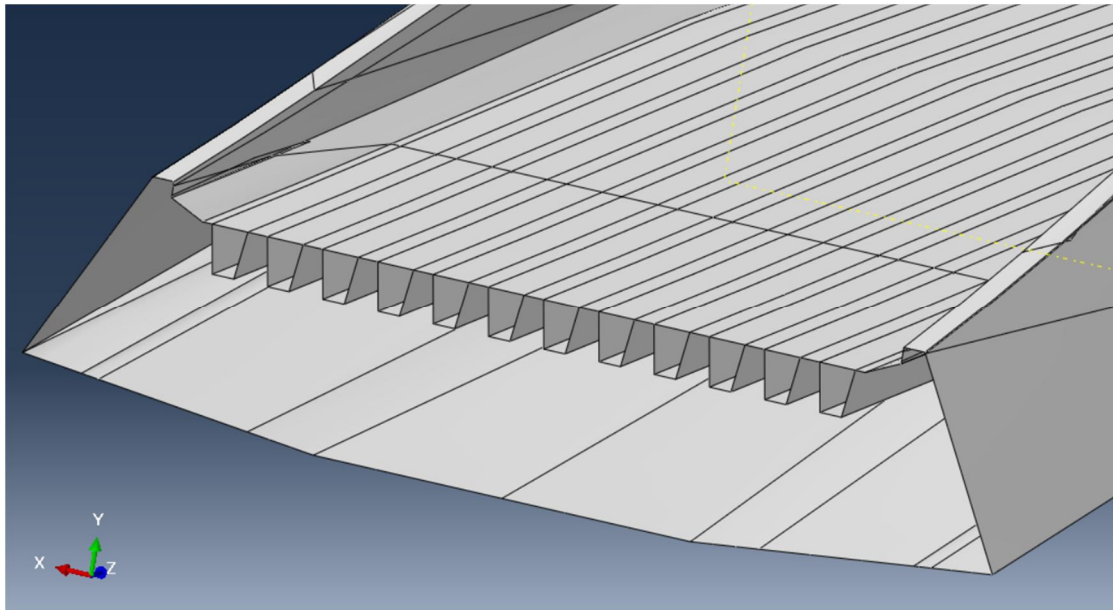
Figure 5.7 – Corrugated deck and remaining structure put together

The Sweep function was used to model the corrugated deck one piece at a time, after the 5 pieces were modeled they were put together to build the entire bridge. The reason for this procedure was that the longer the path on which the extrusion was made, the larger the error. The first attempt was to use the Sweep function for the entire bridge but it was noticeable that the extrusion was not accurate enough and the corrugated deck and the reaming structure did not fit perfectly. Hence, the extrusion was made for each piece and then assembled together.

Despite the accuracy in the drawings/sketches and the meticulous attention to details, Brigade Plus presents still some minor imperfections which will not be discussed in this dissertation. These minor details were fixed and finally a complete model of the bridge with a continuous corrugated deck across the entire bridge was possible to model, *see* Figure 5.8.
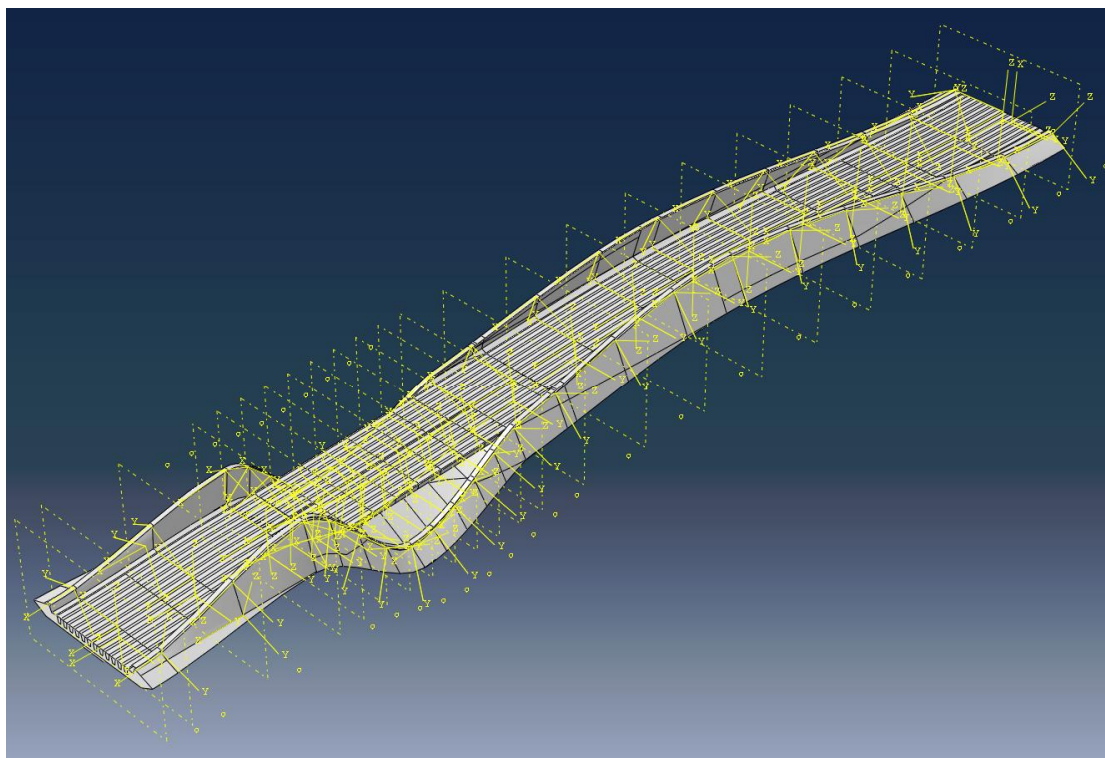
Figure 5.8 – Entire bridge with the continuous corrugated deck

5.4   Carbon fiber reinforcement

Carbon fiber is one of the strongest materials available in the market today; it is slightly heavier than glass fiber but has a higher modulus of elasticity. After some further investigation and advice from experienced engineers, it was understood that the bridge needed a carbon fiber reinforcement to fulfill the deflection limitations. This material may be one of the strongest ones but is also one of the most expensive, for this reason it has to be used wisely to avoid an overpriced structure.

The main idea is to use as little carbon fiber as possible, to do this the area has to be minimized and the lever arm has to be maximized to optimize the carbon fiber contribution. Accordingly, the carbon fiber is placed at the most outer position, over the side wings and under the bridge. As the reinforcement material is to be implemented together with the glass fiber composite, it can be modeled as carbon fiber laminates of stripes. An approximate calculation was made with a simple supported beam with the length of the longest span of the bridge (39 meters) and the contribution of the carbon fiber in an average cross section to estimate the area of carbon fiber needed to fulfill the deflection criteria. The top reinforcements have a thickness of 1 cm and an area of 20 cm2 (20cm x 1cm) and the bottom reinforcement has an area of 510 cm2 (510cm x 1cm), *see* Figure 5.9.
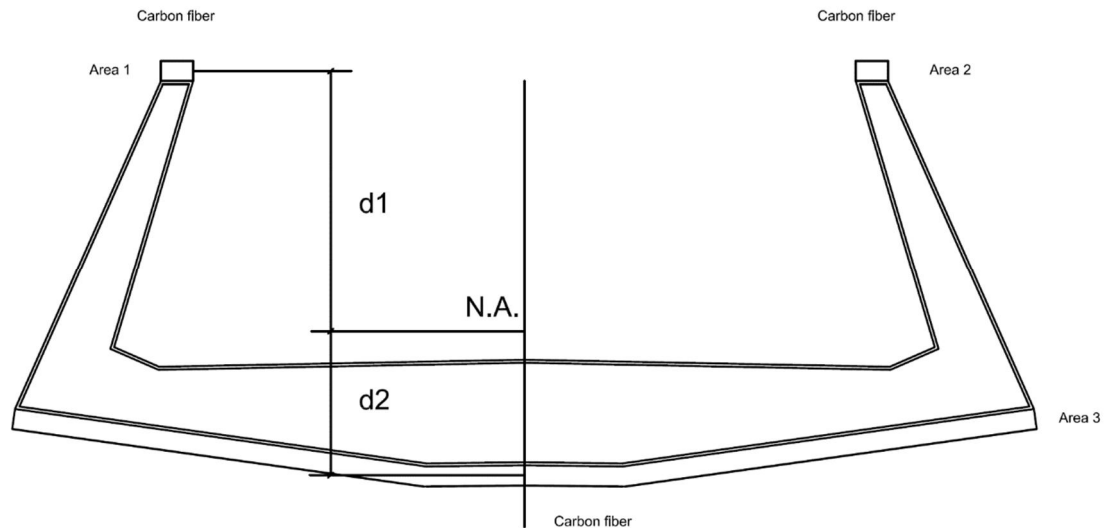
Figure 5.9 – Location of the carbon fiber reinforcement and their distance to the neutral axis

Furthermore, to model the reinforcement into Brigade Plus the carbon fiber stripes were modelled as 2D shell elements using the Sweep function using the path of the location of the reinforcement. To ensure a complete interaction between the carbon fiber and the sandwich panel structure these were connected using the module Interaction in Brigade Plus and connecting the corresponding faces with the Tie function.

Due to the varying form of the bottom part of the structure, the bottom reinforcement was modelled as a narrower strip under the bridge but with the same cross sectional area and the same type of interaction, *see* Figure 5.10. After the carbon fiber reinforcement was incorporated into the model it was possible to study different alternatives and find a satisfying solution.

In this manner, many cases were modelled and studied using different carbon fiber areas, different foam thicknesses, different ply orientations and different ply thicknesses. These different cases made possible understand how changing the properties of the different components of the bridge affected their stiffness and behavior.
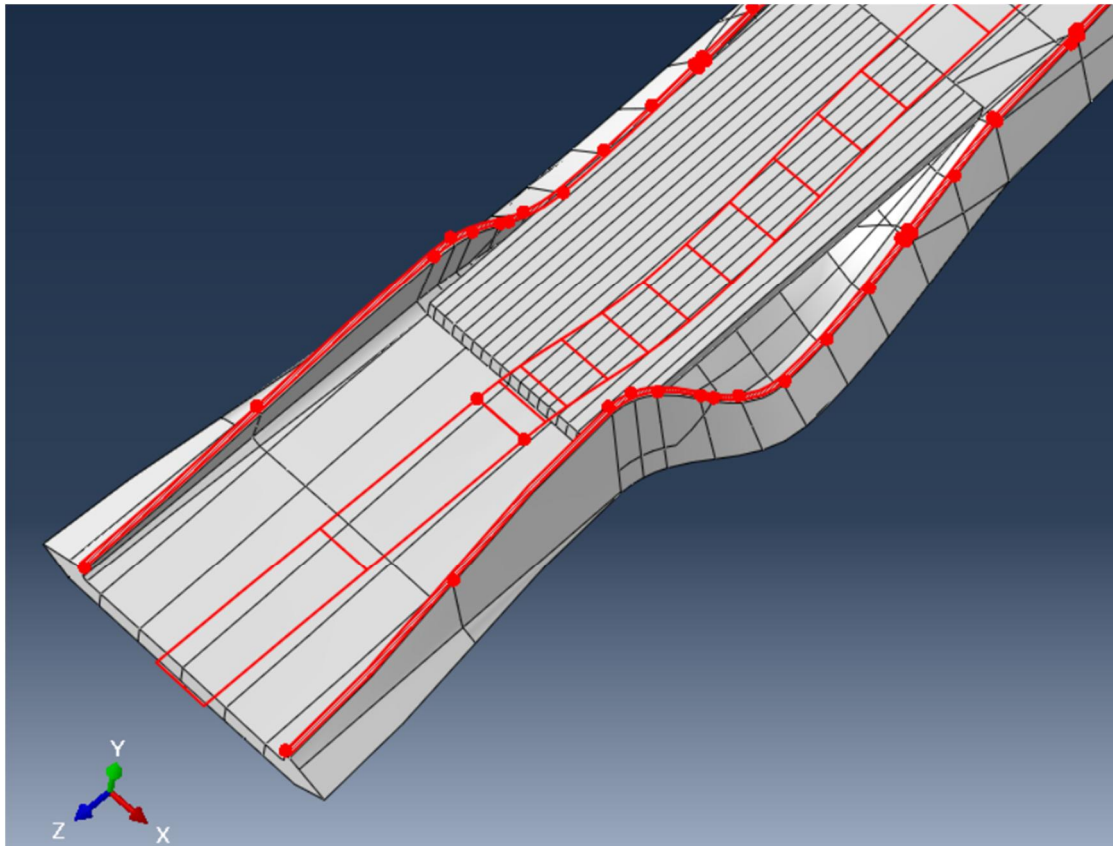
Figure 5.10 – Position of the carbon fiber reinforcement stripes along the bridge

5.5   Orthotropic material definition in Brigade Plus

An orthotropic material is the one that has different properties in different orthogonal directions, in this case longitudinal and transversal denominated axis 1 and 2 respectively. These properties have to be defined in Brigade Plus together with their own local coordinate system. This step is very important because the local coordinate system define the orthogonal orientation (direction) of each particular section of the bridge. If a local coordinate is not defined then the material properties will follow the global coordinates instead (x,y,z).

The entire structure can be divided infinitely increasing the accuracy of the model but the purpose of this study is to divide it enough to provide reasonable results. In this case the bridge as divided every 3 meters where the geometry did not vary too much and every 1 meter where the geometry varied considerably, like the center support section. The geometry was divided both in the longitudinal direction and the transversal direction, *see* Figure 5.11 *and* Figure 5.12.
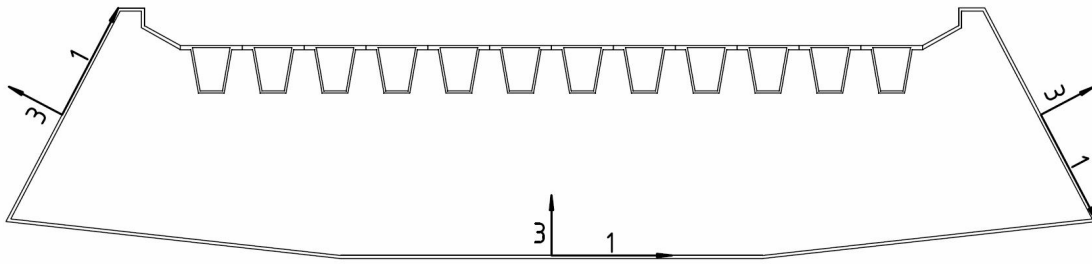
Figure 5.11 – Orientation of the local coordinate system in a transversal cross-section
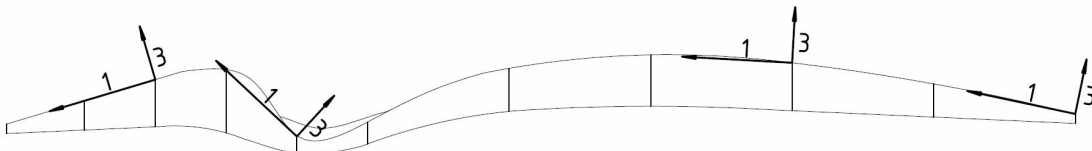
Figure 5.12 – Orientation of the local coordinate system in a longitudinal cross-section
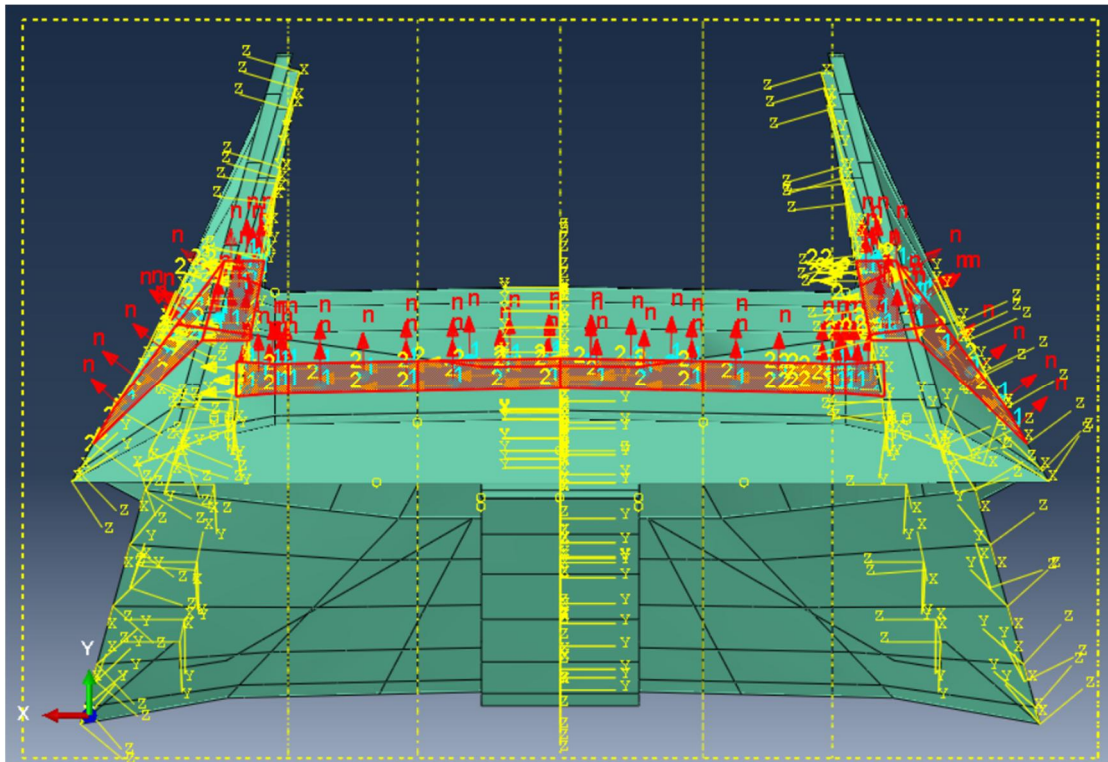
Figure 5.13 – Orientation of the local coordinate system as seen in Brigade Plus

5.6   Sandwich panel configurations

The sandwich panel consists of a combination of different materials with different properties. All these combined to obtain one equivalent material with equivalent properties. The reason to have an equivalent orthotropic material is to simplify the modelling phase. Modelling all the materials in Brigade Plus is time demanding and the difference in the results may not be as significant.

The different materials that compose the sandwich panel are glass fiber and foam filling. Foam is a very light material mainly used to fill empty spaces and provide

formwork. The contribution of the foam in the sandwich panel is to displace the glass fiber layer away from the neutral axis and increase the lever arm.

The equivalent properties are obtained using the developed MatLab routine explained in Chapter 2, to include the contribution of the foam the same principle was used only that in this case the foam is included as a very thick layer with a stiffness matrix equal to zero. With this modification the foams stiffness contribution is neglected and only the spacing between the fiber layers is taken into account, *see* Figure 5.14.

0°	t1
+45°	t2
-45°	t3
90°	t4
Foam	t5
90°	t4
-45°	t3
+45°	t2
0°	t1

Figure 5.14 – Sandwich panel detail for different configurations

Accordingly, the criteria used to organize the different layers after running some tests is to place the strongest orientation on the outer side and neglect the foam's contribution to the stiffness. It is also important to have a symmetric configuration and avoid drastic orientation changes to prevent interlaminate residual stresses. All the different configurations created and used in the model are shown in Table 5.1.

Table 5.1 – Configuration details for the sandwich panel

Configuration Code	001	002	003	004	005	006	007	008	009
t1(mm)	0.250	0.500	0.500	0.500	2	2	2	4	4
t2(mm)	0.125	0.125	0.125	0.125	0.125	0.25	0.25	0.25	0.25
t3(mm)	0.125	0.125	0.125	0.125	0.125	0.25	0.25	0.25	0.25
t4(mm)	0.500	0.250	0.25	0.25	0.25	0.25	0.25	0.25	0.25
t5(mm)	8	8	13	18	15	24.5	34.5	30.5	40.5
E11(MPa)	9.8779	11.166	7.8236	6.0141	17.093	12.673	9.8887	16.897	14.143
E22(MPa)	8.0305	6.960	5.1117	4.0186	5.849	4.779	3.8107	5.132	4.364
G12(MPa)	2.2470	2.160	1.5571	1.2133	1.982	1.790	1.4235	1.92	1.630
G23(MPa)	3.2560	2.732		1.5913	2.233	1.756	1.4014	1.8937	1.6104
υ12	0.2215	0.2442	0.2400	0.2380	0.2533	0.2883	0.288	0.2795	0.2797
υ21	0.1800	0.1522	0.1568	0.1590	0.0867	0.1087	0.111	0.0849	0.0863
υ23	0.2333	0.2740				0.3611	0.3596	0.3551	0.3549
ρ(kg/m3)	420.8	420.8		252.9	504.75	392.37	315.75	483.81	404

During the design process different configurations were studied in order to meet the deflection requirements, Table 5.1 shows all the values the MatLab routine calculates which are used as input in Brigade Plus.

6 Final preliminary design

The ultimate goal of all the modifications and improvements presented in the previous chapters is to build up this final preliminary model. Undoubtedly, this is still a preliminary design and much more can be further developed, however, these are the results from the model obtained according to the time frame provided.

Correspondingly, the two main parameters that guided the development of the model were the deflection and the natural frequency. There are many ways to approach such a procedure, but given the properties of the FRP composite material, these two parameters are the most critical.

6.1 Deflection

As predicted from the very first beginning, the maximum deflection is located on the larger span of 34 meters towards the end support where the height of the bridge tends to reduce, *see* Figure 6.1 Final model perspective view, deflection. The deflection limit is L/400 which gives a value of 8.5 cm, the first models gave us deflections of over 2 meters long from fulfilling the requirement.

However, after many attempts and improvements the deflection in the final model is 7.63 cm. Actually, the total deflection is a bit higher than that but given that the bridge has a chambered form in both spans, these account for the deflection of the self-weight. Consequently, the deflection value has to be measured after the bridge has deflected due to its own weight. To be more specific, the deflection in the model is measured taking into account only the pedestrian live load.
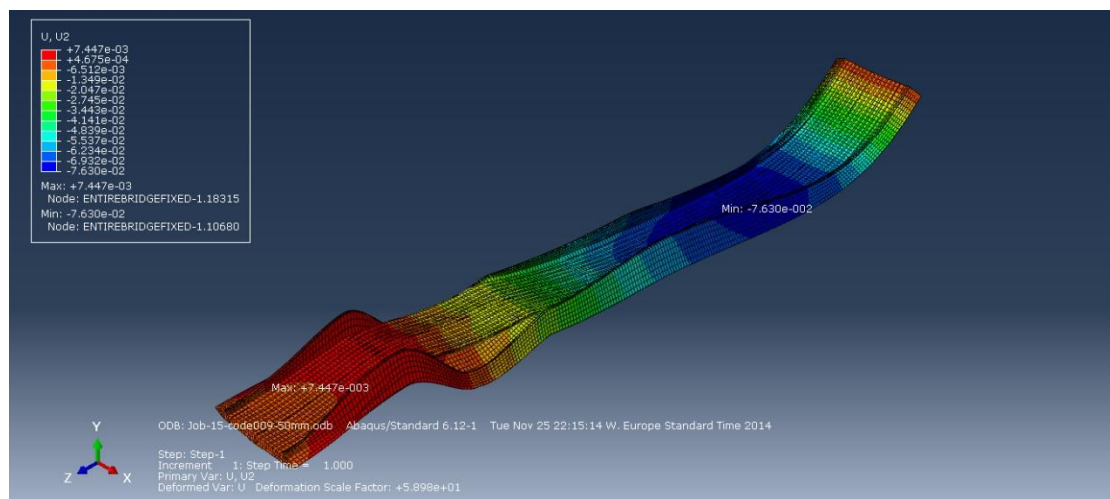
Figure 6.1 Final model perspective view, deflection
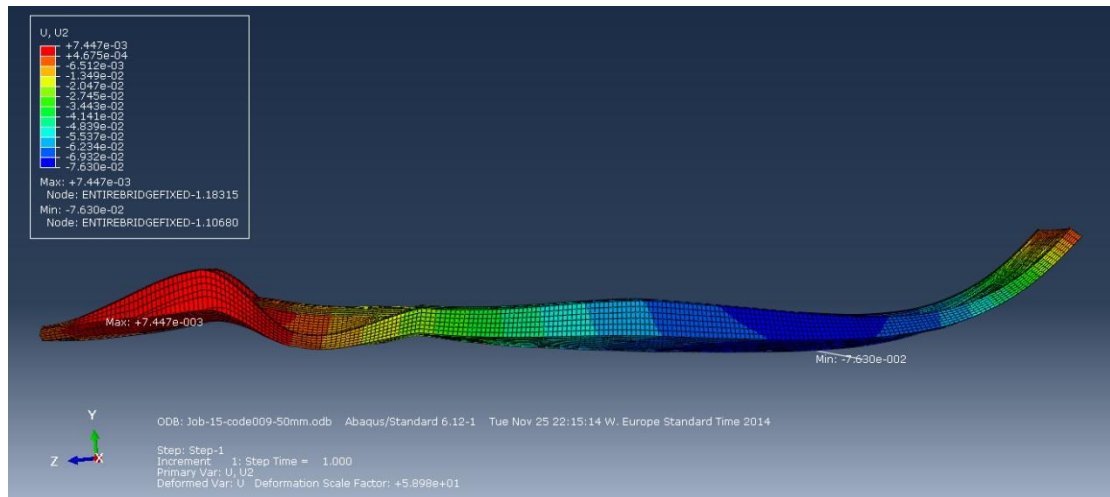
Figure 6.2 Final model side view, deflection

6.2 Frequency

The set frequency parameter was 5 Hz to ensure that the natural frequency could not be caused by a human induced vibration. The first attempts to surpass this value begun at 1.8 Hz and by improving the stiffness of the bridge with a stiffer deck and a sandwich panel cross-section the natural frequency of the bridge increased.

For these reasons, the first mode of the natural frequency of the bridge went up to 3.8 Hz, not reaching the minimum required frequency. This means that a dynamic assessment has to be done to verify the limit accelerations and velocities, but it does not mean that the model can't be improved further to reach the limit frequency. The total weight of the bridge is 24.7 tons, which is quite more than predicted, compared to a preliminary design made by Ramböll of an equivalent structure in steel.
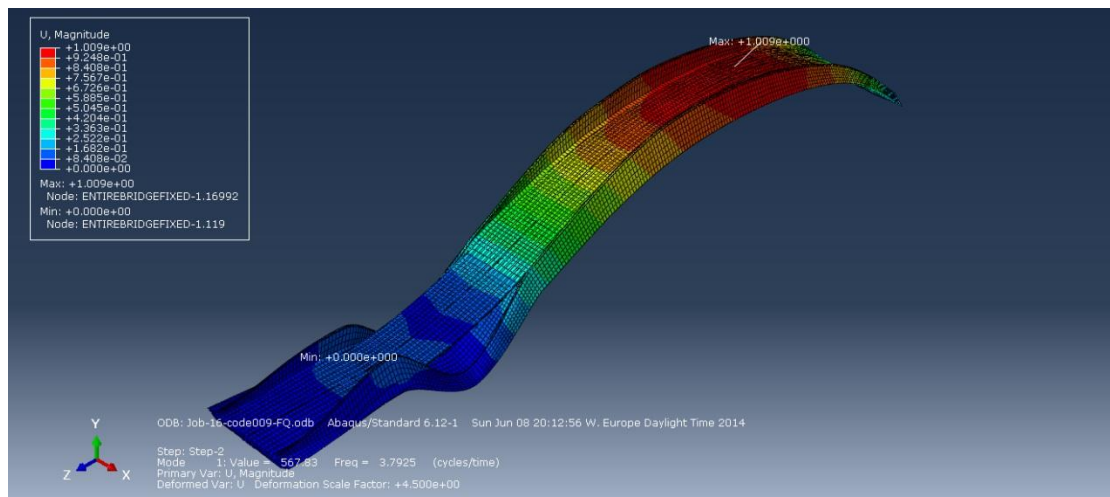
Figure 6.3 Final model, frequency mode 1
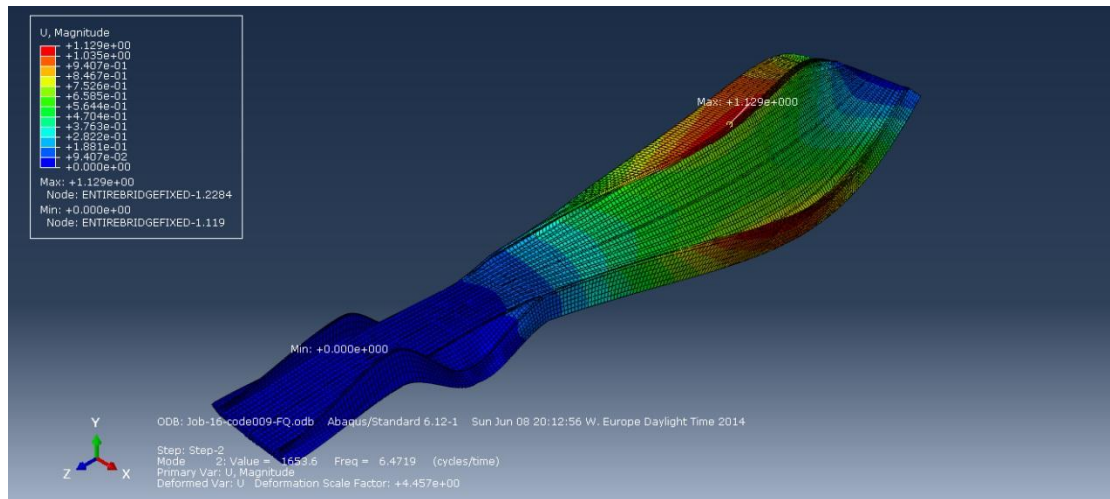
Figure 6.4 Final model, frequency mode 2

Table 6.1 Final results

Final preliminary design	Requirement	First attempt	Final attempt
Deflection	less than 8.5 cm	over 2 m long	7.63 cm
Frequency	more than 5 Hz	1.8 Hz	3.8 Hz

It can be seen from the analysis above that, being this a preliminary design for such an innovative and complex structure, the basic design parameters were identified and tackled. Table 6.1 Final results show that the natural frequency of the structure is not above the one required but there was certainly a big progress towards full filing the requirements.

An equally significant aspect is the lateral frequency, the second mode in this particular case, with a value of 6.47 Hz. This property was not emphasized because it is far above the lateral frequency limit, 2.5 Hz.

CHALMERS, *Civil and Environmental Engineering*, Master's Thesis 2015:141

7 Conclusion and future research

7.1 Conclusion

In this master thesis project, the preliminary design of the FRP pedestrian bridge is accomplished. The authors combined the developed MATLAB routine for particular material like FRP composites with the design philosophy from bridge engineering sector, and this design could solve both aesthetical and geographical problems of the bridge. Last but not least, after being tackled by such practical issues, several major conclusions can be drawn as follow:

- The complexity of the geometry interrupted the continuity of the modelling process due to the lack of skillful manipulation in BRIGADE/PLUS. A lot of trial and errors were performed repeatedly in the modelling part, and that consumed considerable time more than expected.
- In the design of FRP material properties, laminate thickness, selection of constituent materials, the fiber's orientation angle and the lamina stack-up sequence principally affect the overall laminate properties of the material.
- The study indicated that the effect of the carbon fiber reinforcement is reduced if the main structure is not stiff enough to transfer the load to the reinforcement.
- In the design of FRP pedestrian bridge, the sandwich panel with foam core is a promising solution due to lightweight and higher stiffness hence improving the dynamic behavior of the structure.
- The design of the corrugated bridge deck is governed by the choice of maintenance vehicle due to local flexural bending stresses induced by the heavy concentrated vehicle wheel loads. The dimensions of the corrugated deck can be further optimized to a more efficient and economical solution if the weight of maintenance vehicle is appropriately reduced.

7.2 Future research

As the vertical frequency of the FRP pedestrian bridge falls within the critical range, to answer whether the damping devices are required or not, further study on the dynamic assessment of different design situations which are defined by corresponding traffic classes and chosen comfort levels must be performed.

According to the design guidelines for FRP composite materials from AASHTO [16], when choosing individually between bolted connections and adhesive bonding connection in FRP composite structures, bolted connections is a better option since it has been substantially tested and documented. However, one can be used in conjunction with another. Therefore, the identification of needed further research on connection design and detailed analysis such as strength verification of bonded connection is highly compulsory.

When there is change in temperature or moisture content in laminate structures, instant deformation induced by thermal and hygroscopic stresses can occur. Therefore, further investigation on hygrothermal effects should be studied thoroughly.

As discussed with Ramböll AB to further improve the model, if the weight of maintenance vehicle which is the source of heavy concentrated load on the bridge deck is able to change, a lighter solution for corrugated bridge deck is very possible to achieve. This can be realized by further study on optimization analysis regarding with various laminate configurations.

Some other additional topics for further research that should be studied on are

- Life-cycle cost (LCC) analysis
- Life-cycle assessment (LCA) and
- Long term effects

Bibliography

[1]   D. Kendall, "Fibre reinforced Polymer composite bridges," vol. 3, D. Kendall, Ed. National Composites Network, 1992.

[2]   I. Nishizaki, T. Nobufumi, I. Yoshio, and S. Takumi, "A Case Study of Life Cycle Cost based on a Real FRP Bridge," 2006, no. Cice, pp. 99–102.

[3]   Scanscot Technology, "BRIGADE PLUS User's Manual." Scanscot Technology, 2013.

[4]   Scanscot Technology, "BRIGADE STANDARD User's Manual." Scanscot Technology.

[5]   J. L.Clarke, Ed., *Structural Design of Polymer Composites (EUROCOMP Design Code and Handbook)*. E & FN Spon, 2005.

[6]   H. Cristoph, B. Christiane, K. Andreas, S. Mike, G. Arndt, T. Stefan, L. Mladen, C. Bruno, L. Armand, M. Pierre-Olivier, C. Alvaro, and C. Elsa, "Design of Lightweight Footbridges for Human Induced Vibrations," Italy, 2009.

[7]   EN 1990:2002/A1:2005, "Eurocode - Basis of structural design," *Eurocode*, vol. 1990, no. 2002, p. 78, 2002.

[8]   1946 Mallick, P.K., *Fiber-Reinforced Composites-Material, Manufacturing, and Design*, Third edit. Dearborn: Taylor & Francis Group, 2008.

[9]   P. B. Potyrala, "Use of fibre reinforced polymeromposites in bridge construction. State of the art in hybrid and all-composite structures," 2011.

[10]   N. ExpO, "Aramid fiber fabric RA320H5." [Online]. Available: http://www.nauticexpo.com/prod/gurit/product-27794-229518.html.

[11]   S. Dylan, "Carbon fiber fabric." [Online]. Available: www.dylansimon.com/blog/carbon-fiber/.

[12]   V. Mara, "Fibre reinforced polymer bridge decks: A feasibility study on upgrading existing concrete-steel bridges," CHALMERS UNIVERSITY OF TECHNOLOGY, 2011.

[13]   Manoochehr Zoghi, Ed., "The International Handbook of FRP COMPOSITES IN CIVIL ENGINEERING," CPC Press, 2014, pp. 15–77.

[14]   W. VAN PAEPEGEM, "Stacking up sequence of a composite laminate." [Online]. Available: http://www.composites.ugent.be/home_made_composites/what_are_composites.html.

[15]   V. Mara, "Fibre reinforced polymer bridge decks : Sustainability and a novel panel-level connection," Chalmers University of Technology, 2014.

[16]   E.T.Techtonics, "Guide Specifications for Design of FRP PEDSTRIAN BRIDGES." AASHTO, 2008.

[17]   AASHTO, "LRFD Guide Specifications for the Design of Pedestrian Bridges (Final Draft)," vol. 5, 2009.

[18]   F. Jin, P. Feng, and L. Ye, "Study on Dynamic Characteristics of Light-Weight FRP Footbridge," pp. 27–30, 2010.

[19]   K. C. Bhagwan D. Agarwal, Lawrence J. Broutman, *Analysis and Performance of Fiber Composites*, Third Edit. John Wiley & Sons, 2006.

[20]   M. C.Y.Niu, "Composite Airframe Structures," First edit., Hong Kong: CONMILIT PRESS LTD., 1992, p. P.383 to P.446.

[21]   EN 1991-2:2003, "Eurocode 1: Actions on structures, Part 2:Traffic loads on bridges" *Eurocode*, vol. 1991, no. 2003, p. 54, 2003.

APPENDIX A – MATLAB scripts

```
%----------------------FRP composite material design---------------------

clear all
close all
clc


%% Bibliography
%
%
% Ref.1= Analysis Performance of Fiber Composites (Bhagwan D.Agarwal) [19]
%
% Ref.2= Eurocomp:Structural Design of Polymer composites (John.L.Clarke)[5]
%
% Ref.3= Composites Airframe Structures (Michael C.Y.Niu) [20]
%
% Ref.4= The international Handbook of FRP Composites in Civil Engineering
(Manoochehr Zoghi) [13]
%
% Ref.5= Fiber-Reinforced Composites (P.K.Mallick) [8]
%
% Ref.6= FRP bridge decks: sustainability and a novel panel-level
%                         connection. (Valbona Mara) [15]


%% Routine:  Equivalent elastic material properties

%% Input variables

prompt='What is the number of total layers (symmetrical laminates)?\n ';
Total_layers = input(prompt)

fprintf('The unit of ply thickness is in (mm) \n\n');
i=0;
t=zeros(Total_layers,1);
while i<Total_layers
    fprintf('Ply %d:',i+1);
    prompt=' The thickness of the ply is ';
    thickness=input(prompt)
    i=i+1;
    t(i,1)=t(i,1)+thickness;
end

%tt=insert(0,t,2)
if i==Total_layers

    tt=[t(1:i/2);0;t(i/2+1:end)];
end

i=0;
theta=zeros(Total_layers,1);
while i<Total_layers
    fprintf('\n Ply %d:',i+1);
    prompt=' The fiber orientation angle of the ply is ';
    angle=input(prompt)
    i=i+1;
    theta(i,1)=theta(i,1)+angle;
end
t                       % thickness of each lamina          [m]
theta                   %  angle of fiber's orientation   [degree]

num=length(theta);      % total number of laminae in a laminate
```

```
% Core_thickness='What is the thickness of the core (foam)(mm)?\n ';
% CT = input(Core_thickness)

Normal_force='What is the applied normal forces N=[Nx; Ny; Tauxy] (N/m)?\n
';
N = input(Normal_force)

Moment='What is the applied moments M=[Mx; My; mxy] (Nm/m)?\n ';
M = input(Moment)


%
% Fiber properties


Ef=220e9;           % E-glass fiber
v_f=0.2;
Gf=91.7e9;

% Matrix properties

Em=3.6e9;           % Epoxy resin
v_m=0.35;
Gm=1.33e9;

% Fiber volumn fraction

Vf=0.6;             % E-glass epoxy Table A4-1 from Ref.1

% Recommend to use symmetric (balanced) laminates to reduce buckling loads,
% warpage,twisting from residual stress. [Ref.6 P.37]


%% Step 0: Obtain lamina properties

% E11=Vf*Ef+(1-Vf)*Em;          % Eq. 7.3.1 from Ref.3
% E22=Em*Ef/(Ef*(1-Vf)+Em*Vf);  % Eq. 7.3.4 from Ref.3
% v12=v_f*Vf+v_m*(1-Vf);        % Eq. 7.3.3 from Ref.3
% v21=v12*E22/E11;              % Eq. 4.12  from Ref.4
% G12=Gm*Gf/(Gf*(1-Vf)+Gm*Vf);  % Eq. 7.3.5 from Ref.3


% Choose E-glass epoxy ( the material properties are obtained from
%                     Appendix A.4 Table A4-1 P.549 Ref.1)

E11=33.180e9;       % Longitudial elastic modulus [Pa] E_L
E22=7.740e9;        % Transversal elastic modulus [Pa] E_T
v12=0.267;          % major poisson's ratio            v_LT
v21=v12*E22/E11; % minor poisson's ratio            v_TL
G12=2.910e9;        % in-plane shear modulus           G_LT
% v23=v12*(1-v21)/(1-v12);
% G23=E22/(2*(1+v23));
%
% v23
% G23
%
% sigmaLU=1062e6;  % Ultimate tensile strength in Longitudinal direction
[Pa]
% sigmaTU=31e6;    % Ultimate tensile strength in Transverse direction
[Pa]
% TauLTU=72e6;     % Ultimate shear strength
[Pa]

% E11=133.44e9;       % Longitudial elastic modulus [Pa] E_L
% E22=8.78e9;        % Transversal elastic modulus [Pa] E_T
% v12=0.26;          % major poisson's ratio            v_LT
% v21=v12*E22/E11; % minor poisson's ratio            v_TL
```

CHALMERS, *Civil and Environmental Engineering*, Master's Thesis 2015:141

```
% G12=3.254e9;          % in-plane shear modulus           G_LT

sigmaLU=1062e6;  % Ultimate tensile strength in Longitudinal direction [Pa]
sigmaTU=31e6;    % Ultimate tensile strength in Transverse direction   [Pa]
TauLTU=72e6;     % Ultimate shear strength                             [Pa]

sigmaLU_prime=610e6; % Ultimate compressive strength in Longitudinal
direction [Pa]
sigmaTU_prime=118e6; % Ultimate compressive strength in Transverse direction
[Pa]


if N(1)>0 && N(2)>0
    strength=[sigmaLU; sigmaTU; TauLTU];

elseif N(1)<0 && N(2)<0
    strength=[sigmaLU_prime; sigmaTU_prime; TauLTU];

elseif N(1)<0 && N(2)>0
     strength=[sigmaLU_prime; sigmaTU; TauLTU];

elseif N(1)>0 && N(2)<0
     strength=[sigmaLU; sigmaTU_prime; TauLTU];
end
```

Step 1: Determine lamina reduced stiffness values Q_{ij}

% From the pre-determined elastic properties $E_{11}, E_{22}, G_{12}, v_{12}$,
% v_{21} of each lamina, determine the reduced stiffness terms Q_{11},
% $Q_{22}, Q_{66} \,and\, Q_{12}$
%
% $Q_{11} = \frac{E_{11}}{(1-v_{12} * v_{21})},$
%
% $Q_{12} = \frac{v_{21}*E_{11}}{(1-v_{12} * v_{21})},$
%
% $Q_{22} = \frac{E_{22}}{(1-v_{12} * v_{21})},$
%
% $Q_{66} = G_{12}$

```
Q11=E11/(1-v12*v21);       % Eq. 4.52 from Ref.2
Q12=v21*E11/(1-v12*v21);
Q22=E22/(1-v12*v21);
Q66=G12;

Q=[Q11 Q12 0;
   Q12 Q22 0;
    0    0  Q66];
```

Step 2: Calculate lamina transformed reduced stiffness $\bar Q_{ij}$

% Having obtained the lamina reduced stiffness terms Q_{ij} for each
% lamina, calculate the transformed lamina reduced stiffness terms
% $\bar Q_{ij}$ for a given of orientation
%
%
% $U_1 = \frac{3*Q_{11}+3*Q_{22}+2*Q_{12}+2*Q_{66}}{8}$
%
% $U_2 = \frac{Q_{11}-Q_{22}}{2}$
%
% $U_3 = \frac{Q_{11}+Q_{22}-2*Q_{12}-4*Q_{66}}{8}$
%
% $U_4 = \frac{Q_{11}+Q_{22}+6*Q_{12}-4*Q_{66}}{8}$
%
% $U_5 = \frac{Q_{11}+Q_{22}-2*Q_{12}+4*Q_{66}}{8}$
%
% $\bar Q_{11} = U_1+U_2*\cos(2\theta)+U_3*\cos(4\theta)$
%
% $\bar Q_{22} = U_1-U_2*\cos(2\theta)+U_3*\cos(4\theta)$

```
%
% $\bar Q_{12} = U_4-U_3*\cos(4\theta)$
%
% $$\bar Q_{16} = 0.5*U_2*\sin(2\theta)+U_3*\sin(4\theta)$
%
% $\bar Q_{26} = 0.5*U_2*\sin(2\theta)-U_3*\sin(4\theta)$
%
% $\bar Q_{66} = U_5-U_3*\cos(4\theta)$
%
% $\bar Q$=
% $$ \left[
% \begin{array}{ c c c }
%     \bar Q_{11} & \bar Q_{12} & \bar Q_{16}\\
%     \bar Q_{12} & \bar Q_{22} & \bar Q_{26}\\
%     \bar Q_{16} & \bar Q_{26} & \bar Q_{66}
%  \end{array} \right]$

U1=(3*Q11+3*Q22+2*Q12+4*Q66)/8;          % Eq. 3.81 from Ref.5
U2=(Q11-Q22)/2;
U3=(Q11+Q22-2*Q12-4*Q66)/8;
U4=(Q11+Q22+6*Q12-4*Q66)/8;
U5=(Q11+Q22-2*Q12+4*Q66)/8;

Qbar11=U1+U2*cosd(2*theta)+U3*cosd(4*theta); % Eq. 3.80 from Ref.5
Qbar22=U1-U2*cosd(2*theta)+U3*cosd(4*theta);
Qbar12=U4-U3*cosd(4*theta);
Qbar16=0.5*U2*sind(2*theta)+U3*sind(4*theta);
Qbar26=0.5*U2*sind(2*theta)-U3*sind(4*theta);
Qbar66=U5-U3*cosd(4*theta);

% Qbar={Qbar11 Qbar12 Qbar16;
%       Qbar12 Qbar22 Qbar26;
%       Qbar16 Qbar26 Qbar66};

Qbar=cell(num,1);            % [Pa]

 for k=1:num
     if theta(k)==100
        Qbar{k,1}=zeros(3);
     else
        Qbar{k,1}=[Qbar11(k) Qbar12(k) Qbar16(k);
                   Qbar12(k) Qbar22(k) Qbar26(k);
                   Qbar16(k) Qbar26(k) Qbar66(k)];
 end
 end

%% Step 3: Determine coordinates $h_k$ for each lamina from the bottom
surface
% Determine $h_{k-1}$, the distance from the midplane of the laminate to the
% lower surface of the $k^{th}$ layer, and $h_k$, the distance to the upper
layer
% surface of the $k^{th}$ layer for each lamina in a laminate configuration.

% for i=1:num+1
%      h(i)=(i-1)*t-(t*num)/2;
% end

for i=1:num+1
    h(i)=-(sum(tt(i:end))-sum(tt(ceil((num+1)/2):end)));

    if i > (num/2+1)
        h(i)=sum(tt(1:i))-sum(tt(1:num/2));
    end
end

for i=1:num
    ha(i)=h(i+1)-h(i);
    hb(i)=h(i+1)^2-h(i)^2;
```

CHALMERS, *Civil and Environmental Engineering*, Master's Thesis 2015:141

```matlab
    hd(i)=h(i+1)^3-h(i)^3;
end
```

```matlab
%% Step 4: Determine the $A_{ij}, B_{ij}, D_{ij}$ terms for the laminate
% Note: $A_{ij},B_{ij}, and D_{ij}$ are called laminate stiffness matrices
%
% $A_{ij}=\displaystyle\sum_{k=1}^{N} \bar Q_{ij}^{k}*(h_k-h_{k-1})$
%
% $B_{ij}=\frac{1}{2}\displaystyle\sum_{k=1}^{N} \bar Q_{ij}^{k}*(h_k^2-
h_{k-1}^2)$
%
% $D_{ij}=\frac{1}{3}\displaystyle\sum_{k=1}^{N} \bar Q_{ij}^{k}*(h_k^3-
h_{k-1}^3)$
%

A=cell(num,1);

for k=1:num                      % Eq. 4.53 from Ref.2
    for i=1:3
        for j=1:3
            AA{k,1}(i,j)=Qbar{k,1}(i,j)*ha(k);%(h(k+1)-h(k));          %
[N/m]
            BB{k,1}(i,j)=(Qbar{k,1}(i,j)*hb(k))/2;%(h(k+1)^2-h(k)^2))/2;  %
[N]
            DD{k,1}(i,j)=(Qbar{k,1}(i,j)*hd(k))/3;%(h(k+1)^3-h(k)^3))/3;  %
[Nm]
        end
    end
end

A=sum(cat(3,AA{:}),3)
B=sum(cat(3,BB{:}),3)
D=sum(cat(3,DD{:}),3)
%% Step 5: Determine laminate compliances $a_{ij}, b_{ij}, and\,d_{ij}$
% Having obtained the laminate stiffness terms $A_{ij}, B_{ij},
and\,D_{ij}$, calculate
% the corresponding compliance terms $a_{ij}, b_{ij}, and\, d_{ij}$ by
inversing the
% laminate stiffness matrices.


a=inv(A);
b=inv(B);
d=inv(D);

%% Step 6: Determine the equivalent laminate elastic properties $E_{xx},
E_{yy}, G_{xy},v_{xy},v_{yx}$
%
% Having obtained the compliance terms $a_{ij}, b_{ij}, and\,d_{ij}$,
calculate the
% laminate membrane and bending equivalent elastic constants.
%
% The equivalent membrane elastic constants are
%
% $E_{xx}^N=\frac{1}{(num*t)*a_{11}}$
%
% $E_{yy}^N=\frac{1}{(num*t)*a_{22}}$
%
% $G_{xy}^N=\frac{1}{(num*t)*a_{66}}$
%
% $\nu_{xy}^N=-\frac{a_{12}}{a_{11}}$
%
% $\nu_{yx}^N=-\frac{a_{12}}{a_{22}}$
%
% The equivalent bending elastic constants are
%
% $E_{xx}^M=\frac{12}{(num*t)^3*d_{11}}$
```

```
%
% $E_{yy}^M=\frac{12}{(num*t)^3*d_{22}}$
%
% $G_{xy}^M=\frac{12}{(num*t)^3*d_{66}}$
%
% $\nu_{xy}^N=-\frac{d_{12}}{d_{11}}$
%
% $\nu_{yx}^N=-\frac{d_{12}}{d_{22}}$
%

% The equivalent membrane elastic constants are

Exx_N=1/(sum(t)*a(1,1));              % Eq. 4.54 from Ref.2
Eyy_N=1/(sum(t)*a(2,2));
Gxy_N=1/(sum(t)*a(3,3));
vxy_N=-(a(1,2)/a(1,1));
vyx_N=-(a(1,2)/a(2,2));

Equivalent_modulus_Membrane=[Exx_N;Eyy_N;Gxy_N]
Equivalent_poisson_Membrane=[vxy_N;vyx_N]



% The equivalent bending elastic constants are

Exx_M=12/((sum(t))^3*d(1,1));         % Eq. 4.55 from Ref.2
Eyy_M=12/((sum(t))^3*d(2,2));
Gxy_M=12/((sum(t))^3*d(3,3));
vxy_M=-(d(1,2)/d(1,1));
vyx_M=-(d(1,2)/d(2,2));

Equivalent_modulus_Bending=[Exx_M;Eyy_M;Gxy_M]
Equivalent_poisson_Bending=[vxy_M;vyx_M]

v23=vxy_M*(1-vyx_M)/(1-vxy_M);
G23=Eyy_M/(2*(1+v23));

v23
G23



%% Routine: Laminate Stress analysis
% We use lamination theory to determine the stresses and strains in each
% lamina of a thin laminated structures.
%
%
% Step-by-step procedure to compute the stresses and strains in each lamina
%
% 1. Calculate the stiffness matrices for the laminate
%
% 2. Calculate the midplane strains and curvatures for the laminate due to
%    a given set of applied forces and moments
%
% 3. Calculate of in-plane strains for each lamina
%
% 4. Calculate of in-plane stresses in each lamina


%% Step 1: Obtain the laminate membrane, bending, and coupling stiffness
$A_{ij}, B_{ij}, D_{ij}$
% From the given laminate configurations and initial loads, determine
% laminate stiffnesses $A_{ij}, B_{ij}, D_{ij}$
%
% *Calculated from above*

%% Step 2: Calculate corresponding compliance terms $a1_{ij}, b1_{ij},
and\,d1_{ij}$ from $A_{ij}, B_{ij}, D_{ij}$
```

```matlab
% Note: for a symmetric laminate, $[B]=0,$
%                        $so\,   [a1] = [A]^{-1},$
%                               $[b1] = [c1] = [0],$
%                        $and\,  [d1] = [D]^{-1}$
%
% $[D^{*}]=[D]-[B][A^{-1}][B]$
%
% $[a_1]=[A^{-1}]+[A^{-1}][B][(D^{*})^{-1}][B][A^{-1}]$
%
% $[b_1]=-[A^{-1}][B][(D^{*})^{-1}]$
%
% $[c_1]=-[(D^{*})^{-1}][B][A^{-1}]=[B_1]^T$
%
% $[d_1]=[(D^{*})^{-1}]$
%
Dstar=D-B*inv(A)*B;                     % Eq. 3.95 from Ref.5
a1=inv(A)+inv(A)*B*inv(Dstar)*B*inv(A);
b1=-inv(A)*B*inv(Dstar);
c1=b1';
d1=inv(Dstar);


%% Step 3: Calculate the midplane strains and curvatures for the laminate
% From a given set of normal forces and moments, calculate laminate
% midplane deformations (
$\mathring{\epsilon_{xx}},\mathring{\epsilon_{yy}}, \mathring{\gamma_{xy}}$
) and
% curvatures ( $\kappa_{xx},\kappa_{yy}, \kappa_{xy}$ ) in the laminate
% reference axes x-y
%
% $[\mathring{\epsilon}]_{Global}=[a_1][N]+[b_1][M]$
%
% $[\mathring{\kappa}]_{Global}=[c_1][N]+[d_1][M]$
%
epsilon_Dot= a1*N + b1*M;        % Eq. 3.93 and 3.94 from Ref.5
kappa= c1*N + d1*M;


%% Step 4: Determine total strains in laminate reference axes x-y
% Knowing the midplane strains and curvature, for each lamina, calculate
% the total strain ( $\epsilon_{xx},\epsilon_{yy}, \gamma_{xy}$ ) arising
% from the membrane and bending strain contributions
%
%
$[\epsilon]_{Global}^j=[\mathring{\epsilon}]_{Global}^j+Z_j[\kappa]_{Global}
$
%
% * $Z_j$ is the distance from the lamniate midplane to the midplane of the
% $j^{th}$ lamina
%

epsilon_Global=cell(num,1);

for j=1:num
    z(j)=-(sum(t(j+1:num/2))+t(j,1)/2);
    if j==num/2
        z(j)=-t(j,1)/2
    elseif j==num/2+1
        z(j)=t(j,1)/2;
    elseif j>num/2+1
        z(j)=sum(t(num/2+1:j))-t(j,1)/2;
    end
    epsilon_Global{j,1}= epsilon_Dot+z(j)*kappa;  % Eq.3.105 from Ref.5
end

%% Step 5: Tranfrom the lamina strains from the laminate axis x-y to lamina
axis 1-2
% Tranform $\epsilon_{xx},\epsilon_{yy}, \gamma_{xy}\,$ to
$\epsilon_{11},\epsilon_{22}, \gamma_{12}$
%
```

```
% $[\epsilon]_{Local}^j=[T][\epsilon]_{Global}^j$
%

epsilon_Local=cell(num,1);
T=cell(num,1);                               % transformation matrix
for i=1:num
    m(i)=cosd(theta(i));
    n(i)=sind(theta(i));
    T{i}=[m(i)^2 n(i)^2 m(i)*n(i);           % Eq.3.31 from Ref.5
          n(i)^2 m(i)^2 -m(i)*n(i);
      -2*m(i)*n(i) 2*m(i)*n(i) m(i)^2-n(i)^2];

  epsilon_Local{i}=T{i}*epsilon_Global{i};
end

%% Step 6: Convert lamina strains to lamina stresses in lamina axis 1-2
% Calculate the lamina stresses in lamina axis 1-2 from total strains
%
% Convert $\epsilon_{11},\epsilon_{22}, \gamma_{12}\,$ to
% $\sigma_{11},\sigma_{22}, \tau_{12}$
%
% $[\sigma]_{Local}^j=[Q][\epsilon]_{local}^j$
%
sigma_Local=cell(num,1);

for i=1:num
    sigma_Local{i}=Q*epsilon_Local{i};       % Eq.4.14 from Ref.4
end

celldisp(sigma_Local)



%% Routine: Laminate Strength analysis
% The first step in the laminate strength analysis is to carry out laminate
% stress analysis for an assumed load (e.g., a unit load). Below is the
% complete laminate strength analysis procedure
%

%% Step 1: Carry out laminate stress analysis for a unit load on the
laminate
%
% *Calculated from above*
%

%% Step 2: Select an appropriate failure theory
% Use failue criterion to determine first ply failure load
%
% Calculate lamina strength, this will demonstrate whether any lamina has
% failed within the laminate, first ply failure.
%
% Adopting Maximum-Stress Theory:
% This theory states that faiulure will occur if any of the stresses in the
% principle material axes exceed the corresponding allowable stress. Thus
% the following inequalities must be satisfied to avoid failure:
%
% $\sigma_{11} < \sigma_{LU}$
%
% $\sigma_{22} < \sigma_{TU}$
%
% $\tau_{12}   < \tau_{LTU}$
%
% If the normal stresses are compressive, $\sigma_{11}$ and $\sigma_{22}$
% must be replaced by the allowable compress stresses:
%
% $\sigma_{11} < {\sigma_{LU}}^{'}$
%
```

```
% $\sigma_{22} < {\sigma_{TU}}^{'}$
%
%
% $I_f < 1$
%
% * Where
% $I_f=(\frac{\sigma_{11}}{\sigma_{LU}})^2-
\frac{\sigma_{11}\sigma_{22}}{(\sigma_{LU})^2}+(\frac{\sigma_{22}}{\sigma_{T
U}})^2+(\frac{\tau_{12}}{\tau_{LTU}})^2$
%


for i=1:num                % Eq.5.102 & Eq.5.103 from Ref.1

    I(i)=sigma_Local{i}(1)/sigmaLU-...
         sigma_Local{i}(1)*sigma_Local{i}(2)/(sigmaLU)^2+...
         (sigma_Local{i}(2)/sigmaTU)^2+(sigma_Local{i}(3)/TauLTU)^2;

    if I(i)>=1
        fprintf('First ply failure occurs at layer number: "%d" \n',i)
    break
    end
end

I
```

APPENDIX B –Mathcad files

Beam model Verification

Material properties

$L_1 := 7m$

$L_2 := 4m$

$L_3 := 5m$ Span lengths

$L_4 := 10m$

$L_5 := 19m$

$E_{beam} := 20GPa$

           E modulus

$E_{deck} := 20GPa$

$\nu_{beam} := 0.3$

           Poissons's ratio

$\nu_{deck} := 0.3$

Cross sectional area obtained from AutoCAD

$A_1 := 2930295mm^2$

$A_2 := 6205650mm^2$

$A_3 := 4624084mm^2$

$A_4 := 1888727mm^2$

$A_5 := 2278501mm^2$

Hollow cross sectional area obtained from AutoCAD

$A_{h1} := 703098.43mm^2$

$A_{h2} := 778963.44mm^2$

$A_{h3} := 706239.67mm^2$

$A_{h4} := 716595.38mm^2$

$A_{h5} := 708912.34mm^2$

$L_{total} := L_1 + L_2 + L_3 + L_4 + L_5 = 45\,m$ Total span length

$h_{deck} := 300\,mm$ the depth of the bridge deck

$w_{deck} := 3\,m$ Width of the deck

$G_{beam} := 21\,\dfrac{kN}{m^3}$

$G_{deck} := 1\,\dfrac{kN}{m^3}$

$Q_{ped} := 5\,\dfrac{kN}{m^2}$ Pedestrian load

Dead load from each cross-sections

$G_1 := A_{h1} \cdot G_{beam} = 14.765 \cdot \dfrac{kN}{m}$

$G_2 := A_{h2} \cdot G_{beam} = 16.358 \cdot \dfrac{kN}{m}$

$G_3 := A_{h3} \cdot G_{beam} = 14.831 \cdot \dfrac{kN}{m}$

$G_4 := A_{h4} \cdot G_{beam} = 15.049 \cdot \dfrac{kN}{m}$

$G_5 := A_{h5} \cdot G_{beam} = 14.887 \cdot \dfrac{kN}{m}$

$G_{deck.total} := G_{deck} \cdot h_{deck} \cdot w_{deck} \cdot L_{total} = 40.5 \cdot kN$

$G_{deck.distr} := G_{deck} \cdot h_{deck} \cdot w_{deck} = 0.9 \cdot \dfrac{kN}{m}$

$Q_{live} := Q_{ped} \cdot w_{deck} = 15 \cdot \dfrac{kN}{m}$

$G_{total.dead} := G_1 \cdot L_1 + G_2 \cdot L_2 + G_3 \cdot L_3 + G_4 \cdot L_4 + G_5 \cdot L_5 + G_{deck.total} = 716.785 \cdot kN$

Reaction forces from Brigade Standard

$R_1 := -70.9 \cdot kN$

$R_2 := -30.22 \cdot kN$

$R_3 := 319 \cdot kN$

$R_4 := 285 \cdot kN$

$R_5 := 116 \cdot kN$

$R_6 := 112.4 \cdot kN$

$G_{brigade.total} := R_1 + R_2 + R_3 + R_4 + R_5 + R_6 = 731.28 \cdot kN$

$\text{ratio} := \dfrac{G_{total.dead}}{G_{brigade.total}} = 0.98$

Corrugated deck design

Material properties

$E_{glass} := 33.18 GPa$ Isotropic glass fiber

Cross sectional areas

$a_1 := 300mm \cdot 10mm = 3 \times 10^3 \cdot mm^2$ Cross sectional area for top layer 1

$d_1 := 92.27mm$ Distance to neutral axis for area 1

$a_2 := 125mm \cdot 10mm = 1.25 \times 10^3 \cdot mm^2$ Cross sectional area for bottom layer 2

$d_2 := 157.73mm$ Distance to neutral axis for area 2

$a_3 := 59mm \cdot 10mm = 590 \cdot mm^2$ Cross sectional area for top layer 3

$d_3 := 82.27mm$ Distance to neutral axis for area 3
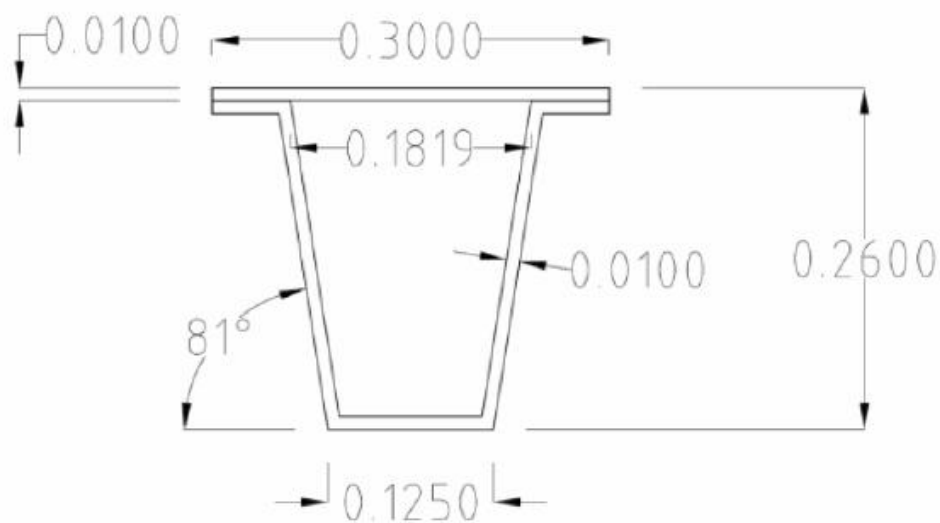
Moment of inertia contribution

$$I_{rib} := a_1 \cdot d_1{}^2 + a_2 \cdot d_2{}^2 + 2 \cdot \left(a_3 \cdot d_3{}^2 \right) = 6.463 \times 10^7 \cdot mm^4$$

Loads

$$g_{snowplow} := 12000 kg \qquad \text{Weight for the snow plow}$$

$$P := \frac{g_{snowplow} \cdot 9.81 \frac{m}{s^2}}{4} = 29.43\ kN \quad \text{Point load for one of the 4 wheels}$$

Deflection

$$defl := \frac{P \cdot (3m)^3}{48 \cdot E_{glass} \cdot I_{rib}} = 7.72 \cdot mm \qquad \text{Deflection for the point load on a 3 meter span}$$

$$\frac{3m}{400} = 7.5\ mm \qquad \text{Deflection limit, L/400}$$